VOLCANIC HISTORY OF WESTERN NICARAGUA AND GEOCHEMICAL EVOLUTION OF THE CENTRAL AMERICAN VOLCANIC FRONT

by

IAN SAGINOR

A Dissertation submitted to the

Graduate School-New Brunswick

Rutgers, The State University of New Jersey

In partial fulfillment of the requirements

For the degree of

Doctor of Philosophy

Graduate Program in Geological Sciences

Written under the direction of

Professor Michael J. Carr

And approved by

_____

_____

_____

_____

New Brunswick, NJ

October, 2008

ABSTRACT OF THE DISSERTATION

Volcanic History of Western Nicaragua and Geochemical Evolution of the Central American Volcanic Front

Dissertation Director:

Professor Michael J. Carr

As part of a long term study on the geochemical evolution of the Central American Volcanic Front led by my advisor, Michael Carr and colleagues at Rutgers University, my dissertation work centers around the development of a better understanding of the duration and scope of a Central America volcanic lull to better constrain and interpret possible causation. To so, I have attempted to improve our knowledge of the volcanic record during this interval by attempting to locate samples that might have erupted during this time period. This effort yielded ages on volcanic samples ranging from 1.1 to 3.6 Ma and, thus, substantially reducing the volcanic gap in Nicaragua. Thus, it may be that while Nicaraguan volcanism was reduced in volume between 7 and 3.6 Ma, activity was still occurring albeit at a substantially reduced rate.

Results of this effort, has given a more complete record that permits more precise analysis of how the volcanic front has evolved since the Miocene. Geochemical analyses of the active and Miocene volcanic fronts document that U/Th values increased by nearly threefold following the Central America, Pacific Coast “carbonate crash” that has been documented at about 10 Ma, related to the closing of the Isthmus of Panama. Although

this transition was considered rather abrupt, data from this study indicate that the transition was somewhat more gradual, occurring over the last 7 myr. An increase in La/Yb Since the Miocene and with increasing distance from the trench, is perhaps due to backward migration of the arc towards the trench. A systematic increase in Zr/Nb towards the trench shows no correlation with age is indicative of a stronger subduction signal near the trench.

Geochemical analysis of Tertiary volcanic rocks from El Salvador to Costa Rica combined with available $^{40}Ar/^{39}Ar$ ages indicate that U/Th values along the Nicaraguan segment of the front have increased since the Miocene, while Ba/La values have not. These values have both remained the same towards the edges of the front.

PREFACE

This dissertation is the culmination of five years of work in Nicaragua and Costa Rica. As part of a long term study on the geochemical evolution of the Central American Arc led by my advisor, Prof. Michael Carr and colleagues at Rutgers University, my dissertation work centers around the development of a better understanding of the duration and scope of the Central America volcanic lull to better constrain and interpret possible causation. The work was funded primarily from NSF Margins support to Prof. Carr and others at Rutgers.

My first trip to Costa Rica during the summer of 2003 provided samples that I analyzed with $^{40}Ar/^{39}Ar$ dating at the Rutgers University Geochronology Laboratory, which is under the direction of Dr. Carl Swisher and Dr. Brent Turrin and published in Carr et al. (2007). These data are included in Chapter One of this dissertation. Fieldwork on this trip focused on collecting samples thought to represent the earliest outpourings of lava from a number of volcanic centers in northwest Costa Rica.

The three fieldtrips during the summers of 2003-2005 were to Nicaragua where I focused on locating samples from 7-0.3 Ma, a period that was not known to contain active Nicaraguan volcanism. Efforts to locate samples from this time period are detailed in chapter two. Samples collected during these trips were also analyzed in the Rutgers Geochronology Laboratory. In addition twenty six of these samples were prepared at Rutgers University and sent to Michigan State University for geochemical analysis. Before this work was done, it was unclear whether this time period was without volcanism or if it was simply that no samples of that age had been found and the majority of my time in the field was spent trying to fill in gaps in the volcanic record.

On my second trip in 2004 to Nicaragua, I collected a sample from an area between Cosigüina and San Cristóbal that I dated to 3.6 Ma. I returned once more to Nicaragua to collect more samples from this area and discovered two previously unknown units that dated from 3.6 to 1.3 Ma, making it possible to see gradual geochemical transitions in the volcanic front since the Miocene.

INTRODUCTION TO THE CHAPTERS

This dissertation is divided into 4 chapters. Chapter One is a manuscript published in *Geochemistry, Geophysics, and Geosystems* (Carr et al., 2007). The goal of this paper was to calculate the flux of incompatible elements from the volcanic front in Costa Rica and Nicaragua. My main contribution to this paper was twenty eight $^{40}Ar/^{39}Ar$ dates, which were used to fill in gaps in the volcanic record and provide maximum ages for several volcanic centers. Those maximum ages were then used to calculate the flux of extrusive volcanism and incompatible elements within the samples area. This paper also includes twenty $^{40}Ar/^{39}Ar$ dates from Brent Turrin of Rutgers University. Brent Turrin and Carl Swisher jointly wrote the methodology sections and the primary author of the manuscript was my advisor Michael Carr. Geochemical analyses were provided by Louise Bolge, Fara Lindsay, Kathy Milidakis, and Mark Feigenson. Guillermo Alvarado also contributed to the writing of the manuscript.

Chapters two through four are written in manuscript format ready for submission to peer reviewed journals. Chapter two will be submitted to the *Revista Geológica de América Central*, which is a publication from the University of Costa Rica's geology department and is intended to describe the efforts I have made in filling in temporal gaps in the volcanic record in Nicaragua and provide some general background on the process, pitfalls, and successes of argon dating Central American volcanic rocks. This paper also presents a basis for interpreting argon ages through an analysis of four case studies that includes reliable as well as unreliable dates.

Chapter three includes all geochemical analyses of samples I collected as well as thirty $^{40}Ar/^{39}Ar$ ages that provide the most complete record of western Nicaraguan

volcanism to date and represents the bulk of my time spent in the field. A number of geochemical indicators are compared as they change through time, with distance along the front, and with distance from the trench. The most important aspect of this chapter is the identification of two previously unknown units of volcanism in western Nicaragua that significantly reduces the gap in the volcanic record of this area.

Chapter four is an analysis of the mechanisms that deliver incompatible elements such as barium and uranium from the subducted sediments, into the mantle, and to the volcanic front in the form of extrusive volcanism. It includes new El Salvadoran data obtained by fellow graduate student Claire Condie's Masters Thesis (Condie, 2004), which increase the range of Miocene samples that can be included in along arc geochemical comparisons. Models are developed to explain the variations in incompatible elements that are evident along the arc and through time with special attention given to barium and uranium.

ACKNOWLEDGMENTS

Writing this dissertation simply would not have been possible without the help and support of my friends, family, and colleagues. Thanks to my committee: Lina Patino for her thoughtful comments, Mark Feigenson for helping run my isotopes, Carl Swisher for teaching me to run “The Machine”, and Mike Carr for trusting me to go to the field without him and giving me the resources to complete my research.

Thanks to all the graduate students who came to my defenses and “relaxed” at the green building, Claire Condie for allowing me to use her Balsamo analyses, and everyone who ever crawled under barb wire to help me get a sample or push the truck out of a ditch (Mike Reilly, Fara Lindsay, Missy Holzer, and Esteban Gazel).

Special thanks to Esteban for never listening to me about how deep the mud is, breaking the car by driving like a maniac, and for ditching me on the streets of Granada at night during a blackout with a San Franciscan pot farmer and a Nicaraguan guy with a habit of breaking bottles over people’s heads. Also for helping me immensely with my figures (“It should look nice”) and for helping me see the big picture. This dissertation would not have been completed without him.

This work is dedicated to Christine, who thinks I’m interesting for some reason.

Table of Contents

Abstract of the Dissertation…….ii

Preface…….. …….iv

Introduction to the Chapters…….……..vi

Acknowledgements……...……...viii

Table of Contents…….……...ix

Chapter 1: Element Fluxes from the Volcanic Front of Nicaragua and Costa Rica

Abstract……1

Introduction…….….2

Data…….…….5

$^{40}Ar/^{39}Ar$ measurements……...……5

Protocol for evaluation of $^{40}Ar/^{39}Ar$ analytical results……7

Volumes of volcanic edifices……...……9

Trace element analysis…….9

Results……...…9

Extrusive volcanic flux for Costa Rica……..……10

Extrusive volcanic flux for Nicaragua……...……12

Does the extrusive volcanic flux vary along Nicaragua and Costa Rica?……..15

Average compositions of volcanic centers and groups……..……15

Models of mantle sources……..……15

Estimating Mantle Contributions……...…16

Flux of subducted components from the volcanic front……18

Discussion……..…19

Magmatic flux versus extrusive volcanic flux……...……19

Subduction derived flux of highly enriched elements……...……20

Conclusions……22

Acknowledgements……22

References……...……23

Tables and Figures…….……29

Chapter 2: Geochronology in Costa Rica and Nicaragua: Progress and Challenges

Abstract……..47

Introduction……....48

Radiogenic Argon……...……50

Methods……..53

Case Studies……...……55

Volcanic History……59

Conclusions……62

References……..……64

Chapter 3: Narrowing the Gap: New geochemical and geochronological results from Western Nicaragua, with an updated Miocene to Recent Volcanic History

Abstract……..…66

Introduction……67

Tectonic Setting…….……68

Study Area……69

Tamarindo Formation……72

Methods……74

Results

Unit 1: Tamarindo Formation……77

Unit 2: Encanto……81

Unit 3: Tinajas……82

Coyol Group……83

Discussion

Volcanic History……86

Geochemical Evolution……88

Origin of the Tamarindo Formation……93

Mid-Miocene Volcanism……96

Conclusions……100

References……102

Chapter 4: Geochemical variations along the Central American volcanic front controlled by subducting input and melting mechanism: A new look at Ba/La and U/Th ratios

Abstract……107

Introduction……108

Stratigraphy of the Cocos Plate……112

The slab contribution……113

Barium Cycle……116

The Papagayo Wind……118

Methods……119

Results……..……120

Trace Element Modeling……..……122

Discussion ……..……126

Conclusions……..……134

References……135

Curriculum Vita……..…….140

Chapter 1

Published 2007 in Geochemistry, Geophysics, and Geosystems

Element Fluxes from the Volcanic Front of Nicaragua and Costa Rica

Michael J. Carr, Ian Saginor
Rutgers University, Department of Geological Sciences, 610 Taylor Rd., Piscataway NJ 08854-8066

Guillermo E. Alvarado
Seismology and Volcanology, Instituto Costarricense de Electricidad, Apartado 10032-1000, Costa Rica

Louise L. Bolge*, Fara N. Lindsay, Kathy Milidakis, Brent Turrin, Mark D. Feigenson and Carl C. Swisher III
Rutgers University, Department of Geological Sciences, 610 Taylor Rd., Piscataway NJ 08854-8066

** Now at Department of Earth Sciences, Boston University, 685 Commonwealth Ave. Boston MA 02215*

Abstract

[1] Geochronologic and geological data define a 600 ka age for the current volcanic front in Costa Rica. In Nicaragua, this age is less constrained but is likely within the range, 600 ka to 330 ka. In Costa Rica, the new geochronologic data significantly improve estimates of the volumes of the volcanoes because they define the contact between the active volcanoes and the previous volcanic front, which is substantially older (2.2 to 1.0 Ma). In addition, the contrast in extrusive volcanic flux between western Nicaragua (1.3 x 10^{10} kg/m/Ma) and central Costa Rica (2.4 x 10^{10} kg/m/Ma) is greatly reduced from previous estimates and within the range of error estimates. These extrusive volcanic flux rates are about a factor of 10 lower than magmatic flux rates estimated for other convergent margins because intrusives, distal tephras, as well as buried and eroded materials are not included in our conservative measurement. We estimate the subducted component of flux for Cs, Rb, Ba, Th, U, K, La, Pb and Sr by subtracting estimated mantle derived contributions from the total element flux. An incompatible element-rich OIB source for the Cordillera Central segment in Costa Rica makes the subducted element flux there highly sensitive to small changes in the modeled mantle-derived contribution. For the other three segments studied, the estimated errors in concentrations of highly enriched, subduction-derived elements (Cs, Ba, K, and Pb) are less than 26%. Averaged over the time of the current episode of volcanism, the subduction-derived component of the fluxes of Cs, Ba, K, Pb and Sr are not significantly different among the four segments of the Central American volcanic front in Nicaragua and Costa Rica. The subduction-derived fluxes of Th and La appear to increase to the SE across Nicaragua and Costa Rica, but the estimated errors in their subduction-derived concentrations are very high, making this variation questionable. The lack of change in the fluxes of Cs, Ba, K, Pb and Sr argues that the well-defined regional variation in Ba/La is the result of changes in the mode or mechanics of fluid delivery into the mantle

wedge, not the total amounts of fluids released from the slab. Concentrated or focused fluids in Nicaragua lead to high degrees of melting. Diffuse fluids in Costa Rica cause lower degrees of melting.

Keywords: Central America, geochronology, geochemistry, subduction, element flux, extrusive volcanic flux

1. Introduction

[2] The cycling of incompatible elements at convergent plate margins, especially those that are more mobile in hydrous fluids or melts of subducted sediments, has become well established since the development of plate tectonics [e.g. *Gill,* 1981]. Specific sources and fluids, coupled with melting and mixing models, have been identified for different arcs; *e.g. Elliot et al.* [1997] and *Stolper and Newman* [1994] for the Izu-Bonin-Marianas system; *Eiler et al.* [2005] for Central America; *Kelemen et al.* [2003] for the Aleutians. The large variety of subducted inputs, especially the sedimentary component, has created considerable diversity among the different convergent margins in their volcanic output [*Plank and Langmuir*, 1988].

[3] Although much progress has been made in understanding the magma generating processes in the subduction factory beneath arc volcanoes, few steps have been made toward the goal of calculating a mass balance across a convergent margin. To quantitatively model element cycling at convergent margins, one must be able to balance the subducted input, the slab and its thin sediment cover, against multiple actual and potential outputs, including mud volcanoes and other shallow releases of fluids and metamorphic products, the volcanic front, the back arc, and transport into the deep mantle. The largest and most easily measured output is the volcanic front and our goal is to make a reliable measurement of the flux of subducted incompatible elements out of the volcanic front. In Central America, the flux of subducted highly incompatible elements out of the volcanic front was estimated by *Patino et al.* [2000] *and Plank et al.* [2002]. However, the age control used was inadequate, consisting of only a few tephra units that were present in piston cores, allowing age determinations from marine stratigraphy [e.g. *Ledbetter,* 1985]. We present more accurate flux determinations based on $^{40}Ar/^{39}Ar$ age determinations of lava flows.

[4] For several reasons, Central America (Figure 1) is an excellent place to make estimates of element fluxes from the volcanic front, especially for elements largely derived from subducted sediment. First, there is a satisfactory geochemical data base posted at http://www.rci.rutgers.edu/~carr/ and derived from *Carr and Rose*, [1987]; *Patino et al.,* [2000] *Carr et al.,* [2003] and Bolge [2005]. Second, from Guatemala to northwestern Costa Rica, there is little or no sediment accretion [*von Huene and Scholl,* 1991] removing a major potential variation in input. However, in southern Costa Rica there is evidence of some sediment accretion [*Ranero and von Huene*, 2000]. Furthermore, just southeast of the end of the volcanic front, there is strong evidence for subduction erosion [*Ranero and von Huene*, 2000; *Vannucchi et al.,* 2001]. The extent of subduction erosion offshore of the volcanic front is not well known but this process may complicate the flux estimate for the central Costa Rica region. Third, $^{10}Be/^{9}Be$, an unambiguous tracer of sediment input,

reaches its global maximum at Masaya volcano in Nicaragua [*Reagan et al.,* 1994]. Fourth, several geochemical tracers of subducted sources (e.g. $^{10}Be/^{9}Be$, $^{87}Sr/^{86}Sr$, Ba/La, U/Th) have large and regular geographic variations that allow comparison of regions of high slab signal, western and central Nicaragua, to nearby regions of low slab signal, central Costa Rica [*Carr et al.,* 2003 and references therein]. These areas in close geographic and tectonic proximity share substantial geologic history, yet have very different geochemistry for the highly incompatible elements that define the typical convergent margin volcanic geochemistry: enrichment in Cs, Rb, Ba, U and K and depletion in Nb and Ta.

[5] Geochemical tracers of the subducted slab define a chevron reaching a maximum in Nicaragua at about the center of the margin. Ba/La, which is well determined for many samples, is an appropriate focus for reviewing the regional geochemical variation (Figure 2a). The symbols in Figure 2 are keyed to tectonics and high field strength element (HFSE) depletion. The tectonic subdivisions are separated by right-stepping jogs, changes in strike and gaps in the volcanic front [*Carr et al.,* 2003]. HFSE depletions are characteristic of arc volcanics and most Central American samples have large HFSE depletions (filled symbols in Figure 2). However, many samples from the volcanic front of Central America have minor HFSE depletions [*Carr et al.,* 2003] or none at all [*Reagan and Gill,* 1989]. These undepleted or less depleted rocks (open symbols in Figure 2) are termed HFSE-rich here because of comparison with the more abundant, strongly depleted rocks. The HFSE-rich samples from the volcanic front are comparable to many Central America back-arc lavas (not included in Figure 2), sharing a lack of HFSE depletion and an enrichment in large ionic radius, lithophile elements (LILE) such as Cs, Rb, Ba, U, K, Pb, Sr.

[6] The Ba/La variation along Central America is quite large and has the shape of a slightly asymmetric chevron, reaching a lower base in central Costa Rica (about 15) than in Guatemala (40). The peak, in Nicaragua, approaches 150. The fluxes calculated below concern the right hand side of the Ba/La chevron, from Nicaragua to Costa Rica, where the ratio has a range of about a factor of 10. Ba/La correlates with $^{10}Be/^{9}Be$ [*Leeman et al.,* 1995], an unambiguous maker of subducted sediment [Morris et al., 1990]. Furthermore, the sediments being subducted on the Cocos Plate are highly enriched in Ba [*Patino et al.*, 2000; *Plank and Langmuir*, 1993]. The expectation then is for changes in the amount of subducted Ba to drive the Ba/La variation. However, Figures 2b and 2c make clear that the regional variation is primarily driven by La, not Ba. Because of this, *Carr et al.*, [1990] and *Feigenson and Carr* [1993] developed a flux focusing model for Central America in which tectonic factors, such as slab dip, control the delivery of flux, making it more and less concentrated. Higher concentrations of flux lead to higher degrees of melting. The high Ba in the flux is diluted as the extent of melting increases, resulting in similar Ba concentrations regardless of the degree of melting. La decreases with extent of melting because the La brought in with the flux is not sufficient to counterbalance the diluting effect of higher extent of melting. This model, which links flux concentration and degree of melting, has been substantially improved as additional geochemical data have been added [e.g. *Reagan et al.*, 1994, *Leeman et al.*, 1994, *Eiler et al.*, 2005]. *Carr et al.* [1990] and *Feigenson and Carr* [1993] implicitly assumed a constant flux across the region but this is a soft assumption, not required by the geochemistry. There could be higher amounts of flux in the areas where geochemistry implies a more concentrated flux. The goal of the current

work is to determine whether or not the absolute amount of flux of highly incompatible elements varies between Nicaragua and Costa Rica. In other words, is the peak in Nicaragua the result of a higher amount of flux, a stronger focusing of a constant flux or some combination of the two?

[7] There are substantial difficulties in making estimates of element fluxes. One of the primary contributions of this work is to highlight those difficulties and outline new approaches that may reduce the uncertainties. On the geochemical side, the major problem is the demonstrated complexity of the sources. The sub-arc mantle is not homogeneous because there is clearly an enriched ocean island basalt (OIB) source affecting central Costa Rica [*Malavassi,* 1991, *Leeman et al.*, 1994, *Herrstrom et al.*, 1995, *Feigenson et al.,* 2004]. The source of the OIB input in central Costa Rica is poorly constrained and could have originated in the mantle wedge or the subducted plate. *Feigenson et al.* [2004] reviewed this problem and found that few of the several hypotheses concerning this issue can be ruled out. Outside of central Costa Rica, REE inverse modeling suggests that the mantle may consist of at least two components, a MORB source and a less depleted source [*Feigenson et al.,* 1993]. The subducted oceanic crustal section adds additional complexity. An East Pacific Rise MORB crust is subducting outboard of Nicaragua and northwestern Costa Rica and a Cocos-Nazca Ridge MORB crust with Galapagos derived seamounts is subducting outboard of Central Costa Rica [e.g. *von Huene et al.* 2000]. The sedimentary stratigraphy includes two units with large differences in geochemistry: a basal carbonate section of roughly 200 m and an upper hemipelagic section of roughly 200 m [*Patino et al.,* 2000]. Recently, *Eiler et al.* [2005] defined plausible depleted mantle (DM) and OIB mantle compositions and identified two separate slab-derived fluxes, one with low $\delta^{18}O$ and one with high $\delta^{18}O$. The former is most likely a hydrous fluid with a strong contribution from the subducted Cocos mantle and the latter is most likely a melt of the subducted sediment.

[8] The mass flux at the volcanic front consists of the existing volcanic edifices, distal tephras, earlier volcanic units, sediments derived by erosion, and a wide range of intrusives including mafic cumulates, which are likely near the Moho [e.g. *Herzberg et al.* 1983], gabbroic-granitic bodies within the crust, and shallow dikes. Obtaining a flux requires defining a volume of igneous output and identifying the time interval over which it was produced. A bottom–up or long-term approach can be achieved in an island arc by measuring the total volume of the arc-related crust using geophysical methods and determining the age of the onset of arc–related igneous activity using stratigraphy and geochronology. One drawback to this approach is that the geochemical patterns along a margin may well change over time, causing a long-term average mass flux to be unrelated to the current geochemistry. In addition, long hiatuses in magmatic activity may generate a long-term rate that rarely or never occurs during magmatically active periods. The top-down or short-term approach, used here, focuses on the actual volcanic output that can be quantified from geologic mapping of lavas and tephras. This restricted approach captures an accurate snapshot of the ongoing magmatic process which allows the use of fresh lavas and tephras. However, the short-term focus on what can actually be measured makes it difficult to measure total magmatic output, because the mass of intrusives resulting from a short time interval cannot be easily measured, even with geophysical imaging. The

approach taken here is to calculate an extrusive volcanic flux, explicitly ignoring the intrusives and the mass removed by erosion.

[9] To provide more accurate estimates of extrusive volcanic fluxes, we report new $^{40}Ar/^{39}Ar$ ages on lava flows that geologic mapping and geomorphic expression indicate are the basal units of the current episodes of cone construction in Costa Rica and Nicaragua. In addition to providing a datum for the active centers, the new ages allowed us to improve the geologic mapping of Costa Rican volcanoes. Our results add to a growing body of geochronological data. *Ehrenborg* [1996] and *Plank et al.* [2002] recently summarized and added to the previous geochronological work in Nicaragua. *Alvarado et al.* [1992] summarized the geochronology of Costa Rican volcanics and *Gillot et al.* [1994] provided several new K-Ar ages and estimates of the volume of the major volcanic units. *Vogel et al.* [2004] and *Pérez et al.* [2006] defined the age framework of several Costa Rican ignimbrite sheets. A substantial number of new $^{40}Ar/^{39}Ar$ ages have allowed *Gans et al.* [2002, 2003] to propose that a series of discrete volcanic episodes has constructed the volcanic provinces of Costa Rica.

[10] The geochronologic data presented here, combined with previously published results, allow us to calculate an extrusive volcanic flux for the volcanic front cones along with their contemporaneous tephra sheets. After making assumptions about the nature of the mantle and the extent of melting, we estimate a flux of subducted incompatible elements out of the Central American volcanic front, improving on the subduction derived flux estimates of *Patino et al.* [2000] and *Plank et al.* [2002].

2. Data

2.1 $^{40}Ar/^{39}Ar$ measurements

[11] Samples for geochemistry and $^{40}Ar/^{39}Ar$ dating were obtained from the cores of large boulders or lava blocks. Many of the samples of the oldest flows were of dense rock cores remaining after intense weathering. This was particularly the case on the NW or Caribbean side of the Costa Rican volcanic front. GPS provided accurate locations for samples collected since 1999, including most of the samples for which we obtained ages. The $^{40}Ar/^{39}Ar$ ages determined for this project are in Table 1. The data from the step-heating measurements are included in the supplemental material. We include six previously published ages for Irazú volcano [*Alvarado et al.*, 2006] because we subsequently adopted a new age for the Alder Creek standard (1.194 Ma). This increased the Irazú ages by about 0.6%.

[12] Samples for $^{40}Ar/^{39}Ar$ dating were selected by evaluation of petrographic thin sections, choosing only those samples with little or no visible weathering and minimal interstitial glass. The samples were crushed using a steel plated micro jaw crusher and sieved to >300 μm and <425 μm. This fraction was rinsed and then washed in distilled water in an ultrasonic cleaner for about 10 minutes to remove dust, clays or adhering fine particles, and then dried at less than 100° C. Magnetite was removed using a hand magnet, and most plagioclase phenocrysts were removed using a Frantz Isodynamic Separator.

Remaining loose plagioclase phenocrysts were hand-picked from the matrix fraction under a binocular microscope. In a few cases, biotite and plagioclase phenocrysts were separated from the sample, cleaned and hand picked for analyses using similar techniques outlined above.

[13] The "cleaned" >300μ <425μ matrix or mineral separates were then loaded into individual sample wells of aluminum irradiation disks, along with aliquots of the irradiation monitor mineral Alder Creek (AC-1). The loaded sample disks were wrapped in Al foil, sealed in quartz glass tubes, and then irradiated for 0.25 hours in the Cadmium-Lined, In-Core Irradiation Tube (CLICIT) facility of the Oregon State University Triga Research Reactor (OSTR).

[14] Ten to 80 milligrams of the irradiated samples (depending on approximate age) were loaded into individual six mm diameter wells in ~60 mm diameter stainless steel disks, loaded onto one of the two extraction line sample chambers, and baked out at approximately 100° C for six hours. Gases were extracted using a 40 watt CO_2 laser to apply stepwise incremental heating. The laser is focused through a II-VI ZnSe faceted transmissive beam integrator lens resulting in a 6 mm square flat top beam profile with minimal temperature gradients. The use of the CO_2 laser to heat samples permits the heating of 10 to 80 milligrams of sample and provides adequate "clean-up" of extracted gases for up to 10 minutes without significantly raising background values, a problem with larger volume metal resistance furnaces. The ability to heat samples and yet keep backgrounds at an ultra low level enables us to obtain high-resolution plateau ages on a few tens of milligrams of sample instead of several hundreds of milligrams.

[15] The use of the laser, as opposed to a more conventional vacuum furnace system, permits two to ten times the percent radiogenic ^{40}Ar yields on geologically young, low potassium (0.3 to 1% K_2O) bearing samples by minimizing extraction line volumes, avoiding heating of metal surfaces releasing interference Ar isotopes, and removing a significant proportion of atmospheric argon contamination in the lower temperature steps, thus significantly reducing accompanying combined analytical uncertainties.

[16] Calibration and determination of the irradiation parameter J was determined by multiple total fusion analyses of the co-irradiated monitor mineral Alder Creek Rhyolite Sanidine (ACS-1) using a published reference age of 1.194 ± 0.006 Ma [*Turrin et al.,* 1994, *Renne et al.*, 1998]. Interference isotopes produced from Ca during irradiation of the samples using the Oregon TRIGA were corrected using previously published values $(^{36}Ar/^{37}Ar)_{Ca} = 2.72\pm0.06$ $(x10^{-4})$ and $(^{39}Ar/^{37}Ar)_{Ca} = 7.11\pm0.02$ $(x10^{-4})$ [*Renne et al*. [1998] and *Deino et al.* [2002]. During the analysis of the samples and standards, mass discrimination was regularly monitored through measurement of air aliquots delivered via an on-line automated air pipette system and varied between 1.000 and 1.007 AMU. System baselines, Ar isotope backgrounds and mass discrimination measured for a typical sample loading and run period (approximately one week) were time averaged though linear regressions of the measured data. Resultant curves were then applied to the standards and unknown sample measurements. This approach of "modeling" baseline, background, and mass discrimination throughout the run period significantly improves the analytical data for

both the standard and unknowns by minimizing spurious low signal measurements on backgrounds and blanks due to electronic and mechanical noise. Automation laser heating, gas extraction and clean-up, spectrometer measurement and data reduction were made using automated software written by A. Deino.

2.2 Protocol for evaluation of $^{40}Ar/^{39}Ar$ analytical results

[17] The basalts and andesites that dominate the mass of the volcanic front in southern Central America present several problems that complicate the task of obtaining reliable ages from $^{40}Ar/^{39}Ar$ measurements. The difficulties include the young ages of many samples, the low K_2O contents (except for Central Costa Rica), assimilation, magma mixing and tropical weathering. Nevertheless, our experience with Central American samples (and geologically young samples in general) demonstrates that CO_2 laser techniques provide accurate analyses on low potassium mineral phases such as plagioclase, biotite, and whole rock matrix if a rigorous approach to selection of $^{40}Ar/^{39}Ar$ dating results is followed. Careful evaluation of the Ar isotopic data used for age calculation is critical because about half of the samples measured to date indicate a non-atmospheric $^{40}Ar/^{36}Ar$ ratio and slightly disturbed step-heating spectra.

[18] We used the following protocol to evaluate the $^{40}Ar/^{39}Ar$ results obtained in this study and consider those data that meet the following criteria the most reliable ages.

[19] I. In an incremental heating release spectrum, individual apparent ages derived from the argon isotopes released at discrete temperature steps are plotted relative to the cumulative percentage of $^{39}Ar_K$ released in each increment relative to the total $^{39}Ar_K$ released from the completed experiment (Figure 3). Those experiments that result in release patterns forming age plateaus are considered more reliable than those whose apparent ages vary widely relative to temperature. We use the commonly used definition of a plateau as defined by gases released from a minimum of three consecutive temperature increments whose relative ages overlap at the 95-percent confidence level and total 50% or more of the total $^{39}Ar_K$ released from the completed incremental heating experiment, [*Fleck et al.,* 1977]. Plateaus incorporating more increments and greater total percentages of the total $^{39}Ar_K$ released during the experiment are considered of better quality and reliability. Sample CR-IZ-02-05 (Figure 3) meets all these criteria. Seven discrete temperature steps yield apparent ages that overlap at the 95-percent confidence interval and form a plateau with a weighted mean age of 598 ± 16 ka. The plateau-age, defined by 94% of the total $^{39}Ar_K$ released, is concordant with the total fusion or integrated age of 580 ± 50 ka at the 95-percent confidence level

[20] II. The second group of criteria relates to the plotting of the Ar isotopes obtained from the incremental heating experiments on inverse isochron plots, where the Y-axis ($^{36}Ar/^{40}Ar$) relates to the atmospheric components of the total gases, the X-axis ($^{39}Ar/^{40}Ar$) the radiogenic component and the slope from the fit of the plotted increments, the age. We consider those analyses most reliable with an isochron derived age that is analytically indistinguishable from the plateau age and the total fusion age (weighted sum of the individual relative increment ages). The initial $^{40}Ar/^{36}Ar$ ratio derived from the Y-intercept

should be analytically indistinguishable from the atmospheric ratio of 295 ± 1 (Figure 3). The qualities of the incremental heating experiments are also evaluated on the fit of the $^{36}Ar/^{40}Ar$ and $^{39}Ar/^{40}Ar$ ratios for the different temperature steps on the isochron plot. The better defined the mixing line between the initial $^{36}Ar/^{40}Ar$ ratio and the $^{39}Ar/^{40}Ar$ ratio, the better the fit of the slope, thus the higher the quality and more reliable the isochron age. This goodness of fit is defined as the mean sum of the weighted deviates of the individual temperature ages or MSWD [*York*, 1969]. The MSWD is essentially the ratio of the measurement error to the observed scatter about the regression line through the points on the isochron plot. A value of 1.0 indicates that the scatter about the regression line is accounted for by the measurements errors. A value less than one suggest that the errors for the individual measurements may be over estimated. We consider ages whose isochron plots resulted in MSWDs close to 1.0 to be the most reliable. In our example, CR-IZ-02-05 (Figure 3), the isochron data meets all these criteria. The isotopic data indicate an initial $^{40}Ar/^{36}Ar$ ratio of 293 ± 7, analytically indistinguishable from the accepted atmospheric ratio of 295 ± 1. The MSWD is 1.9 and the resultant isochron age is 598 ± 20 ka, concordant with the plateau and total fusion ages.

[21] III. An additional criterion used to provide further indication of the reliability of a sample's age, is the order that the isotopic data appear on the isochron plot relative to increasing or decreasing $^{36}Ar/^{40}Ar$ and $^{39}Ar/^{40}Ar$ ratios for the individual step-heating measurements. These points define the "mixing line" between the initial $^{36}Ar/^{40}Ar$ ratio (atmospheric component) and the $^{39}Ar/^{40}Ar$ ratio (radiogenic component) of the sample. With each increasing temperature age, the isotopic composition commonly moves along a mixing line from the initial $^{36}Ar/^{40}Ar$ (atmospheric) ratio toward the $^{39}Ar/^{40}Ar$ (radiogenic) ratio corresponding to the sample age until the sample reaches a unique temperature or step. In cases where increased atmospheric components are released at high temperatures, the isotopic composition should evolve back toward the initial $^{36}Ar/^{40}Ar$ intercept along the same mixing line as obtained from lower temperature increments (Figure 3). In our example, CR-IZ-02-05 (Figure 3), the isochron data also meet this criterion. On the inverse isochron, the low temperature steps of plot near the y-intercept corresponding to accepted atmospheric ratio of 295. With each increasing temperature step, the isotopic composition moves along a mixing line toward the $^{39}Ar/^{40}Ar$ ratio corresponding to an age of 598 ± 20 ka until the 8-watt step (approximately 890° C). Then the isotopic composition evolves back toward the atmospheric ratio intercept along the sample mixing line.

[22] In the case of samples where the isochron analysis does not indicate an atmospheric ratio but the MSWD is ≤2 and the mixing line is well defined, then the isochron age is considered the most reliable age measurement because no assumptions are made about the isotopic composition of the initial Ar in the sample.

2.3 Volumes of volcanic edifices

[23] The volume of each volcanic center was calculated using digitized areas within 100 m contour intervals on topographic maps of 1:50,000 scale for smaller volcanoes or 1:250,000

scale for larger volcanoes. A formula for a frustrum was used to calculate the volume between two contours with areas b1 and b2; $V = 0.1 \cdot (b1+b2+(b1 \cdot b2)^{0.5})/3$. Many volcanoes have irregular bases that required adding in wedge or slab like volumes.

[24] Some volcanoes have produced ashflow sheets that extend beyond the current topographic limits of the volcanic edifice. All of the ashflow units with ages of 600 ka or less and whose volumes have been determined have been included in the volumes in Table 2. The Alto Palomo tephra near Platanar volcano in Costa Rica [*Villegas,* 2004; *Vogel et al.*, 2005] has an appropriate age but lacks a well-determined volume and was not included. Similarly, the las Banderas pyroclastic flow is not yet included in the volume of the Masaya/Las Sierras volcanic center but should be in the future. The ashflow sheets near Malpaisillo, Nicaragua are not included in any volume because the source, the Malpaisillo Caldera, proposed by *van Wyk De Vries* [1993], has not been proven and the age is thought to be late Tertiary.

[25] Volumes critically depend on the determination of the base which relies heavily on a geologic understanding of each volcanic center. For example, *Stoiber and Carr* [1973] estimated a volume of only 11 km^3 for Masaya volcano, based on the size of the most recent caldera. Masaya has now become the Masaya/Las Sierras volcanic center, a much larger edifice, over 200 km^3 in volume. The recognition that Masaya caldera was part of a of an ignimbrite shield [*van Wyk de Vries,* 1993] was key for this improvement. The large changes in the published volumes of some Central American volcanoes have been the result of improved geologic understanding, not fluctuations from random error. Included in the supplemental material are the data and assumptions from which the volumes were calculated.

2.4 Trace element analysis

[26] Many previously published geochemical data for Central America [e.g. *Patino et al.,* 2000] were re-determined after powdering the samples in alumina containers. These samples, collected from 1972-1990, were originally powdered in tungsten carbide vessels, rendering their Nb and Ta analyses suspect or completely misleading. Comprehensive and precise trace element analyses were made on a HR-ICP-MS during the last five years by various students following the procedures of *Bolge et al.* [2006]. Many new samples have been added to the CaGeochem data base by *Bolge* [2005], *Reilly* [2005], F. Lindsay (unpublished) and K. Milidakis (unpublished).

3.0 Results

[27] The calculation to determine the flux of highly incompatible elements derived from subduction beneath the volcanic front of Nicaragua and Costa Rica has two steps. The first is to determine an extrusive volcanic flux, which requires measurements of the volumes of volcanic centers and determination of an appropriate time interval. The new $^{40}Ar/^{39}Ar$ ages in Table 1 allow us to make substantially improved estimates of the extrusive volcanic flux for the two Costa Rican segments of the volcanic front and modestly improved estimates of the extrusive volcanic flux for the two Nicaraguan segments. Our data and a few additional

$^{40}Ar/^{39}Ar$ ages from *Vogel et al.* [2005] indicate a well-defined pulse of volcanic activity beginning at about 600 ka (Figure 4) and continuing to the present. The second step is to determine average compositions of the volcanic centers and then apportion the total for each element into mantle-derived and slab-derived components. We estimate mantle derived components using primarily the methods and assumptions of *Eiler et al.* [2005]. Estimating the mantle contribution introduces substantial error. However, for selecting elements that have very large enrichments over plausible mantle derived compositions, we can determine subduction derived fluxes that have minimal dependence on assumptions about the nature of the mantle or the degree of melting.

3.1 Extrusive volcanic flux for Costa Rica

[28] In Costa Rica, a rich background of geochronologic work [*Alvarado et al.* 1992; *Gillot et al.*, 1994, *Gans et al*., 2003] and geologic mapping [*Tournon and Alvarado,* 1997] guided our sampling, allowing us to select critical areas not addressed by previous work. The extensive geochronologic survey of the Costa Rican volcanic belt by *Gans et al.* [2003] suggested several post-Miocene peaks of volcanic activity separated by apparent lulls: with peaks at 6-4 Ma, 2-1 Ma, 600-400 ka and 100-0 ka. We designed our sampling to better define the boundaries between these age peaks, especially the contact mapped by [*Tournon and Alvarado,* 1997] between the 2-1 Ma volcanics and the volcanics younger than 600 ka. The 2-1 Ma volcanics will be referred to here as the Monteverde volcanic front (VF) and the 600 ka and younger volcanics will be referred to as the active VF.

[29] Geochronologic work since the 1997 map of *Tournon and Alvarado* has improved the geologic boundaries, increasing the extent of the Monteverde VF at the expense of the active volcanoes. Figure 5 sketches the currently recognized boundaries of the Monteverde VF and the active VF. Our $^{40}Ar/^{39}Ar$ data made substantial contributions to this mapping in the Cordillera de Guanacaste by obtaining new ages for flows on either side of the contact. Four samples have ages (1.13 Ma, 1.60 Ma, 2.16 Ma and 2.18 Ma) that place them in the Monteverde VF and slightly extend the range of the 2 to 1 Ma peak to 2.2 Ma. At Rincón de la Vieja volcano, the largest volcano in the Cordillera de Guanacaste, we obtained an age of 564 ka on a flank lava selected for its high degree of erosion. Similarly, at Miravalles and Tenorio volcanoes we obtained ages of 548 (coincidentally equal) on eroded flow fields from the lower flanks. These data verify the presence of the 600-400 ka peak in the Guanacaste region.

[30] Our sampling also sought to define a geologic boundary separating the 600-400 ka and 100-0 ka peaks proposed by *Gans et al.*[2003]. However, we obtained 9 new ages between 400 ka and 100 ka. Therefore, we doubt there was a regional lull in extrusive volcanic activity after 400 ka. From our perspective, we treat all the volcanics from 600 ka to the present as a single unit. There are geomorphological differences, apparent on topographic maps, air photos and satellite images, that suggest pauses in activity at individual volcanoes, but the ages obtained to date indicate that such pauses are local, not segment wide. In contrast, we were successful in using geomorphology to locate the oldest flows; six samples yielded ages between 548 and 598 ka. We, therefore, agree with *Gans et al.* [2003] that there was a substantial outpouring of lava starting at about 600 ka.

[31] Two of our samples from Costa Rica have ages in the lull between the Monteverde VF and 600 ka. One is a lava from Tenorio volcano with an age of 740 ka. The other is the San Jerónimo ash flow tuff with an age of 855 ka. We sampled this welded tuff because geologic mapping [*Krushensky*, 1972; *Alvarado et al.*, 2006] places it beneath the basaltic and andesitic lavas that comprise the lower flanks of Irazú volcano. These two ages clearly shows that volcanism did not entirely cease between 1 Ma and 600 ka.

[32] The active volcanoes primarily occur in two major ranges, the Cordillera de Guanacaste and the Cordillera Central (Figure 5). They are separated by a volcanic gap of 80 km that is interrupted only by the small Arenal volcanic center. This gap was not present as recently as 1 My ago [*Gillot et al.,* 1994], during the eruption of the Monteverde VF. The location of the Monteverde volcanic front is similar to that of the present volcanic front in the Cordillera de Guanacaste and the Cordillera Central, but profoundly different in the intervening region. In the Cordillera de Guanacaste, the Monteverde VF is wider than the present volcanic front. It includes a line of volcanic remnants and lava plateaus, located slightly trenchward of the present volcanic front but also extends under and behind the present front. In the Cordillera Central, the Monteverde volcanic front and the active volcanic front coincide and the Monteverde volcanic front is largely buried because of the great extent of the younger volcanics. However, in the area of the gap, pierced only by the small Arenal volcanic center, the Monteverde VF makes a large ridge whose axis is about 15 km trenchward of Arenal. Therefore, the substantial change in the Costa Rican volcanic front after about 1 Ma was the near cessation of activity in the area between the Cordillera de Guanacaste and the Cordillera Central. Furthermore, when volcanism resumed near Arenal about 100 ka ago [*Gillot et al.*, 1994], it was located 10 to 15 km NE of its former axis.

[33] Our new $^{40}Ar/^{39}Ar$ ages confirm the proposed peak in volcanic activity starting at about 600 ka. With the exception of Arenal volcanic center, which apparently began only about 100 ka ago at Cerro los Perdidos, the other mafic Costa Rican volcanic centers all have lava fields in the 600-500 ka age range [this work, *Gans et al.*, 2003, *Gillot et al*., 1994 and *Alvarado et al.*, 1992]. The peak, starting at 600 ka, followed a reorganization of the volcanic front; specifically, the near cessation of volcanism and the repositioning of the volcanic front in the 80 km region, centered on Arenal. These two factors lead us to use 600 ka as the datum for estimating an extrusive volcanic flux for Costa Rica.

[34] Table 2 provides new and substantially lower estimates for the volumes of the Costa Rican volcanic centers. The interaction between geochronological and geological investigations that defined a 600 ka base for the active volcanoes also outlined much more realistic areal extents and volumes for the active volcanoes. This geologic insight came from the 1:500,000 scale geologic map of *Tournon and Alvarado* [1997], as revised by new age dates and ongoing mapping by G. E. Alvarado and co-workers from the Central American School of Geology at the University of Costa Rica.

[35] The key change lowering the volumes of the volcanic centers in the Cordillera Central was the recognition of older volcanics and sediments at roughly 1500 m elevations

throughout the Cordillera Central. The basal lavas at Irazú in the valley of the Rio Reventazón outcrop as low as 1500 m. Previous volume estimates used this geologic data and so the base at approximately 1500 m on the SW side of the Cordillera Central has not changed. However, geologic observations define a higher base for the center of the Cordillera and its NE or Caribbean flank. For example, Miocene sediments and Pliocene lavas comprise the lower SE flank of Turrialba volcano with uppermost outcrops that just reach the 1500 contour. At Barva volcano, recent fieldwork uncovered sediments on the SE flank that extend from 700 to 1500 m. At Platanar volcano, older volcanics crop out on the SW flank at elevations as high as 2000 m.

[36] The active volcanoes, (600 ka and younger volcanics) of the Cordillera Central cover and nearly obscure an older volcanic and sedimentary massif that extends the entire length of the Cordillera and has a summit elevation of roughly 1500 m. Therefore, nearly all the topography above 1500 m belongs to the active volcanoes. This volume comprises 75% of the total. The lavas of the active volcanoes extend to about 1500 m into the Valle Central on the SW or Pacific side. However, on the NE or the Caribbean side, young lavas reach elevations as low as 300 m. Geologic cross sections indicate that these flank lavas and tephras make a thin cover on a buried massif of Monteverde age and older volcanics and sediments. We estimated volumes of this cover using a thickness of 100 m for the lower flank (areas located at elevation below 1000 m) and a thickness of 200 m for the upper flank (areas between 1500 and 1000 m elevations). These flank veneers comprise 25% of the total volume of the active volcanoes of the Cordillera Central and we use that percentage as the error estimate for the Cordillera Central volumes. In the Guanacaste segment, the contact between the active VF and the Monteverde VF can be mapped and so the estimated error in volume is less and assumed to be 20%.

3.2 Extrusive volcanic flux for Nicaragua

[37] *Patino et al.* [2000] estimated ages for several segments of the volcanic front in Central America, primarily using the ages of large pyroclastic deposits assumed to predate all the active basaltic to andesitic volcanoes. The Nicaraguan estimate (135 ka) was based on the age of the J1 tephra, found in piston cores offshore of Nicaragua and dated via paleontological methods [*Ledbetter,* 1985]. The tephra has distinctly high FeO, making the Masaya-Las Sierras complex, the only volcanic center in Central America with strong Fe-enrichment [*Walker et al.* 1993], the likely source. Towards the Pacific coast from Masaya volcano, the initial volcanic deposits resting on underlying Plio-Pleistocene marine sediments are thick andesitic to dacitic pyroclastic flows. The J1 tephra was assumed to be a fall deposit associated with these pyroclastic flows and the entire Nicaraguan volcanic front was assumed to be younger than the J1 tephra. This obviously weak chain of assumptions was a primary motivation for our current work. Although we can substantially improve the estimate by *Patino et al.* [2000], we cannot define a clear age boundary separating the active volcanoes from earlier volcanics or sediments.

[38] The Nicaraguan volcanic front is roughly parallel to and within the Nicaraguan Depression (Figures 1 and 6). The two major Nicaraguan lakes and the Gulf of Fonseca, separating Nicaragua from Honduras and El Salvador, lie within the Nicaraguan

Depression, suggesting it is a region of active subsidence. However, most shallow earthquakes occur along the volcanic axis, rather than along either the NE or SW side of the Depression. The flat topography of the Depression simplifies measurement of the volumes of the volcanoes, but at least some subsidence, along with active alluvial and lacustrine sedimentation, has led to the burial of the earliest lavas of the active volcanoes, making it difficult to determine a time of onset for the active volcanoes. Because the flanks of the Nicaraguan volcanoes, with the exception of SW side of the Masaya volcanic center, merge into alluvial and lacustrine sediments and tephra deposits, the contact between the earliest lavas of the active volcanoes and the previous generation of volcanic deposits is not exposed. Therefore, some additional assumptions are needed to calculate rates of extrusive volcanic flux.

[39] Our new $^{40}Ar/^{39}Ar$ ages for Nicaraguan lavas and tephra fall into four groups. First, two samples are from Miocene volcanics on the NE border of the Nicaraguan Depression. These samples, with ages of 9.5 Ma and 7.1 Ma, are located within the 7-9 Ma age band mapped by *Plank et al.*, [2002] and consistent with it. Second, one sample, with an age of 3.5 Ma, from the volcanic remnants outcropping along the volcanic front between San Cristóbal and Cosigüina volcanoes (Figure 6), third, between the Miocene volcanics on the NE border of the Nicaraguan Depression and the active volcanic front is a roughly 20 km wide zone of sediments surrounding a few low volcanic hills. We obtained two ages from these partially buried volcanic remnants (1.13 and 1.48 Ma), which fall within the age range of the Monteverde VF in Costa Rica. Finally, the samples making up the main group are lavas collected from the regions of the active volcanoes that appear from geomorphological criteria to be the oldest exposed lavas from the active volcanoes. Topographic maps and satellite images of the active volcanoes reveal relatively few highly dissected areas that are likely to expose old lavas. Figure 7 shows the result of sampling of the highly dissected Cerro los Portillos area of Telica volcano. Three age determinations from the flanks of the highly dissected area indicate an age of at least 330 ka. We sampled the flank region because the cores of volcanoes are commonly subjected to severe hydrothermal alteration. The $^{40}Ar/^{39}Ar$ ages we obtained from the oldest available sectors of the active volcanoes range from 65 to 330 ka. The oldest lava sampled is slightly more than half as old as the 600 ka datum we determined for Costa Rica.

[40] Our interpretation of the data is that the active volcanoes of Nicaragua are part of the volcanic pulse, described above for Costa Rica, that began at 600 ka and whose base commonly outcrops and has been repeatedly sampled along the volcanic front of Costa Rica. The immediately preceding peak in volcanic activity in Costa Rica is the Monteverde volcanic front at 2.2 to 1.0 Ma. Two Nicaraguan samples, located 10 to 15 km NE of the current volcanic axis, are time equivalent to the Monteverde VF. Because of these similarities in ages, we interpret the Nicaraguan volcanic history to be the same as Costa Rica's over the last two Ma; specifically, a peak between 2.2 to 1.0 Ma and an ongoing pulse that began at 600 ka.

[41] Because the bases of the active Nicaraguan volcanoes are covered by sediments, we cannot locate and sample the contact with older volcanics that would provide both age control and volume control. We can calculate reasonably precise volume measurements of

the active volcanoes, using the surrounding plain as the base level. We estimate an extrusive volcanic flux based on these volumes and the age of the oldest Nicaraguan lava sampled to date, 330 ka. This approach gives extrusive volume fluxes (in units of km^3/km/Ma) for western Nicaragua (4.7) and eastern Nicaragua (6.9) that bracket the volume flux for the Cordillera de Guanacaste (5.3) and are slightly less than the flux for the Cordillera Central (8.5). We expect that further efforts in geochronology will discover lavas somewhat older than the oldest current sample but expect that the oldest lavas will not be recovered except by drilling. We estimate the error in age as half the difference between the 600 ka datum from Costa Rica and the age of our oldest current sample. This gives an error estimate of 40%. The resulting extrusive volcanic flux errors for the two Nicaraguan segments are larger than those of the Costa Rican segments, even though the errors in the Nicaraguan volumes are lower.

[42] We test the reasonableness of our extrusive volcanic flux rates for Nicaragua by assuming a 600 ka date for the beginning of current cone construction and adding volume to the cones based on the depth to the pre-volcanic surface, following the estimates of *van Wyk de Vries* [1993]. Two arguments indicate that the depth to the base of the current volcanoes is not great. The first is a drill hole at the geothermal development on Momotombo volcano that intersected a dacitic ash flow, thought to be the top to the Tertiary volcanics, at a depth of only 150 m below the present surface [*van Wyk de Vries*, 1993]. The second argument is the presence, within 15 km NE of the current volcanic front, of volcanic remnants whose ages are the same as the Monteverde volcanic front. Similarly, in the Nicaraguan Depression between San Cristóbal and Cosigüina volcanoes, there are low hills made of Tertiary volcanics, so that the depth of cover there is zero. Therefore, we agree with *van Wyk de Vries* [1993] that the sediments that obscure the bases of the active volcanoes do not appear to be very deep. We choose the drilling result at Momotombo volcano as the most reliable basis for estimating the depth to the bases of the volcanoes. We assume an interfingering relationship between the volcanic deposits and sediments, implying a roughly cylindrical shape. Volumes representing the time between 600 ka and the current topographic base of the volcano can be determined by multiplying the area within the outer boundary of each volcano by 150 meters, the depth determined by drilling at Momotombo. These assumptions add 176 km^3 to the volumes of western Nicaraguan volcanoes and 212 km^3 to the volumes of eastern Nicaraguan volcanoes. The resulting volume fluxes are 4.4 km^3/km/Ma for western Nicaragua and 6.4 for eastern Nicaragua, slightly reduced from our preferred estimates in Table 2 but clearly consistent with it. To achieve the same flux rate for both the 330 ka datum and the 600 ka datum, the depth to the pre-volcanic surface needs to be increased to only 180 m.

3.3 Does the extrusive volcanic flux vary along Nicaragua and Costa Rica?

[43] *Carr et al.* [1990] reported a paradoxical inverse correlation between degree of melting and volcano size in Central America. Degree of melting, inferred from rare earth element data, was high in Nicaragua but low in the Cordillera Central of Costa Rica. Surprisingly, the volumes of Nicaraguan volcanoes were small compared to the volumes of the Cordillera Central, which had huge estimated volumes. This paradox is solved by the recognition of a late Pliocene to early Quaternary volcanic front, the Monteverde VF.

Removing the older volcanics from the volumes of the Costa Rican volcanic centers substantially removes the disparity in size between the Nicaraguan and Costa Rican volcanic fronts. The Nicaraguan magmas still appear to have formed from a higher degree of melting than the Costa Rican magmas but that difference may involve regional differences in the geochemistry of the source of the magmas, specifically the general agreement now that the source in the Cordillera Central of Costa Rica is more enriched [e.g. *Malavassi*, 1991, *Herrstrom et al.*, 1995, *Feigenson et al.*, 2004].

[44] Although new geochronologic and geologic data have reduced the extrusive volcanic flux estimate for the Cordillera Central of Costa Rica, it remains larger than the flux estimates for the two Nicaraguan segments and the Cordillera de Guanacaste (Table 2 and Figure 8). However, the errors estimated for the calculation of extrusive volcanic flux are large enough to explain the remaining disparity. Thus, the extrusive volcanic flux is considered constant along the volcanic front of Nicaragua and Costa Rica.

3.4 Average compositions of volcanic centers and groups

[45] We selected the most complete and accurate geochemical data from each volcano in Nicaragua and Costa Rica. Many studies have shown that distinct magma types are sometimes present within the same volcanic center in Central America, even erupting from the same vent [e.g. *Ui,* 1972; *Walker*, 1984; *Alvarado and Carr*, 1993; *Patino et al.*, 2000; *Carr et al.*, 2003; *Alvarado et al.*, 2006]. Furthermore, there are large differences in the sizes of volcanic centers (Table 2). Therefore, we decided to base our geochemical averages on individual volcanic centers and individual magma groups within a volcanic center. To calculate a flux for each center we made averages for each magma group at the center and then estimated the percentage of the total volume each group represented (Table 2). In most cases there was just one magma group. *Patino et al.* [2000] and *Plank et al.* [2002] took a simpler route and used average values for entire segments of the volcanic front.

3.5 Models of mantle sources

[46] The total flux of an incompatible element at an arc volcano consists of a mantle contribution and a subducted contribution. Separating these two is not straightforward. *Patino et al.* [2000] created mantle estimates by inverting the EMORB values of *Sun and McDonough* [1989] and then made models of mantle contribution by using batch melting and degrees of melting between 10 and 20%. *Plank et al.* [2002] used the NMORB of Sun and McDonough [1989] divided by 3 as the mantle source. We derive mantle models similar to the DM and OIB of *Eiler et al.* [2005] but based on different lava samples (Figure 9). *Eiler et al.* derived an OIB source by assuming that a Turrialba lava with minimal evidence of slab contribution was derived via a 5% batch melt of OIB. We examine a slightly expanded set of elements, so we repeated that procedure using a similar lava (CR-IZ-D5) but the same mantle mineral mode (51.6% olivine, 28.7% orthopyroxene, 16% clinopyroxene and 3.7% spinel) and the same partition coefficient table with some additions. Partition coefficients for missing REEs were interpolated from adjacent REEs. Rb partition coefficients were assumed equal to K, Cs equal to K/2, P equal to Sr and Ta

equal to Nb. The DM of *Eiler et al.* has a high K_2O concentration and very low Ba (Figure 9). We derive a somewhat more enriched DM source from an alkaline basalt from Utila island off the north coast of Honduras. Utila and Yojoa are alkaline volcanoes in Honduras that erupted along faults generated by the Caribbean-North America plate boundary (Figure 1). They represent the cleanest window into the unmodified Central American mantle. There are small Ba and Pb enrichments at Yojoa, consistent with O-isotope data indicating a minor slab contribution [*Eiler et al.*, 2005]. Therefore, we chose Utila (Hon-UT-1) as the basis for the DM source. Employing the same mantle mode and partition coefficients used to derive the OIB source, we obtain a DM source by assuming the Utila lava was the result of 0.5% batch melt of DM. Because Hon-UT-1 lacks values for Nb, Ta and Pr, we estimated values by interpolation from adjacent elements on the spider diagram. The DM source, derived from Utila, has about 10 times the Ba concentration as the DM source of *Eiler et al*. [2005] (Figure 9). This seemingly radical difference has minimal effect on the subduction-derived Ba flux because the mantle contribution to Ba in Nicaragua, where this source is primarily used, is only 2 to 4% of the total. Using the lower Ba value from *Eiler et al.* [2005] would make the mantle contribution much smaller but only slightly increase the already large subduction-derived contribution.

3.6 Estimating Mantle Contributions

[47] Although most of the samples used to determine average values were mafic, the resulting averages vary in SiO_2 and MgO content. To minimize any bias this variation would introduce, we made a fractionation correction prior to estimating a mantle contribution. Least squares fractional crystallization modeling of representative lava suites showed that a change of 1 wt % SiO_2 required 5% crystallization. We picked the least silicic average composition in each segment as the reference for that region and adjusted the other averages to it based on the difference in SiO_2 contents. *Eiler et al.* [2005] made a similar correction but instead diluted with olivine to make MgO equal to 6.0 wt. % .

[48] The mantle contribution to the total incompatible element flux in Central America can be estimated from mixtures of the two mantle sources subjected to appropriate degrees of melting. For seven of the magma groups in Nicaragua and Costa Rica we had an initial model, the source percentages and degrees of melting determined by *Eiler et al.* [2005]. With these models as starting points, we varied the proportions of the two mantle sources and the degrees of melting to fit the HREEs and the lowest elements on the spider diagrams, usually Nb and Ta. Some examples of modeled mantle contributions are shown in Figures 10 and 11. For most groups, the modeling was simple and the fits very good. Table 4 lists the mantle source assumptions and the best fitting extents of melting for each group. The modeling also assumed the partition coefficients and mantle mode of *Eiler et al.* [2005] and batch melting. Table 4 also lists the mantle sources and extents of melting derived by *Eiler et al.* [2005].

[49] Many of the magma groups listed in Tables 2 and 4 have very similar patterns on spider diagrams and effectively define clusters. In Nicaragua, the groups modeled with a pure DM source have nearly identical trace element patterns with the exception of Masaya, Granada and the Telica group with high Ba/Th. The peak in the regional Ba/La variation

occurs in the western Nicaragua cluster (Figure 10a), which consists of seven groups that differ primarily in extent of melting, with a range from 10 to 25%. The mantle contribution model appropriate for the Cerro Negro-Las Pilas group, a 20% melt of DM, is included in Figure 10a. The spider diagram and the fitted mantle contribution model for Masaya (Figure 10c) suggests a lower extent of pure DM melting but this is likely an artifact. Masaya has a well-defined pattern of open-system magma evolution with at least two distinct inputs [*Walker et al.*, 1993]. The increase in incompatible element contents at constant SiO_2 content caused by open system fractionation makes the HREE contents higher and our simple model sees that as a lower extent of melting. The Telica group with high Ba/Th cannot be closely fit using any combination of the two current mantle models. This misfit and similar problems for three of the HFSE-rich groups (discussed below) indicate that the OIB mantle may not be an appropriate enriched mantle source for western Nicaragua. The Granada HFSE-rich group has a notable lack of Nb and Ta depletion, no enrichment in K or Rb and moderate enrichments in Cs, Ba, U, Pb and Sr. The baseline is reasonably well fit as a 15 % melt of DM.

[50] The groups that required an OIB component in the mantle source are shown in Figure 11. The groups with the poorest fits are the HFSE-rich groups from Telica, Las Pilas and Nejapa (Figure 11a). These groups differ from Granada by having enrichments in K and Rb. They differ from the other western Nicaragua groups by lacking Nb or Ta depletions and by having no suggestion of Zr or Ti depletions. The two Costa Rican clusters, Guanacaste and Cordillera Central are easily fit. This is not surprising given that the OIB source was derived from a lava from the Cordillera Central. The most plausible fit to the Concepcion and Maderas cluster (Figure 10b) has a mantle source derived equally from DM and OIB.

[51] The change in mantle source composition is not smooth along the volcanic front. The volcanic groups in Table 4 are ordered from NW to SE. In western Nicaragua the major source is DM but a more enriched source is likely always present but only revealed in low degree melts (HFSE-rich samples) that erupt before mixing into large magma chambers dominated by high degree melts. Proceeding southeast, the proportion of OIB source increases at Mombacho and then increases even more at Concepción and Maderas. The Guanacaste segment follows the large trenchward step in the volcanic front after Maderas and here the OIB component decreases. These results favor the complex intermingling of different sources in eastern Nicaragua and the Guanacaste proposed by *Reagan et al.* [1994] on the basis of U-series isotopes, rather that the abrupt transition at Tenorio volcano proposed by *Feigenson et al.* [2004] on the basis of Pb isotope variations.

[52] Our modeled mantle contributions primarily fit Nb and the HREEs, implicitly assuming that Nb, Ta and the heavy REEs are derived almost entirely from the mantle. For this assumption to hold, the fluids metasomatizing the mantle should have low Nb contents or La/Nb of about 20. The high $\delta^{18}O$ slab phase of *Eiler et al.* [2005] has these characteristics but the low $\delta^{18}O$ slab phase has too much Nb. Most of the samples with low $\delta^{18}O$ are from Nicaragua and several of these are HFSE-rich lavas. These were not treated as a separate group and including them with the other Nicaraguan samples may have biased

the calculated Nb for the low $\delta^{18}O$ phase. Furthermore, the Nb values available at that time were two to three times higher than our new data based on re-powdering the rocks.

3.6 Flux of subducted components from the volcanic front

[53] The contribution from the subducted slab is the difference between the modeled mantle contribution and the mean analysis (examples are shown in Figures 10 and 11 and the calculations are available as supplementary material). These differences were then adjusted for fractionation in a procedure that was the reverse of the fractionation correction described above. In this case, the mean SiO_2 that was adjusted to was not the mean for the relatively few analyses with high quality trace element data but the mean for the entire available major element suite, which is more representative of the volcano's actual composition. These concentration data were then multiplied by the mass flux, the last column of Table 2. The resulting subduction-derived element flux values are in the top section of Table 5.

[54] The error involved in calculating a subduction-derived element concentration require propagating errors from a large number of assumptions that are not easily quantified. Instead, we estimate percentage errors in concentration from the sensitivity of the subduction-derived element flux to assumptions about the mantle contribution. Our preferred subducted element fluxes, based on the *Eiler et al* [2005] approach, are the top section of Table 5. We estimate maximum subduction-derived fluxes as the total fluxes (second section of Table 5). We define a first estimate of concentration error as one half of the difference between our maximum flux and our preferred flux. We estimate a minimum subduction-derived flux by assuming that a line through the Th and Zr values on a spider diagram defines the mantle contribution. The values for the mantle component obtained this way are analogous to the Eu* parameter often used to define Europium enrichment or depletion on a REE plot. We did not extrapolate beyond Ba. We define a second estimate of concentration error as the differences between our preferred flux and the flux estimated relative to the Th-Zr line. We take the largest of the two concentration errors as the error that we propagate with the mass error to obtain a flux error.

[55] The concentration errors in Table 5 are large for the Cordillera Central, where the source is thought to be a variety of OIB. The large size of these errors is partly real because we do not have good control on the actual mantle contribution and the incompatible element concentrations are quite high. However, some of the error may be caused by the awkwardness of the sensitivity approach. We consider the subduction-derived element concentrations for the Cordillera Central poorly determined. Outside of the Cordillera Central, the concentration errors are small for the elements strongly enriched above the modeled mantle contribution (Cs, Rb, Ba, U, K, Pb). The errors for La, Th and, to a lesser extent, Sr are substantially larger.

[56] The errors in element flux, obtained by combining the mass flux errors (Table 2) and the largest of the two concentration errors, range from 24% to 155% of the totals for each element and each segment (bottom section of Table 5). These are generous errors because the inter-segment variations in subduction-derived flux are small for Cs, Ba, K and Pb and

Sr (top section of Table 5). In fact, the standard deviations of the inter-segment variations for these elements are less than 20% of the means, substantially less than the estimated flux errors.

[57] If the regional variation in subduction signal, e.g. Ba/La (Figure 2), is the result of variations in flux, then the fluxes of highly enriched elements (top section of Table 5) should decrease from the NW Nicaragua segment to the Cordillera Central segment. Furthermore, the decrease should be substantial because Ba/La decreases by a factor of 10 across this region. However, the Ba fluxes do not decrease across the region and, in fact, do not significantly change. Other highly enriched elements, whose fluxes show no regional variation, include Cs, K, Pb and Sr. What does change is the flux of Th and La, which increases from NW to SE. The range in La flux variation in Table 5 is roughly a factor of 5, similar to the range for Ba/La. However, the large errors estimated for the La and Th concentrations make us doubt that the regional variation in these modestly enriched elements is real. For these elements, a small decrease in extent of melting raises the mantle concentration and substantially reduces the subducted concentration. Alternatively, the southeastward increases in Th and La are real and reflect changes in the subduction component caused by additions of Galapagos derived volcanics that are highly enriched in incompatible elements. These inputs could be from seamounts or volcaniclastic sediments on the subducting slab or from subduction erosion of the Costa Rican forearc [Goss and Kay, 2006].

4.0 Discussion

Magmatic flux versus extrusive volcanic flux

[58] The extrusive volcanic flux estimates for Central America (Table 2) are considerably lower than mass fluxes reported at many other convergent margin settings. The range of extrusive volcanic flux observed in Central America, about 5 to 9 km^3/km/Ma, is about a factor of 10 less than the means of various fluxes estimated for continental arcs and oceanic arcs, compiled by *White et al.* [2006]. However, most of these much higher flux estimates are total magmatic fluxes, which include large assumptions about the extent of buried intrusives and dispersed volcanic sediments and ash. Future work that would expand and improve the top-down approach taken here includes geomorphology to measure rates of erosion, volcanology for rates of distal ash deposition, and petrology to infer the mass of cumulates required to make the basaltic andesites and andesites most common at the volcanoes. Geophysics and structural geology may allow measurements of intrusive masses or better volume estimates for buried volcanic material along the active volcanic front in Nicaragua.

[59] A bottom-up or long-term approach, applied to the Aleutian arc, yields an astonishingly high time-averaged magma production rate of 110-205 km^3/km/Ma. [*Jicha et al.*, 2006] or a slightly lower rate of 82 km^3/km/Ma [*Holbrook et al.*, 1999]. *Clift and Vannucchi* [2004] estimated rates of magmatic productivity for arcs worldwide using rates of crustal growth derived from seismic refraction profiles of oceanic arcs such as the

Aleutians. They estimate a global magmatic arc productivity rate of 90 km^3/km/Ma, just enough to replenish the crust that they calculate is lost via subduction erosion. Their rate for Costa Rica, derived by adjusting the global rate to account for differences in the rates of plate convergence, is 108 km^3/km/Ma, about 12 times the rate we measured.

Subduction derived flux of highly enriched elements

[60] Our primary result is that the fluxes of Cs, Ba, K, Pb, and Sr are not significantly different along the Central American volcanic front from Nicaragua to Costa Rica. This constant flux is easy to reconcile with the similar rates of plate convergence and sediment thickness along the Middle America Trench. If the regional variation in slab signal (e.g. Ba/La in Figure 2) was caused by variations in flux, then the fluxes of Cs, Ba, K, Pb and Sr would be substantially greater for Nicaragua than for Costa Rica. This is not the case and the range of error is small compared to the large variation along the margin. Alternatively, the fluxes of denominators in the slab signal ratios, La and Th, would be substantially smaller for Nicaragua than for Costa Rica. This is consistent with our estimates but the concentrations errors for La and Th are substantially larger and much more model dependent. The uncertainty in the Th and La fluxes could be substantially reduced by expanding our work to the northwestern half of the margin into El Salvador and Guatemala. The main difficulty with Th and La fluxes arises at the Cordillera Central segment in Costa Rica, where an OIB-rich source component, either in the mantle [*Feigenson et al.,* 2004] of from subduction [*Goss and Kay,* 2006], greatly complicates the problem of determining elemental fluxes. Present isotopic and trace element evidence shows that this complication is not present across El Salvador and into southeast Guatemala [*Carr et al*., 2003].

[61] The chemical stratigraphy of the Cocos Plate sediments features an uppermost 100 meters of hemipelagic sediment that contains modest amounts of Ba but nearly all of the inventory of ^{10}Be and U [*Morris et al.,* 2002; *Patino et al.,* 2000]. The Ba flux will be modestly affected by sequestering part of the section but the ^{10}Be/^{9}Be signal will be greatly reduced. Therefore, the regional variations in ^{10}Be/^{9}Be might be explained by differential subduction of the uppermost hemipelagic sediments. Subduction of the entire hemipelagic section offshore of Nicaragua and sequestering of the ^{10}Be-rich uppermost sediments offshore of Costa Rica are what is required. This possibility is well within the errors in our flux estimates.

[62] Several weaknesses qualify our conclusion that the subduction derived flux of highly fluid mobile elements is roughly constant along the margin. The first is the lack of any estimate of three prominent outputs from the volcanic front; the dispersed ashes, the eroded volcanics, making their way to the Caribbean and the Pacific, and the masses of intrusives. However, it is unlikely that differences in these unmeasured parameters would be just the right size to greatly increase the flux in Nicaragua over Costa Rica. A second weakness is the appropriateness, or lack thereof, of the time frame we chose. We calculate the extrusive volcanic flux of the current generation of volcanoes. This approach includes an assumption that there are different generations of volcanics, that volcanic activity is episodic. This episodicity is the clear impression from field geology and it is the conclusion reached by

detailed studies of Costa Rican geochronology and geology [*Alvarado, et al.*, 1992; *Gillot et al.,* 1994; *Gans et al.*, 2003]. The larger problem is to measure the volcanic output over several volcanic pulses and calculate maximum, minimum and long-term rates. *Goss and Kay* [2006] estimated a long-term flux (over a 6 Ma period) for Pb and Th using the magmatic productivity rate of *Clift and Vannoucchi* [2004]. Their fluxes are far higher than the ones we estimate because the magmatic productivity rate they start from is 15 times the volcanic flux we start from. The contrast between these two approaches makes clear that much work remains to be done.

[63] The largest geochemical problem is the appropriateness, or lack thereof, of the mantle-derived component of total flux. The work of *Eiler et al.* [2005] provides an appropriate way forward and we suggest several improvements. The enriched component may be more variable than the OIB estimated from Cordillera Central lavas. Away from Costa Rica, fits using this component were generally poor. The best places to seek a better enriched component are the Granada and Nejapa volcanic lineaments in central Nicaragua. Volcanics from the back-arc region of Nicaragua should be reinvestigated. The alkaline cones near Pearl Lagoon on Nicaragua's Caribbean coast are the best candidates for finding a clear window into the mantle beneath Nicaragua.

[64] We implicitly assumed that all elements are coursing through the system at the same rate and storage within the mantle wedge is not a factor. U-Series isotopes clearly show types of disequilibrium that suggest storage of some elements in the mantle wedge [*Regan et al.*, 1994; *Thomas et al*., 2002].

[65] We provide no constraint on the flux of water and so it may well vary along the lines proposed by *Ruepke et al.* [2002], *Ranero et al.* [2003] and *Patino et al.* [2000] and *Abers et al.* [2003]. However, *Sadofsky et al*. [2005] presented melt inclusion results that argue strongly for no change in the flux of water along the Central American margin.

[66] A variety of regional geochemical variations have been identified in Central America, including iodine isotopes [*Snyder and Fehn,* 2002], Li isotopes [*Chan et al.*, 1999], chalcophile elements [*Noll et al.*, 1996], B/Be [*Leeman et al.*, 1994]. Most explanations of the regional geochemical variation in Central America have employed a variant of the model that couples slab signal and degree of melting. These models were free to also assert that there was a higher flux in Nicaragua than in Costa Rica. Future models should incorporate a constant regional flux of Cs, Ba, K, Pb and Sr.

[67] The lack of regional gradients in the best defined subduction-derived element fluxes strongly suggests that the cause of the pronounced regional gradients in subduction signals lies either in changes in mantle composition or physical changes such as the dip of the subducted slab or the physical or thermal structure of the upper plate.

5.0 Conclusions

[68] New geochronologic and geological data make a strong case for a 600 ka age for the beginning of the current volcanic front in Costa Rica. The primary change at that time was

a near cessation of volcanic activity in the gap between the Cordillera de Guanacaste and the Cordillera Central. A basal age of 330 ka is proposed for the two volcanic segments in Nicaragua. This datum is less well established than the basal age for the two volcanic segments in Costa Rica.

[69] The flux of extrusive volcanics along Nicaragua and Costa Rica varies between 1.3 and 2.4 x 10^{10} kg/m/Ma. These extrusive fluxes are about a factor of 10 lower than flux estimates published for other convergent margins, but most of these are total magmatic fluxes which are expected to be higher.

[70] Uncertainty over the trace element characteristics of the mantle beneath Central America make the calculated subduction-derived component of flux unreliable for elements that are only slightly or moderately enriched, such as Th and La. However, for Ba and other elements with very large enrichments over plausible unmodified mantle compositions, the uncertainly about the actual mantle composition becomes a relatively small factor in calculating the element flux.

[71] The subduction component of the fluxes of Cs, Ba, K, Pb, and Sr are not significantly different along the Central American volcanic front from Nicaragua to Costa Rica.

6.0 Acknowledgements

[72] We thank our many friends in Central America who made this work possible. C.T Herzberg and E. Gazel provided helpful criticism. Constructive reviews by Mark Reagan, Seth Sadofsky and an anonymous reviewer are sincerely appreciated. This work was supported in part through NSF grants EAR9628251, EAR9905167 and EAR0203388.

7.0 References

Abers, G.A., T. Plank, B.A. Hacker (2003), The wet Nicaraguan slab, *Geophys. Resch. Lett. 30*, 1098, doi: 10.1029/2002GL015649

Alvarado, G.E. and M.J. Carr (1993), The Platanar-Aguas Zarcas volcanic centers, Costa Rica: Spatial-temporal association of Quaternary calc-alkaline and alkaline volcanism, *Bull. Volcanol. 55,* 443-453.

Alvarado, G.E., Carr, M.J., Turrin, Brent D., Swisher, C.C., Schmincke, H.-U., and Hudnut, K.W., (2006), Recent volcanic history of Irazú volcano, Costa Rica: Alternation and mixing of two magma batches, and pervasive mixing, *in* Rose, W.I., Bluth, G.J.S., Carr, M.J., Ewert, J., Patino, L.C., and Vallance, J., Volcanic hazards in Central America: Geological Society of America Special Paper 412, p. 259–276, doi: 10.1130/2006.2412(14).

Alvarado, G.E., S. Kussmaul, S.Chiesa, P.-Y. Gillot, H. Appel, G. Wörner and C. Rundle (1992), Resumen cronostratigráfico de las rocas ígneas de Costa Rica basado en dataciones radiométricas, *J. South American Earth Sciences 6*, 151-168.

Bolge, L.L. (2005), *Constraining the magmatic sources of Hawaiian and Central American volcanics.* Ph.D. Thesis, Rutgers University. 280pp.

Bolge, L L., Carr, M.J, Feigenson, M.D., and Alvarado, G.A., (2006) Geochemical stratigraphy and magmatic evolution at Arenal Volcano, Costa Rica. J. Volc. Geotherm. Res. V. 157, Pp. 34-48, doi:10.1016/j.jvolgeores.2006.03.036

Carr, M.J., M.D. Feigenson, and E.A. Bennett (1990), Incompatible element and isotopic evidence for tectonic control of source mixing and melt extraction along the Central American arc, *Contrib. Mineral. Petrol 105*, 369-380.

Carr, M.J., Feigenson, M.D., Patino, L.C. and J.A. Walker (2003), Volcanism and Geochemistry in Central America: Progress and Problems, in *Inside the Subduction Factory,* AGU Geophysical Monograph 138, Edited by Eiler, J. and G. Abers, pp. 153-179.

Carr, M.J., and W.I. Rose Jr. (1987), CENTAM-a data base of analyses of Central American volcanic rocks, *J. Volc. Geotherm. Res.*, *33*, 239-240.

Chan, L. H., W. P. Leeman and C.-F. You (1999), Lithium isotope composition of Central American volcanic arc lavas: implications for modifications of subarc mantle by slab-derived fluids, *Chemical Geology, 160*, 255-280.

Clift, P., and P. Vannucchi (2004), Controls on tectonic accretion versus erosion in subduction zones: Implications for the origin and recycling of the continental crust, *Rev. Geophys., 42*, RG2001, doi:10.1029/2003RG000127

Deino, A., L. Tauxe, M. Monaghan and A. Hill (2002), $^{40}Ar/^{39}Ar$ geochronology and paleomagnetic stratigraphy of the Lukeino and lower Chemeron Formations at Tabarin and Kapcheberek, Tugen Hills, Kenya, *Journal of Human Evolution, 42*, 117-140.

Ehrenborg, J. (1996), A new stratigraphy for the Tertiary volcanic rocks of the Nicaraguan highland, *Geol. Soc. Am. Bull. 108*, 830-842.

Eiler J.M., M.J. Carr, M. Reagan, E. Stolper (2005), Oxygen isotope constraints on the sources of Central American arc lavas, *Geochem. Geophys. Geosyst. [G^3], 6 (7)*, 28 pp.

Elliott, T., T. Plank, A. Zindler, W. White, and B. Bourdon, B., (1997), Element transport from subducted slab to volcanic front at the Mariana arc, *Journal of Geophysical Research 102*, 14991–15019.

Feigenson, M.D. and M.J. Carr (1993). The source of Central American lavas: inferences from geochemical inverse modeling, *Contrib. Mineral. Petrol., 113*, 226-235.

Feigenson, M.D., M.J. Carr, S.V. Maharaj, L.L. Bolge and S. Juliano (2004), Lead Isotope Composition of Central American Volcanoes: Influence of the Galapagos Plume, *Geochem. Geophys. Geosyst. [G³], 5* (6), 14pp.

Fleck, R.J., J.F. Sutter and D.H. Elliot (1977), Interpretation of discordant $^{40}Ar/^{39}Ar$ age-spectra of Mesozoic tholeiites from Antarctica, *Geochim. Cosmochim. Acta, 41*, 15-32.

Gans, P.B., G. Alvarado-Induni, W. Peréz, I. MacMillan and A. Calvert (2003), Neogene evolution of the Costa Rican Arc and development of the Cordillera Central. *Geol. Soc. America, Cordilleran Section, 99th annual meeting, Abstracts with Programs (April 1-3, Puerto Vallarta), 35:4,* 74.

Gans, P.B., I. MacMillan, G. Alvarado-Induni, W. Pérez and C. Sigarán (2002), Neogene evolution of the Costa Rican arc. *Geol. Soc. America 2002 Annual meeting, Abstracts with Programs (Oct. 27-30, Denver), 34 (6),* 513.

Gill, J.B., 1981, Orogenic Andesites and Plate Tectonics: Berlin, Springer-Verlag, 390 p.

Gillot, P.Y., S. Chiesa, G.E. Alvarado (1994), Chronostratigraphy of upper Miocene-Quaternary volcanism in northern Costa Rica, *Rev. Geol. Am. Cent., 17*, 45–53.

Goss, A. R. and S. M. Kay (2006), Steep REE patterns and enriched Pb isotopes in southern Central American arc magmas: Evidence for forearc subduction erosion? *Geochem. Geophys. Geosyst. [G³], 7* (5), Q05016, doi:10.1029/2005GC001163

Herrstrom, E. A., M. K. Reagan, and J. D. Morris (1995), Variations in lava composition associated-with flow of asthenosphere beneath southern Central America, *Geology 23*, 617-620.

Herzberg, C.T., W.S. Fyfe and M.J. Carr (1983), Density constraints on the formation of the continental Moho and crust. *Contrib. Mineral. Petrol.*, 54:1-5.

Holbrook, W. S., Lizarralde, D., McGeary, S., Bangs, N., Diebold, J., (1999) Structure and composition of the Aleutian island arc and implications for continental crustal growth, *Geology*, 27, 31-34.

Jicha, B.J., Scholl, D.W.,Singer, B.S., Yogodzinski, G.M. and Kay, S.M.,(2006),Revised age of Aleutian Island Arc formation implies high rate of magma production,*Geology*, 34-8, 661-664; DOI: 10.1130/G22433.1

Kelemen, P. B., K. Hanghoj and A.R. Greene (2003), One view of the geochemistry of subduction-related magmatic arcs, with an emphasis on primitive andesite and lower crust, in *The Crust, Vol. 3,* Edited by Rudnick, R. L. in *Treatise on Geochemistry,* Edited by Holland, H. D. and K.K. Turekian, Oxford: Elsevier– Pergamon, pp. 593–659.

Krushensky, R.D. (1972), Geology of Irazú Quadrangle, *U.S.G.S. Bulletin 1353*, 46 p.

Ledbetter, M.T. (1985), Tephrochronology of marine tephra adjacent to Central America, *Geol. Soc. America Bull. 96*, 77-82.

Leeman, W.P., Carr, M.J. and Morris, J.D., (1994), Boron geochemistry of the Central American arc: Constraints on the genesis of subduction-related magmas. *Geochim. Cosmochim. Acta 58,* 149-168.

Malavassi, E. (1991), *Magma sources and crustal processes at the southern terminus of the Central American volcanic front*. PhD. Thesis, 435pp., Univ. Calif. Santa Cruz.

Morris, J. D., W. P. Leeman and F. Tera,(1990), *The subducted component in island arc lavas; constraints from B-Be isotopes and Be systematics*, *Nature, 344 (6261)*, 31-36.

Morris, J., R. Valentine and T. Harrison, (2002), ^{10}Be imaging of sediment accretion and subduction along the northeast Japan and Costa Rica convergent margins, *Geology, 30-1*, 59–62.

Noll, P.D., H.E. Newsom, W.P. Leeman and J.G. Ryan (1996), The role of hydrothermal fluids in the production of subduction zone magmas: Evidence from siderophile and chalcophile trace elements and boron. *Geochim. Cosmochim. Acta 60*, 587-612.

Patino, L.C., M.J. Carr and M.D. Feigenson (2000), Local and regional variations in Central American arc lavas controlled by variations in subducted sediment input, *Contrib. Mineral. Petrol. 138,* 265-283.

Pérez, W., G.E. Alvarado and P.B. Gans (2006), The 322 ka Tiribí Tuff: stratigraphy, geochronology and mechanisms of deposition of the largest and most recent ignimbrite in the Valle Central, Costa Rica, *Bull. Volcanol.* DOI: 10.1007/s00445-006-0053-x

Plank, T. and C.H. Langmuir (1988), An evaluation of the global variations in the major element chemistry of arc basalts, *Earth Planet. Sci. Lett. 90*, 349-370.

Plank, T. and C.H. Langmuir (1993), Tracing trace elements from sediment input to volcanic output at subduction zones, *Nature, 362*,.739-743.

Plank, T., V. Balzer and M.J. Carr (2002), Nicaraguan volcanoes record paleoceanographic changes accompanying closure of the Panama Gateway, *Geology 30*, 1087-1090.

Ranero, C and R. von Huene (2000) Subduction erosion along the Middle America convergent margin, *Nature 404*, 748-752.

Ranero, C.R., J. Phipps Morgan, K. McIntosh and C. Reichert (2003), Bending-related faulting and mantle serpentinization at the Middle America trench, *Nature 425*, 367-373.

Reagan, M.K. and J.B. Gill (1989), Coexisting calcalkaline and high-niobium basalts from Turrialba Volcano, Costa Rica; implications for residual titanates in arc magma sources. *J. Geohys. Res. B 94:4*, 4619-4633.

Reagan, M.K., J.D. Morris, E.A. Herrstrom and M.T. Murrell (1994), Uranium series and beryllium isotope evidence for an extended history of subduction modification of the mantle below Nicaragua, *Geochim. Cosmochim. Acta 58*, 4199-4212.

Reilly, Jr. M. J. (2005), A revised perspective on trace element and rare earth element geochemistry of the Central American volcanic front. MS thesis Rutgers University, 40 pp.

Renne, P.R., C.C. Swisher, A.L. Deino, D.B. Karner, T.L.Owens and D.J. DePaolo (1998) Intercalibration of standards, absolute ages and uncertainties in $^{40}Ar/^{39}Ar$ dating, *Chemical Geology 145*, 117-152.

Ruepke, L.H., J. Phipps Morgan, M. Hort, and J.A.D. Connolly (2002), Are the regional variations in Central American arc lavas due to differing basaltic versus peridotitic slab sources of fluids? *Geology 30-11*, 1035-1038.

Sadofsky, S., K. Hoernle, P. van den Bogaard (2005), Volatile cycling through the Central American volcanic arc from melt inclusion studies of Nicaraguan and Costa Rican magmas, *Abstracts of the 15th annual V. M. Goldschmidt conference, Geochim. Cosmochim. Acta, 69-10-Suppl.*, 663.

Snyder, G.T. and U. Fehn (2002), Origin of iodine in volcanic fluids; ^{129}I results from the Central American volcanic arc, *Geochim. Cosmochim. Acta 66-21*, 3827-3838.

Stoiber, R.E., and M.J. Carr (1973), Quaternary volcanic and tectonic segmentation of Central America, *Bull. Volc., 37*, 304-325.

Stolper, E. and S. Newman (1994), The role of water in the petrogenesis of Mariana Trough magmas, *Earth Planet. Sci. Lett. 121,* 293-325.

Sun S., and W. F. McDonough, (1989), Chemical and isotopic systematics of oceanic basalts: implications for mantle composition and processes, in *Magmatism in the Ocean Basins* edited by A. D. Saunders and M. J. Norry, *Geological Soc. Special Publ., 42*, 313-345.

Thomas, R. B., M. M. Hirschmann, H. Cheng, M. K. Reagan, R. L. Edwards (2002), $^{231}Pa/^{235}U$-$^{230}Th/^{238}U$ of young mafic volcanic rocks from Nicaragua and Costa Rica and the influence of flux melting on U-series systematics of arc lavas, *Geochimica et Cosmochimica Act*a, 66 (24), 4287-4309.

Tournon, J. and G.E. Alvarado (1997), Carte géologique du Costa Rica: notice explicative; Mapa geológico de Costa Rica: folleto explicativo, échelle-escala 1:500,000. -Ed. Tecnológica de Costa Rica, 80 pp. + Mapa geológico de Costa Rica.

Turrin, B.D., J.M. Donnelly-Nolan, B.C. Hearn Jr. (1994), $^{40}Ar/^{39}Ar$ ages from the rhyolite of Alder Creek, California; age of the Cobb Mountain normal-polarity subchron revisited, *Geology, 22-3*, 251-254.

Ui, T., (1972), Recent volcanism in the Masaya-Granada area, Nicaragua, *Bull. Volcanol. 36*, 174-190.

Vannucchi, P., D.W. Scholl, M. Meschede, and K. McDougall-Reid (2001), Tectonic erosion and consequent collapse of the Pacific margin of Costa Rica; combined implications from ODP Leg 170, seismic offshore data, and regional geology of the Nicoya Peninsula, *Tectonics, 20-5*, 649-668.

van Wyk de Vries, B. (1993), *Tectonics and magma evolution of Nicaraguan volcanic systems*, Ph.D. Thesis, 328pp., Open University, Milton Keynes, UK.

Villegas, A. (2004), La Formación Alto Palomo: flujos pumíticos de le Cordillera Volcánica Central, Costa Rica, *Rev. Geol. Amér. Central 30*: 73-81.

Vogel, T.A., L.C. Patino, G.E. Alvarado and P.B Gans (2004), Silicic ignimbrites within the Costa Rican volcanic front: evidence for the formation of continental crust, *Earth and Planet. Sci. Lett. 226,* 149-159.

von Huene, R., C. R. Ranero, W. Weinrebe and K. Hinz, (2000), Quaternary convergent margin tectonics of Costa Rica: Segmentation of the Cocos Plate, and Central American volcanism, *Tectonics, 19*, 314-334.

von Huene, R. and D. W. Scholl (1991), Observations at convergent margins concerning sediment subduction, subduction erosion, and the growth of continental crust, *Reviews of Geophysics 29*, 279–316.

Walker, J.A. (1984), Volcanic rocks from the Nejapa and Granada cinder cone alignments, Nicaragua, *J. Petrol., 25*, 299-342.

Walker, J.A., Williams, S.N., Kalamarides, R.I., and Feigenson, M.D., (1993), Shallow open-system evolution of basaltic magma beneath a subduction zone volcano: the Masaya Caldera Complex, Nicaragua: . *J.Volcanol.Geotherm. Research*, 56, 379-400.

White, S.M., Crisp, J.A. and F. J. Spera 2006. Long-term volumetric eruption rates and magma budgets. *Geochem. Geophys. Geosyst. [G^3], 7 (3)*, 20 pp.

York, D., (1969), Least squares fitting of a straight line with correlated errors, *Earth and Planet. Sci. Lett., 5*, 320-324.

Table 1. Age determinations for volcanic rocks from Nicaragua and Costa Rica. Preferred ages in bold.

Sample ID	Lat.	Lon.	material	Plateau Age (ka)	Total Fusion Age (ka)	Isochron Age (ka)	$^{40}Ar/^{36}Ar$ Intercept	MSWD	$\%^{39}Ar$ release on plateau	Note	Volcano
Nicaragua											
SJ-3	12.319	-85.985	matrix	No plateau	6800 ± 70	**7110 ± 60**	287 ± 5	3.0	88%		San Jacinto
LL-4	12.385	-85.874	matrix	**9480 ± 30**	8740 ± 50	9540 ± 70	281 ± 6	3.3	66%		Las Lajas
C-51	12.742	-87.249	matrix	**3500 ± 30**	3440 ± 40	3550 ± 50	294 ± 0.6	1.0	94%		unnamed
C-51	"	"	matrix	**3590 ± 30**	3550 ± 40	3640 ± 50	294 ± 0.8	1.0	98%		"
LN-6	12.680	-86.601	matrix	**1130 ± 50**	1060 ± 40	1560 ± 150	286 ± 3	1.0	80%		"
LN-7	12.684	-86.609	matrix	**1480 ± 20**	1470 ± 40	1480 ± 60	295 ± 1.9	2.0	97%		"
NIC- SC-2000-1	12.602	-87.047	matrix	**160 ± 60**	320 ± 120	190 ± 70	299.3 ± 1.3	1.2	77%		San Cristóbal
NIC-TE-111	12.619	-86.887	matrix	**330 ± 20**	400 ± 30	300 ± 30	303 ± 3	1.3	76%		Telica
NIC-TE-114	12.618	-86.889	matrix	**172 ± 16**	170 ± 30	260 ± 70	292 ± 3	0.3	100%		"
NIC-TE-120	12.639	-86.766	matrix	**173 ± 11**	150 ± 20	215 ± 19	293.1 ± 1	0.5	100%		"
NIC-LP-106	12.514	-86.631	matrix	**65 ± 11**	150 ± 40	17 ± 6	301.9 ± 1.8	4.3	79%		Las Pilas
NIC-MT-2000-2	12.478	-86.607	matrix	**71 ± 9**	100 ± 15	20 ± 6	305 ± 3	4.9	57%		Momotombo
NIC-MT-2000-6	12.387	-86.525	matrix	**283 ± 12**	290 ± 20	290 ± 20	295 ± 2	0.6	100%		"
NIC-MT-2000-6	"	"	matrix	**280 ± 20**	280 ± 30	280 ± 30	295 ± 2	0.9	100%		"
NIC-M-10	11.485	-85.493	matrix	**76 ± 6**	87 ± 7	52 ± 16	301 ± 5	3.0	78%		Maderas
Costa Rica											
CR-RV-201	10.787	-85.259	matrix	**380 ± 20**	360 ± 40	290 ± 70	295.2 ± 1.4	1.3	99%		Rincón
CR-RV-04-12	10.769	85.278	matrix	**564 ± 5**	555 ± 7	557 ± 8	300 ± 4	1.4	76%		"
CR-RV-02-62	10.780	-85.421	matrix	**1138 ± 30**	1258 ± 60	1,238 ± 50	284 ± 5	1.7	76%		pre-Rincón
CR-RV-02-66	10.815	-85.416	matrix	**1611 ± 200**	1611 ± 600	906 ± 500	307 ± 13	0.3	98%		"
CR-RV-04-13	10.730	85.392	matrix	**2176 ± 19**	2144 ± 14	2179 ± 14	294.2 ± 1.3	2.5	91%		"
CR-MV-02-40	10.852	-85.148	matrix	**5654 ±30**	5356 ± 30	5537 ±170	320 ± 70	15.0	56%	2	pre-Miravalles
CR-MV-04-9	10.716	-85.175	matrix	**75 ± 4**	116 ± 4	68 ± 7	301.2 ± 1.5	2.7	66%		Miravalles
CR-MV-04-11	10.681	-85.145	matrix	**548 ± 11**	560 ± 20	580 ± 70	294 ± 70	3.5	88%		"
CR-TE-02-38	10.596	-85.049	matrix	1913 ± 20	1681 ± 60	**2174 ± 40**	221 ± 9	1.2	90%		pre-Tenorio
CR-TE-04-5	10.596	-85.029	matrix	**740 ± 30**	743 ± 18	740 ± 16	287 ± 4	2.7	75%		"
CR-TE-02-31	10.710	-84.980	matrix	**95 ± 8**	70 ± 20	124 ± 14	291.7 ± 1.3	1.5	75%		Tenorio
CR-TE-02-32	10.785	-84.955	matrix	372 ± 30	513 ± 80	**209 ± 40**	330 ± 10	0.2	94%	1	"

CR-TE-04-6	10.609	-85.039	matrix	**548 ± 6**	543 ± 8	550 ± 8	294 ± 2	1.3	94%		"
CR-TE-04-7	10.614	-85.043	matrix	**90 ± 4**	102 ± 6	81 ± 5	303 ± 3	1.1	90%		"
CR-TE-04-8a	10.623	-85.049	matrix	**266 ± 19**	280 ± 20	270 ± 30	309 ± 13	1.5	61%		"
CR-TE-04-8b	10.623	-85.049	matrix	**371 ± 12**	368 ± 16	390 ± 30	294 ± 3	0.5	100%		"
CR-PO-02-22	10.341	-84.446	matrix	**252 ± 30**	232 ± 100	312 ± 70	290 ± 6	0.4	100%		Platanar
CR-PP-02-26	10.280	-84.264	matrix	No plateau	2380 ± 170	440 ± 40	325.4 ±1.7	5.1		3	"
CR-PP-02-27	10.284	-84.263	wr	**554 ± 20**	705 ± 50	352 ± 40	315 ± 3	2.3	76%	1	"
CR-PO-02-28	10.363	-84.236	wr, plg	260 ± 18	302 ± 40	**201 ± 30**	301 ± 2	2.3	67%		Poás
CR-PO-02-29	10.351	-84.221	wr, plg	293 ± 18	383 ± 40	**201 ± 30**	305 ± 3	1.5	76%		"
CR-B-02-8	10.324	-84.167	matrix	238 ± 6	224 ± 11	**262 ± 10**	289.6 ± 1.7	0.3	74%		Barva
CR-B-02-9	10.320	-84.156	matrix	**201 ± 20**	201 ± 30	282 ± 50	286 ± 5	0.7	93%		"
CR-B-02-15	10.400	-84.081	matrix	**259 ± 9**	221 ± 50	272 ± 12	294.0 ± 0.7	1.5	95%		"
CR-B-02-16	10.408	-84.076	matrix	335 ± 7	386 ± 19	**246 ± 17**	321 ± 4	0.2	93%	1	"
CR-IZ-02-1	9.891	-83.855	matrix	8 ± 7	26 ± 15	**57 ± 13**	287 ± 2	1.3	50%		Irazú
CR-IZ-02-2	9.899	-83.835	matrix	**20 ± 12**	7 ± 19	9 ± 3	289 ± 3	0.8	54%		"
CR-IZ-02-5	9.884	-83.751	matrix	**598 ± 16**	584 ± 50	602 ± 20	293 ± 7	1.9	94%		"
CR-IZ-02-19	9.952	-83.929	biotite	**137 ± 5**	135 ± 10	147 ± 10	293 ± 2	1.1	99%		"
CR-IZ-02-20	9.987	-83.943	matrix	**544 ± 3**	516 ± 6	**573 ± 6**	269 ± 4	0.7	88%		"
CR-IZ-02-17	9.862	-83.795	biotite	**861 ± 6**	856 ± 8	872 ± 9	292 ± 3	1.2	100%		San Jeronimo
CR-IZ-02-17	"	"	"	**868 ± 9**	868 ± 10	843 ± 16	304 ± 8	1.1	98%		"
CR-IZ-02-17	"	"	plag	830 ± 8	819 ± 9	**853 ± 11**	284 ± 3	0.6	96%		"

Notes

1. Saddle Shaped spectra
2. Three step plateau, first two steps not used in isochron
3. No plateau, no reliable age, meets none of the reliability criteria

Table 2. Mass flux for Nicaragua and Costa Rica

Volcanic center (subgroup)	fraction of volume	Volume[1] km^3	Length km	Age Ma	Volume flux $km^3/km/Ma$	Mass Flux[2] $10^{10}kg/m/Ma$
Cosigüina	1.00	57	-	-	-	0.29
San Cristóbal	1.00	109	-	-	-	0.56
Telica (high U/La)	0.43	12	-	-	-	0.06
Telica (high Ba/Th)	0.43	12	-	-	-	0.06
Telica (HFSErich)	0.14	4	-	-	-	0.02
Rota	1.00	7	-	-	-	0.04
Las Pilas-Cerro Negro	0.82	23	-	-	-	0.12
Las Pilas (HFSErich)	0.18	5	-	-	-	0.03
Momotombo	1.00	17	-	-	-	0.09
Apoyeque	1.00	12	-	-	-	0.06
Western Nicaragua totals		259	166	0.33	4.7	1.32
error estimate in %		15	5	40	43	43
Nejapa	0.75	2	-	-	-	0.01
Nejapa (HFSErich)	0.25	1	-	-	-	0.00
Masaya-Las Sierras-Apoyo	1.00	203	-	-	-	1.04
Mombacho	0.95	34	-	-	-	0.17
Granada (HFSErich)	0.05	2	-	-	-	0.01
Zapatera	1.00	9	-	-	-	0.05
Concepción	1.00	31	-	-	-	0.16
Maderas	1.00	30	-	-	-	0.15
Eastern Nicaragua totals		312	137	0.33	6.9	1.59
error estimate in %		20	5	40	45	45
Orosí	1.00	76	-	-	-	0.39
Rincón de la Vieja	1.00	102	-	-	-	0.52
Miravalles	1.00	62	-	-	-	0.31
Tenorio	1.00	53	-	-	-	0.27
Guanacaste totals		293	92	0.60	5.3	1.49
error estimate in %		20	10	10	24	24
Arenal	1.00	11	-	-	-	0.03
Platanar	1.00	84	-	-	-	0.26
Poás	1.00	97	-	-	-	0.30
Barba	0.50	99	-	-	-	0.31
Barba (HFSErich)	0.50	99	-	-	-	0.31
Irazú-Sapper	0.50	130	-	-	-	0.40
Irazú-Haya (HFSErich)	0.50	130	-	-	-	0.40
Turrialba	1.00	112	-	-	-	0.35
Cordillera Central totals		761	150	0.60	8.5	2.37
error estimate in %		25	15	10	31	31

1. Total volumes for each center with subgroups can be obtained by summing the groups.
2. Density assumed to be 2800 kg/m^3. Length and age factors of flux taken from segment totals.

Table 3. Composition of mantle sources

	Cs	Rb	Ba	Th	U	Nb	Ta	K_2O	La	Ce	Pb	Pr	Sr
DM	0.002	0.21	2.03	0.032	0.006	0.25	0.014	0.013	0.42	1.08	0.029	0.18	16.3
OIB	0.006	1.22	32.13	0.271	0.093	1.21	0.060	0.066	2.10	5.07	0.220	0.70	52.9

	P_2O_5	Nd	Zr	Sm	Eu	Gd	TiO_2	Tb	Dy	Y	Yb	Lu
DM	0.015	0.75	8.69	0.24	0.12	0.25	0.25	0.15	0.66	5.68	0.60	0.11
OIB	0.028	2.66	12.18	0.64	0.20	0.52	0.20	0.14	0.75	5.01	0.48	0.08

Table 4. Models of mantle contribution.

Volcanic center or group	*Eiler et al.* [2005]		Melt	Mantle source		Melt
	DM	OIB	%	DM	OIB	%
Cosigüina				100		15.0
San Cristóbal	95	5	15	100		10.0
Telica (high U/La group)				100		15.0
Telica (high Ba/Th group)				100		25.0
Telica (HFSE-rich group)				95	5	10.0
Rota				100		15.0
Las Pilas-Cerro Negro	100		25	100		20.0
Las Pilas (HFSE-rich group)				95	5	7.5
Momotombo and Apoyeque				100		15.0
Nejapa				100		25.0
Nejapa (HFSE-rich group)	100		12	95	5	10.0
Masaya				100		7.5
Mombacho and Zapatera				80	20	7.5
Granada (HFSE-rich group)	100		12	100		15.0
Concepcion				50	50	10.0
Maderas				50	50	10.0
Orosí				80	20	10.0
Rincón de la Vieja				80	20	10.0
Miravalles				80	20	7.5
Tenorio	80	20	7	80	20	15.0
Arenal				50	50	20.0
Platanar					100	10.0
Poás					100	10.0
Barba					100	10.0
Barba (HFSE-rich group)		100	6		100	4.5
Irazú-Sapper					100	10.0
Irazú-Haya (HFSE-rich group)		100	6		100	4.0
Turrialba					100	10.0

Table 5. Fluxes and error estimates. Fluxes in units of 10^4 kg/m/Ma

Element	Cs	Rb	Ba	Th	U	K_2O	La	Pb	Sr
	Subducted Element flux								
NW Nicaragua	0.84	20.0	899	0.90	1.00	1.17	4.2	3.71	566
SE Nicaragua	1.04	25.0	1076	1.60	1.75	1.40	7.2	4.48	392
C. Guanacaste	0.73	27.4	892	1.75	1.14	1.42	9.6	3.55	554
C. Central	1.01	44.8	755	6.88	2.25	1.70	22.5	5.21	523
	Total flux (maximum)								
NW Nicaragua	0.86	22.7	926	1.31	1.08	1.34	9.2	3.77	741
SE Nicaragua	1.09	32.2	1201	2.90	2.11	1.82	19.6	5.53	745
C. Guanacaste	0.78	34.3	1028	3.07	1.53	1.81	21.4	4.61	877
C. Central	1.24	89.1	1900	16.51	5.61	4.11	90.8	12.46	1948
	Subducted flux from Th-Zr (minimum)								
NW Nicaragua			819		0.77	0.96	1.1	3.29	523
SE Nicaragua			962		1.44	1.03	2.8	4.00	321
C. Guanacaste			775		0.84	1.05	5.6	3.24	505
C. Central			578		2.08	0.82	25.9	7.42	650
	Concentration Error in % (Total flux-subducted flux)/(2*subducted flux)								
NW Nicaragua	1	7	2	23	4	7	60	1	15
SE Nicaragua	2	14	6	41	10	15	87	12	45
C. Guanacaste	3	13	8	38	17	14	61	15	29
C. Central	11	49	76	70	75	71	152	70	136
	Concentration Error in % (ThZr base-subducted flux)/(subducted flux)								
NW Nicaragua			9		23	18	74	11	8
SE Nicaragua			11		18	26	61	11	18
C. Guanacaste			13		26	26	42	9	9
C. Central			23		8	52	-15	-43	-24
Segment (mass error)	Flux error in % (mass error and largest concentration error)								
NW Nicaragua (43%)	43	44	44	49	49	47	85	44	46
SE Nicaragua (45%)	45	47	46	61	48	52	98	47	64
C. Guanacaste (24%)	24	27	27	45	36	35	66	28	38
C. Central (31%)	33	58	82	77	81	77	155	76	140

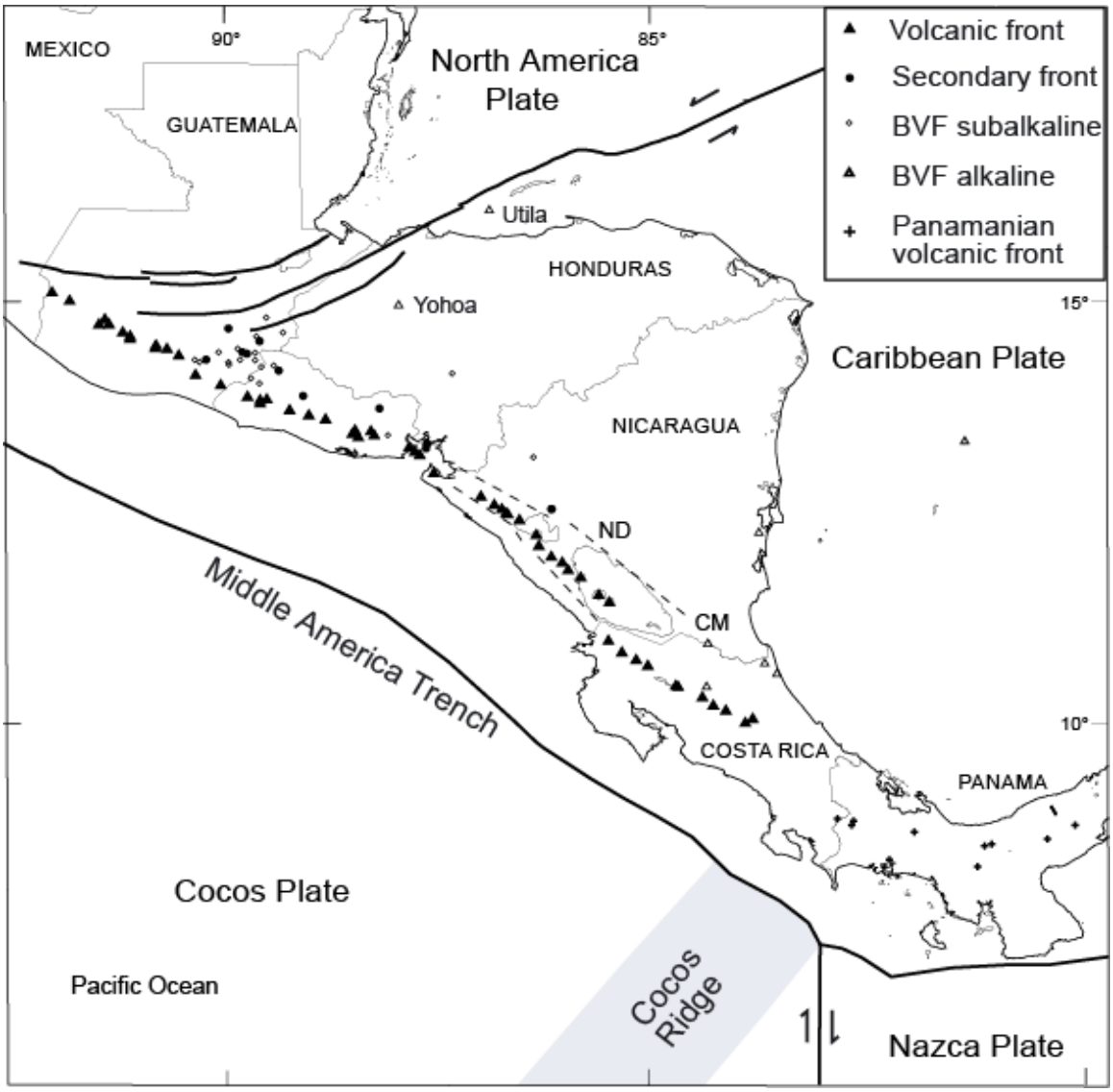

Figure 1. Location map for Central American volcanoes.
CM marks the location of Cerro Mercedes. Dashed lines mark position of Nicaraguan Depression (ND).

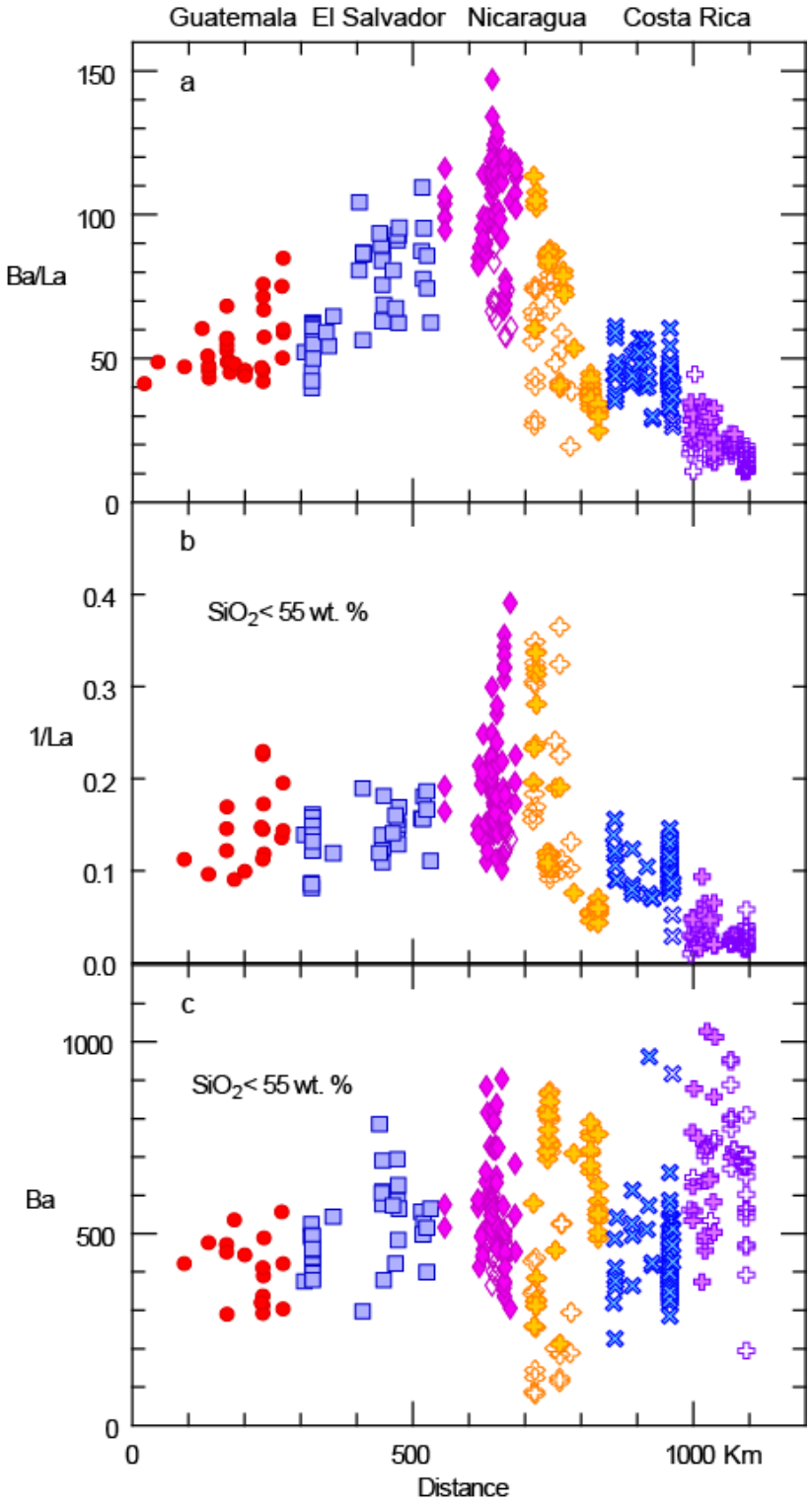

Figure 2. Subduction signal, Ba/La, and its two components along the volcanic front. Symbols mark segments defined primarily by right stepping jogs in the volcanic front.

Filled symbols are the volcanics with HFSE depletions. Open symbols are the HFSE-rich suites in Nicaragua and Costa Rica

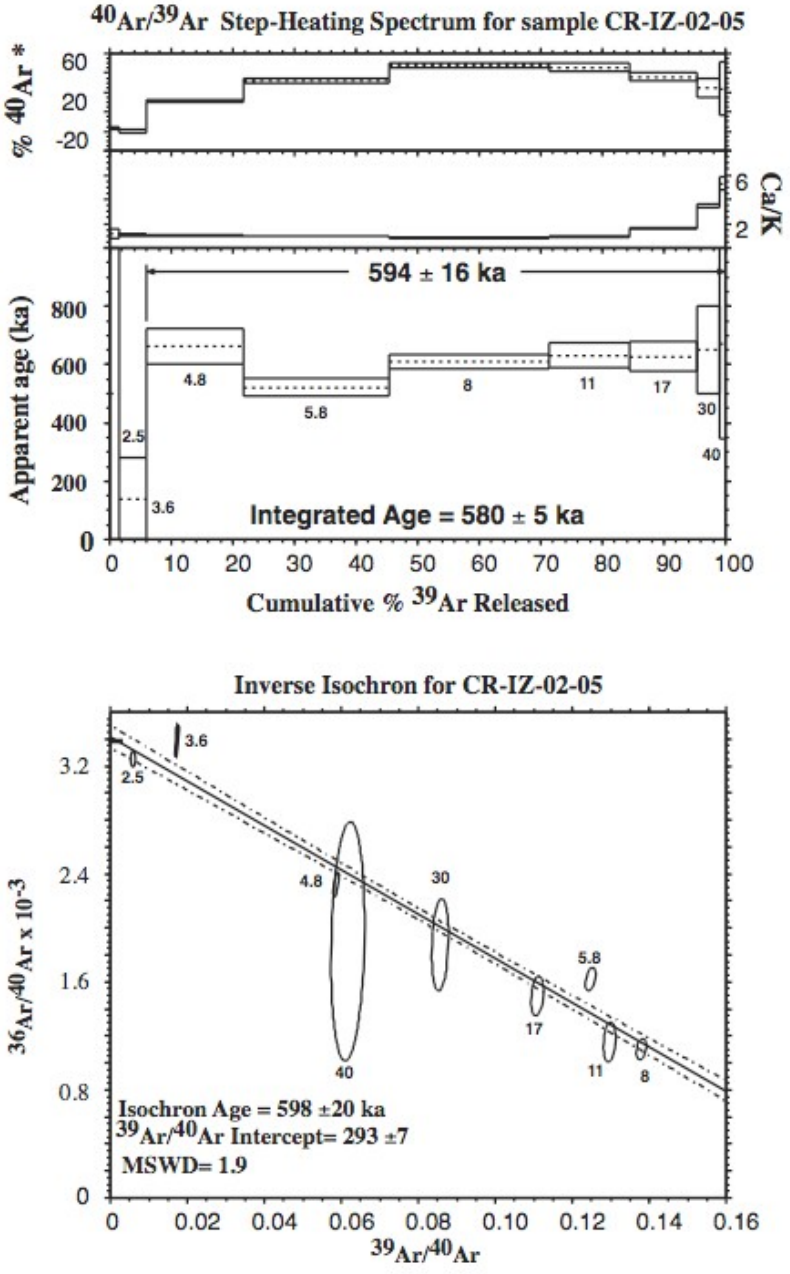

Figure 3

Figure 3. Step heating spectra for sample CR-IZ-02-05 from Irazú volcano. The heating steps, in watts are written below Ar release steps in the plateau diagram and adjacent to the error ellipses in the inverse isochron diagram.

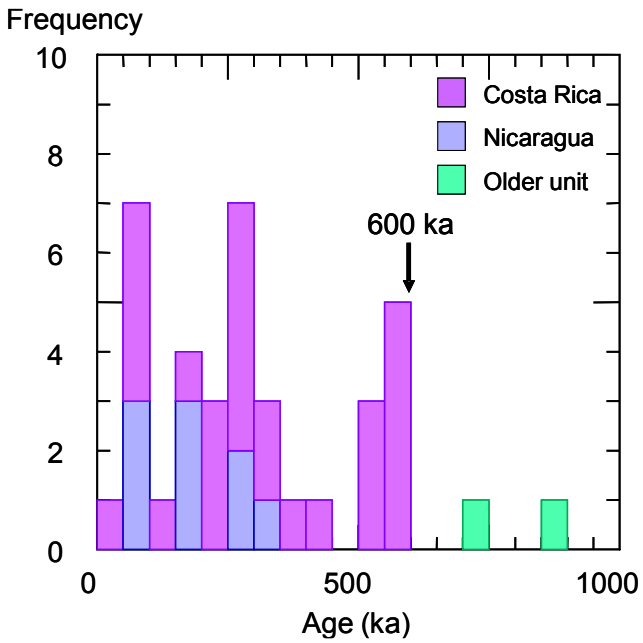

Figure 4. Histogram of $^{40}Ar/^{39}Ar$ ages for recent Costa Rican and Nicaraguan volcanics.

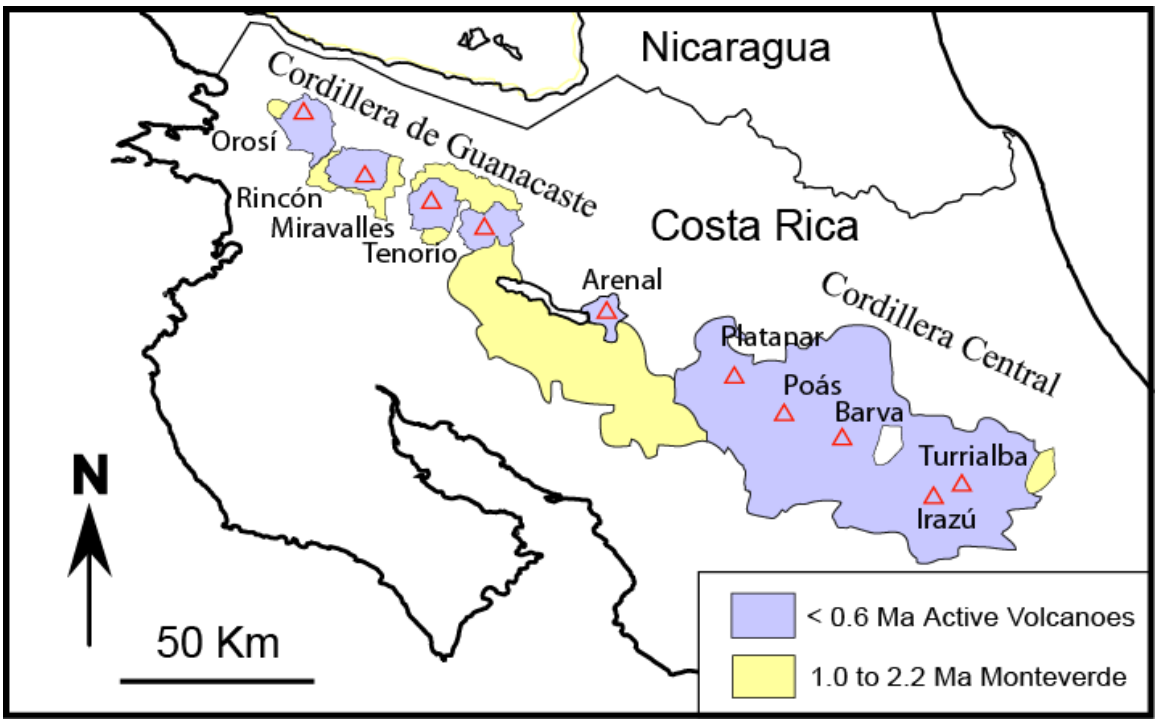

Figure 5. Map of active volcanic front and Monteverde volcanic front in Costa Rica.

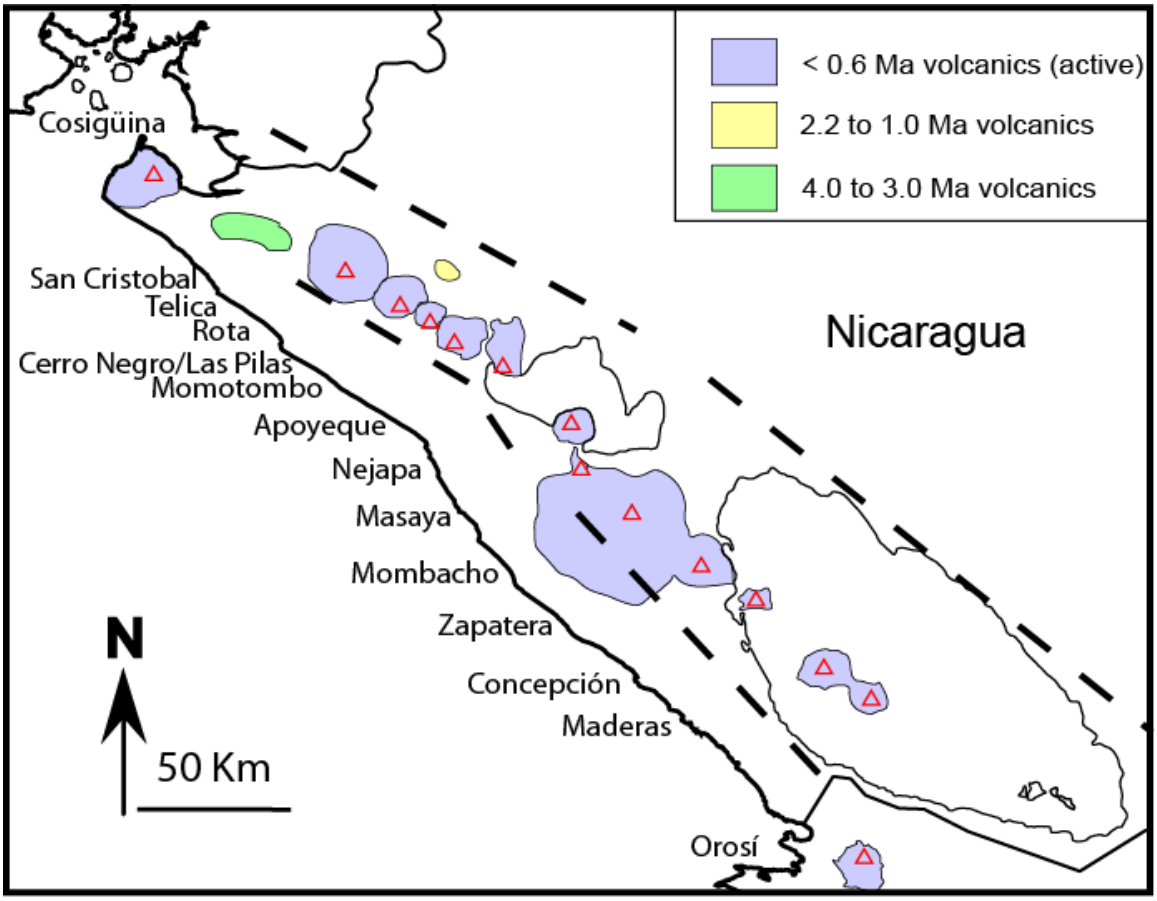

Figure 6. Map of post-Miocene volcanics in Nicaragua. Dashed lines are borders of Nicaraguan Depression.

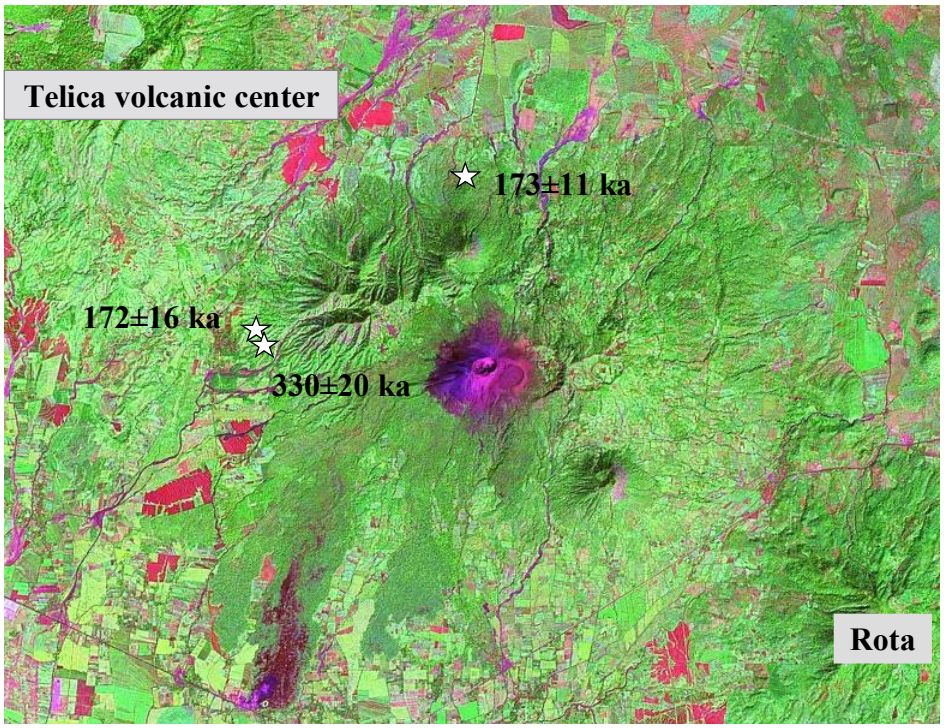

Figure 7. Satellite image of Telica volcano, Nicaragua, from NASA MrSID image N-16-10_2000.

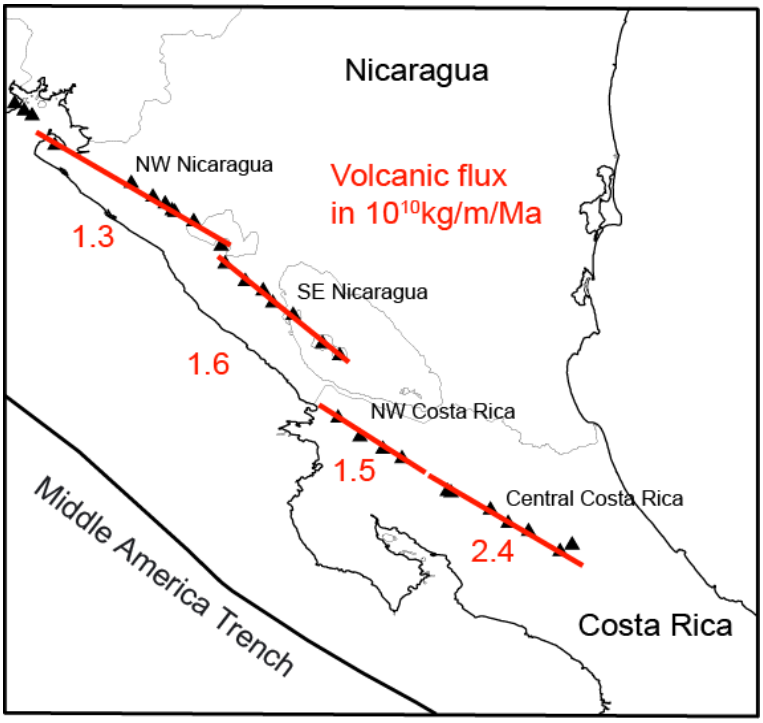

Figure 8. Extrusive volcanic flux by segment.
The NW Costa Rica segment of the volcanic front includes the Cordillera de Guanacaste volcanoes. The central Costa Rica segment includes Arenal volcano and the Cordillera Central volcanoes.

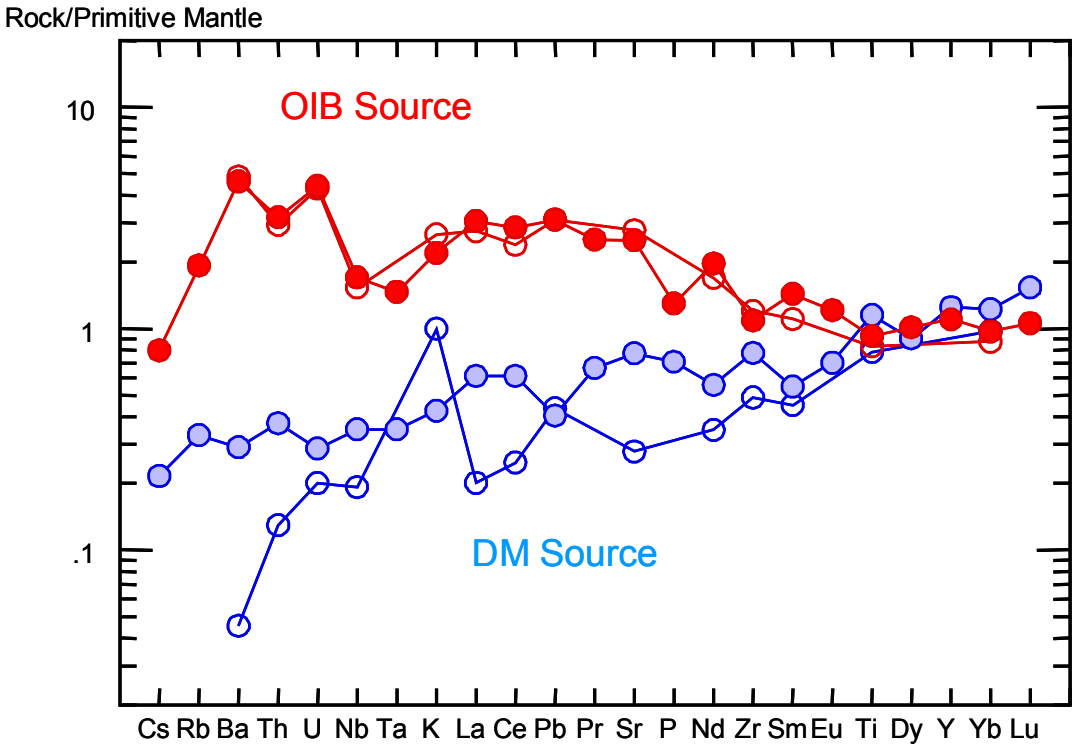

Figure 9. Sources for Central American volcanics.
Open symbols from *Eiler et al.* [2005]

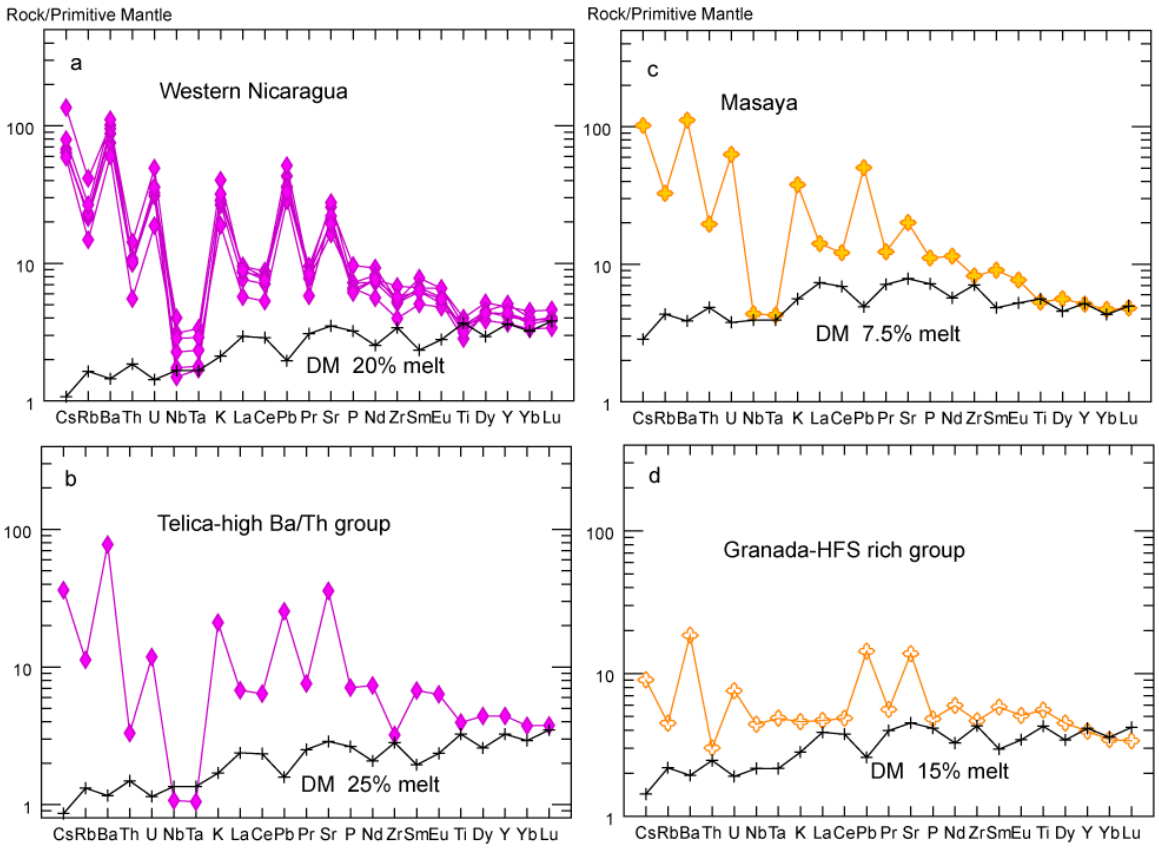

Figure 10. Spider diagrams of Nicaraguan volcanoes, whose modeled mantle-derived components are derived solely from DM. Selected models of mantle-derived component shown in black.

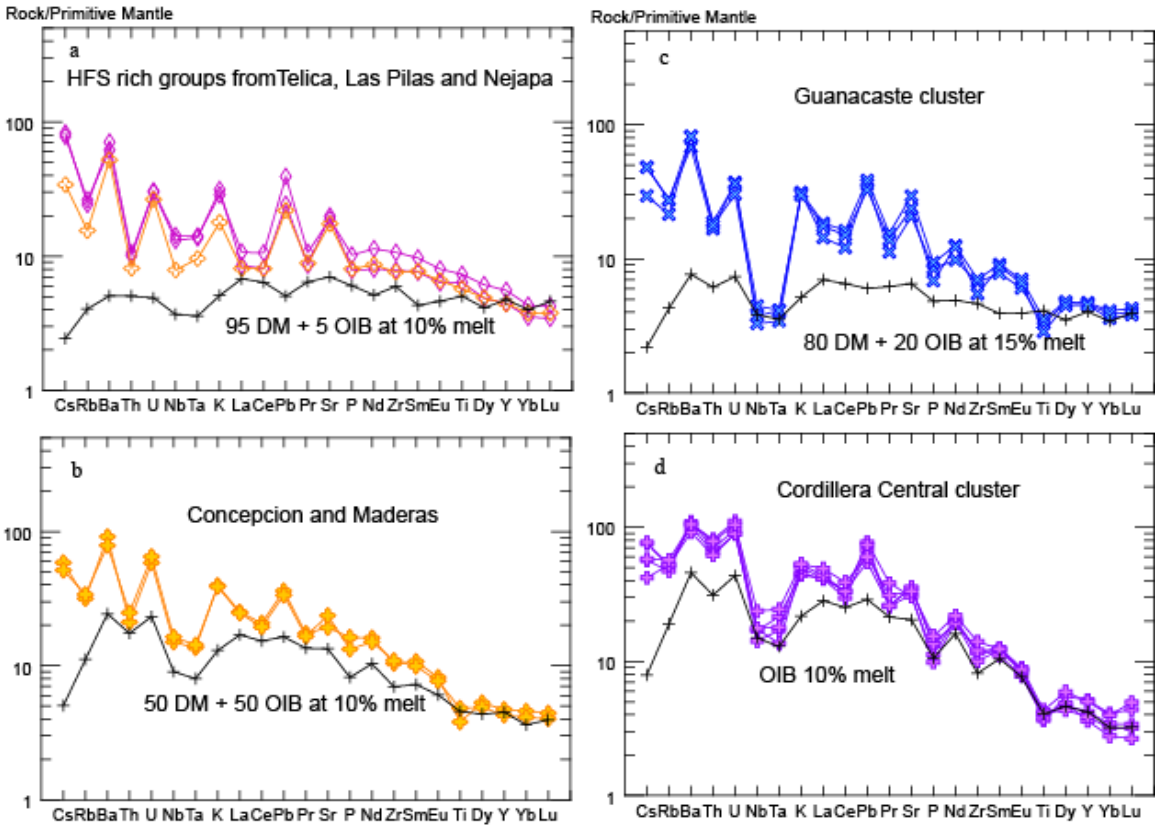

Figure 11. Spider diagrams of Nicaraguan and Costa Rican volcanoes, whose modeled mantle derived components are derived from mixtures of DM and OIB or from pure OIB. Selected models of mantle-derived component shown in black.

Chapter 2

Geochronology in Costa Rica and Nicaragua: Progress and Challenges

Ian Saginor, Esteban Gazel, Michael J. Carr, Carl C. Swisher III, Brent Turrin
Rutgers University, Department of Geological Sciences, 610 Taylor Rd., Piscataway NJ 08854-8066

Abstract

To better estimate the extrusive flux of the Central American Arc, from 2002-2008, we obtained sixty one high precision $^{40}Ar/^{39}Ar$ ages on geographically well-situated lavas and tephra from Costa Rica and Nicaragua. Here, we describe a number of observations encountered during this study using four examples that well document the precision, accuracy and general reliability of the $^{40}Ar/^{39}Ar$ ages. First, low K_2O values, particularly in samples from Nicaragua, is a major limitation in or attempts to obtain reliable dates on samples under 1 Ma. Second, extensive weathering of samples due to the tropical climate of Central America has resulted in various levels of argon loss even when the hand sample appeared unaltered. Third, our field and geochronological data lead us to conclude that eruptive rates have not been constant over the past 15 to 20 myr, but rather appears punctuated by gaps of up to several million years.

We attempted to address the temporal gaps in several ways. First, geochemical analyses were used to identify samples that may have erupted during time periods without known volcanism. For example, U/Th values in the active Central American arc are significantly higher than those obtained from the Miocene Coyol Group except for four samples with intermediate values that were dated to determine if their ages were intermediate as well. However, all of these samples were found to be from a period with known volcanism. Second, we sought to locate the oldest sections of the active arc and the

youngest sections of the Coyol Group in order to better constrain the timing and duration of the apparent gap in volcanic productivity. This approach also failed to locate samples from periods without known volcanism. When these methods proved largely unsuccessful, our focus shifted to dating regions of minor volcanism between the active and Coyol volcanic fronts as well as between Cosigüina and San Cristóbal, the longest stretch of the Central American Volcanic Front without active volcanism. This effort yielded ages on samples ranging from 1.1 to 3.6 Ma and, thus, substantially reduced the apparent volcanic gap in Nicaragua.

Introduction

The development of $^{40}Ar/^{39}Ar$ dating methods made it possible to obtain high precision ages from a wide variety of igneous material. Radiometric dates appear simple to interpret, but this accessibility often leads to misunderstandings about how these dates are obtained and even what geologic events in the rock's history the dates refer to. It is therefore important to be clear about what argon ages mean, how they are derived, and what affects their reliability.

The basis of the $^{40}Ar/^{39}Ar$ dating technique is a modification of the ^{40}K-^{40}Ar dating method based on the decay of ^{40}K to ^{40}Ar with a half-life of 1.26 Ga (Beckinsale and Gale, 1969). The $^{40}Ar/^{39}Ar$ technique differs from the ^{40}K-^{40}Ar method in that the K of a sample, is measured by conversion of ^{39}K to ^{39}Ar by neutron bombardment in nuclear reactor. Since the ratio of ^{39}K to ^{40}K is known, the derived ^{39}Ar can be used as proxy for ^{40}K measurement (Merrihue and Turner, 1966). This technique has an advantage over conventional K-Ar dating, because both the radioactive parent $^{39}Ar_K$ and the daughter ^{40}Ar

can be measured by the same method, mass spectrometry, on the same sample split at the same time. This permits the measurement of smaller sample sizes (since splits are not needed for K and Ar measurement) and reduces measurement errors associated with weighing and homogeneity. Since these are now direct ratio measurements, not recombined yields per sample weight, samples can be incrementally heated, yielding series of relative increasing temperature ages that yield insight into the thermal history of the sample. Likewise these data can be plotted on isochron plots that give added information as to the initial argon concentration of the sample at the time of cooling.

The $^{40}Ar/^{39}Ar$ technique can be applied to any K-bearing igneous rock or mineral phase that has not undergone extensive weathering or reheating since its formation. Within each rock, ^{40}K is perpetually decaying, however ^{40}Ar will not begin to accumulate until the material drops below its "blocking" temperature; the temperature below which crystal structure is strong enough to block the diffusion of argon. ^{40}Ar is a relatively large atom and cannot escape the typical silicate mineral crystal lattice unless the sample is reheated or physically abraded. Once the mineral has cooled beneath its blocking temperature, the "clock" begins and the daughter ^{40}Ar accumulates. Blocking temperatures vary for different minerals, with amphibole ~500ºC (Hanson and Gast, 1967), biotite ~400ºC, and plagioclase ~200ºC (Berger and York, 1981). It is important to note that when we refer to a $^{40}Ar/^{39}Ar$ "age", we are referring to this moment in time and not necessarily the formation age. For example, plutonic rocks can remain above their blocking temperature for millions of years and metamorphic rocks can have their radiometric clocks reset by subsequent reheating, which means that these rocks can form long before the radiometric clock begins (Berger and York, 1981). In contrast, extrusive volcanic rocks typically cool below their

blocking temperature soon after the time of eruption and can yield true formation ages. All ages referred to in this paper are considered to be eruption ages.

While $^{40}Ar/^{39}Ar$ dating is an extremely useful tool, it is not without its drawbacks, particularly in Central America and obtaining reliable dates is dependant on a number of factors, each of which can affect the reliability of the resulting age data.

Radiogenic Argon

Prior to the eruption of a lava or tephra, the magma is generally well above the blocking temperature of most K-bearing minerals, and normally is in equilibration with the $^{40}Ar/^{36}Ar$ ratio of the atmosphere (295.5, Steiger and Jager, 1977). All extrusive volcanic rocks therefore contain some ^{40}Ar at the time of formation, but ^{40}Ar of radiogenic origin (abbreviated $^{40}Ar^*$) only begins to accumulate after they cool below their blocking temperature. A reliable date can be obtained if sufficient amounts of $^{40}Ar^*$ accumulates to distinguish from ^{40}Ar derived from equilibration with the atmosphere.

The accumulation of $^{40}Ar^*$ is controlled by two main factors: The initial potassium content of the sample and the elapsed time since it dropped below the blocking temperature. A high potassium sample can accumulate sufficient $^{40}Ar^*$ to yield a reliable age in less time than a low potassium sample. A problem arises however, when trying to date young rocks with low potassium content, because there is very little $^{40}Ar^*$ to measure.

While potassium contents of Central American arc basalts are comparable to basalts from other arcs, (generally between 0.5 and 2 wt.%, Luff, 1982; Marsh, 1982; Smith et al., 1980; Wills, 1974), there is significant internal variability with central Costa Rican values almost doubling those in northwest Nicaragua (Figure 1, Carr et al., 2003). Northwest

Costa Rican samples are also higher on average than those from Nicaragua, although there is significant overlap. This regional difference may be in part responsible for the large number of reliable dates obtained from the Costa Rican volcanic front and the paucity of similar data in Nicaragua.

Volcanic material as young as a few thousand years has been successfully dated using $^{40}Ar/^{39}Ar$ dating techniques (Renne et al. 1997, Lanphere et al., 1999), but those samples had potassium levels at least 10 times that of typical in Central America. It is likely the combination of young age and low potassium content that makes dating Nicaraguan volcanic front samples challenging. Thirty one Nicaraguan volcanic front samples have been dated at the Rutgers University Geochronology Lab and of those, only eight yielded reliable ages. Thirty five Costa Rican volcanic front samples have been dated at the Rutgers University Geochronology Lab and of those, thirty three yielded reliable ages, a significantly higher percentage than the Nicaraguan samples. Measuring K_2O contents and selecting only those samples with the highest levels can help solve this problem.

Weathering and hydrothermal alteration can also be problematic for argon geochronology of lavas, because both of these processes can cause the release of $^{40}Ar^*$ that has been building up since the time of eruption or differential K and Ar loss during weathering. This is common in volcanic rocks, particularly in the tropical climate of Central America, and often affects only the phases that crystallized at the lowest temperatures as well as secondary phases, such as zeolites that are the result of low temperature alteration (Figure 2; Ching-Hua Lo et al., 1994). Under certain conditions, weathering and hydrothermal alteration can cause the release of all pre-eruption $^{40}Ar^*$, even

in samples less than 100 ka. For example, on the southern flank of San Cristóbal, one smooth, lobe-shaped lava was found (12.7315ºN/87.0540ºW) to be so hydrothermally altered that it could be easily broken by hand. This sample was not collected, but is a reminder of how quickly alteration can occur. K is often lost from glassier phases during weathering and hydration.

Another factor that can cause unreliable dates is incomplete degassing or trapping of pre-eruption ^{40}Ar. When erupted lava is allowed to fully equilibrate with the atmosphere, the initial ratio of ^{40}Ar to ^{36}Ar will be 295.5. However, if pre-eruption ^{40}Ar is not allowed to degass, the sample is said to have "excess" argon. This can be seen in an isochron diagram of sample VE-071605-2 (Figure 2), which is described later in this paper.

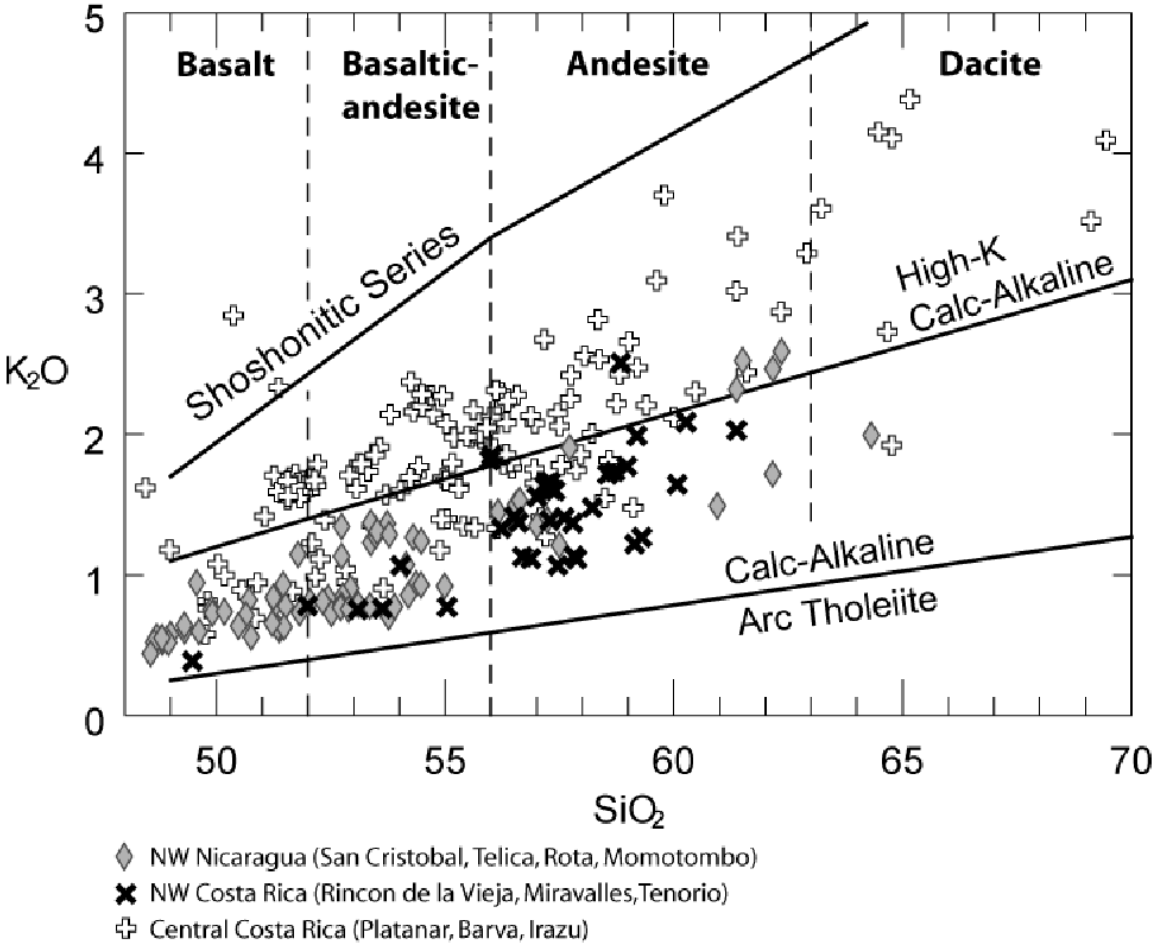

Figure 1. Geochemical classification diagram (Peccerillo and Taylor, 1976). Gray diamonds are Nicaragua, black Xs are northern Costa Rica, open crosses are central Costa Rica. Data from Carr et al. (2003).

Methods

Samples for $^{40}Ar/^{39}Ar$ dating discussed here, were obtained from the cores of large boulders or lava blocks collected from the study areas. Samples were observed under binocular and petrographic microscopes and those that showed clear evidence of weathering or alteration were eliminated. For most samples, only the fine-grained matrix (composed mainly of microlitic plagioclase) was analyzed, because its lack of phenocrysts suggest that it was formed at the time of eruption. Phenocrysts were removed through a combination of hand picking and magnetic separation. A biotite mineral separate was analyzed for sample C-06-NIC-2, a biotite rich tephra. Samples were prepared and analyzed following methods outlined in Carr et al. (2007) and will not be described in detail here.

It is worth noting that all ages are based on either matrix or mineral separates as opposed to whole rock analysis. The main difference is that with the whole rock method, the entire sample is analyzed and may include radiogenic argon from weathered phases, pre eruption phenocrysts, or xenolithic contamination. By analyzing only the fine-grained matrix, we minimize these factors and limit the possibility of obtaining anomalously old ages. Even with this precaution, it can be difficult to eliminate pre-eruption phases entirely, particularly if they are small and of the same minerals that make up the matrix. Low temperature alteration can also be difficult to completely eliminate during sample preparation.

For these reasons, samples were incrementally heated with up to 15 increasing temperature steps and the released gases measured each time. Each temperature step is

based on an increase in laser power wattage (typically between 2 and 32 watts) and those power limits have been empirically determined to vary the temperature of the sample between 500ºC and 1150ºC. This method yielded the incremental heating release spectra diagrams seen throughout this paper as opposed to total fusion ages, which are generated by releasing trapped argon with a single high temperature step. Total fusion analysis includes the radiogenic argon component of the entire sample in a single measurement and can mask internal variability and evidence of weathering and xenolithic contamination. Release spectra diagrams plot the apparent age of each individual temperature step, which may or may not be the same throughout the sample. Ideally, apparent ages from consecutive temperature steps representing at least 50% of the total ^{39}Ar would form an age plateau at the 95% confidence level. Typically, the plateau age (if there is one) is reported along with the integrated age, which is simply the weighted average of each individual temperature step and is essentially the same as a total fusion age.

The incremental-heating method is also beneficial because multiple steps can be plotted on an inverse isochron diagram (examples in Figure 2). In this type of diagram, $^{36}Ar/^{40}Ar$ is plotted against $^{39}Ar/^{40}Ar$. In an ideal sample, the individual temperature steps plot along a single line, such that the slope provides the age and the *y*-intercept provides the initial $^{36}Ar/^{40}Ar$ value.

Case Studies

The first sample case study is RO-4 (Figure 2A), a lava collected from Rota Volcano in Nicaragua (Figure 5, Chapter 1). RO-4's extremely low radiogenic argon yields (–1.1 to 1.9%) is typical of Nicaraguan active front lavas. Negative values simply

reflect the fact that the error exceeds the amount of the measured gas. This can be clearly seen in the first temperature step, which accounts for approximately 30% of the total released ^{39}Ar, yet the apparent age is below 0. The low $^{40}Ar^{*}$ yield is most likely due to its relatively young age (the Nicaraguan front is no more than 350 ka, Carr et al., 2007) rather than it's potassium content, which at 1.22 wt.% (Carr et al., 2003), is one of the highest in Nicaragua. Although evidence of weathering was not detected in hand sample or thin section, due to the sample's location in a tropical climate and proximity to active volcanism (and therefore sources of hydrothermal activity), low-temperature alteration cannot be entirely ruled out. In addition, the apparent age seems to increase in the last 5 temperature steps, which could suggest that radiogenic argon was released only at the lower temperature phases. This sample is considered not to have yielded a reliable date and is included here only to illustrate the difficulty in evaluating the age of a sample when the radiogenic argon yield is low.

In the absence of a reliable plateau, how should this data be interpreted? The isochron yields a negative age and an atmospheric initial $^{40}Ar/^{36}Ar$, so we can conclude that there is simply too little radiogenic argon to obtain a reliable age. In the absence of clear evidence of chemical or physical alteration, we can simply conclude that the sample is of 0 age, or more precisely, that the sample's age is indistinguishable from 0.

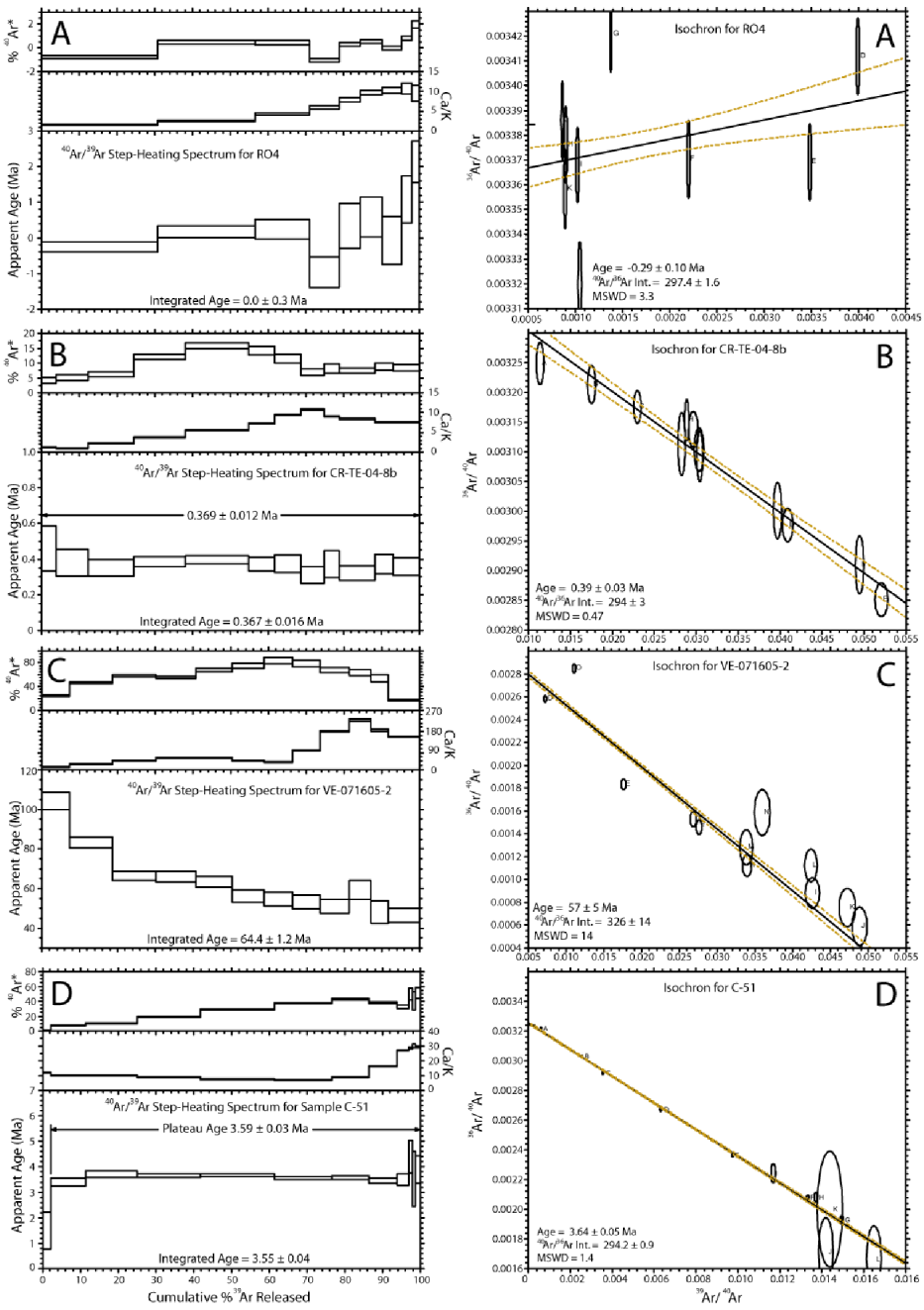

Figure 2. Step-heating spectra and Isochron plots for A) RO-4 from Rota in Nicaragua B) CR-04-TE-8b from Tenorio in Costa Rica C) VE-071605-2 from Isla Venado off the Nicoya Peninsula in Costa Rica D) C-51 from between Cosigüina and San Cristóbal in Nicaragua.

The next sample case study is CR-TE-04-8b (Figure 2B), a lava collected from Tenorio Volcano along the Costa Rican volcanic front (Figure 5, Chapter 1). All temperature steps form a 0.369 ± 0.012 Ma plateau at the 95% confidence level and the

$^{40}Ar^{*}$ yields range from 4 to 16%. The isochron age agrees with the plateau age within the margin of error at 0.39 ± 0.03 Ma and the initial $^{40}Ar/^{36}Ar$ ratio is within the range of atmospheric values at 294 ± 3. In addition, the mean squared weighted deviation (MSWD) of the individual steps is only 0.47, which means that the errors fully account for the scatter about the isochron line. The large plateau and the high $^{40}Ar^{*}$ yield (relative to Nicaraguan volcanic front samples) is consistent with the majority of other Costa Rican samples. For all of these reasons, this is considered to be an excellent example of a reliable age in contrast to the previous sample RO-4.

The third case study is a pillow basalt from Isla Venado off Costa Rica's Nicoya Peninsula (VE-07165-2; Figure 2C). This sample is overlain by a unit of reworked volcaniclastic sediments that was dated using biostratigraphy to 100 Ma. This sample had an initial $^{40}Ar/^{36}Ar$ ratio of 326 ± 14, higher than atmospheric ratios and evidence of excess argon and is likely due to its submarine eruption, which prevented complete degassing and equilibration with the atmosphere. The release spectra (Figure 2C) show the individual temperature steps falling from 105 Ma to 45 Ma throughout the analysis. Not only does this sample lack a plateau, but the isochron is also problematic with a mean squared weighted deviation of 14, well above the variation accounted for by the errors. One could attempt to refit the isochron with a different line by including only the high temperature steps that appear to be approaching a plateau. This approach would increase the age and the initial $^{40}Ar/^{36}Ar$ ratio, but we believe that would be over interpreting very low-quality data. Although a reliable age cannot be obtained from this sample, the high initial $^{40}Ar/^{36}Ar$ ratio suggests that it the age is probably much younger than the >100 Ma estimate based on field data. This may simply mean that the contact between the pillow basalts and the

overlying unit is a thrust fault and not depositional, however further fieldwork is needed to make this determination. Given the glassy nature of pillow basalts, the spectra may also reflect K-loss during hydrothermal alteration.

The last sample case study is C-51 (Figure 2D), a lava collected from a low lying area between the volcanic front volcanoes of Cosigüina and San Cristóbal in northwest Nicaragua. This sample has a plateau age of 3.59 ± 0.03 in agreement with an isochron age of 3.54 ± 0.05. These ages were first reported in Carr et al. (2007) and are included here as an example of how low degrees of weathering or alteration can affect the release spectra of a sample. Although, the plateau includes 98% of the total released ^{39}Ar, the first temperature step is not included and is almost 2 Ma younger than the rest of the plateau. This is common even in samples with robust ages and is evidence of low-temperature alteration, which releases radiogenic argon trapped in low-temperature phases within the lava.

Volcanic History

Previous geochronological work in Nicaragua (Ehrenborg, 1996; Elming et al., 2001; Plank et al., 2002, Carr et al., 2007) suggest that the NW/SE trending Coyol Arc migrated steadily toward the southwest until ~7 Ma when volcanic production abruptly ceased. The Coyol volcanic front lasted from 25 Ma to 7 Ma (Plank et al., 2002) and consists of extensive lavas and ignimbrites throughout the Nicaraguan Highlands. Volcanism wouldn't resume until 3.6 Ma and then only between Cosigüina and San Cristóbal (Carr et al., 2007). Several attempts were made aimed at filling in this missing period in the volcanic record.

First, U/Th values in Nicaraguan volcanics experienced a significant increase between the Miocene and present arc (Figure 3, Plank et al., 2002), however there were three samples thought to be Miocene that had U/Th values between those typical for the Miocene and active arcs. These samples were selected for dating, because their intermediate U/Th values raised the possibility that their ages were intermediate as well. Sample LL-4 is from the Las Lajas volcano just east of the Nicaraguan depression and samples Bal-8 and Bal-10 are from the Balsamo Formation in El Salvador. LL-4 was found to be 9.5 Ma, which places it firmly within the Coyol Group (Carr et al., 2007). Samples Bal-8 and Bal-10 were found to be older than the active volcanic front and yielded ages of 1.3 and 1.1 Ma respectively.

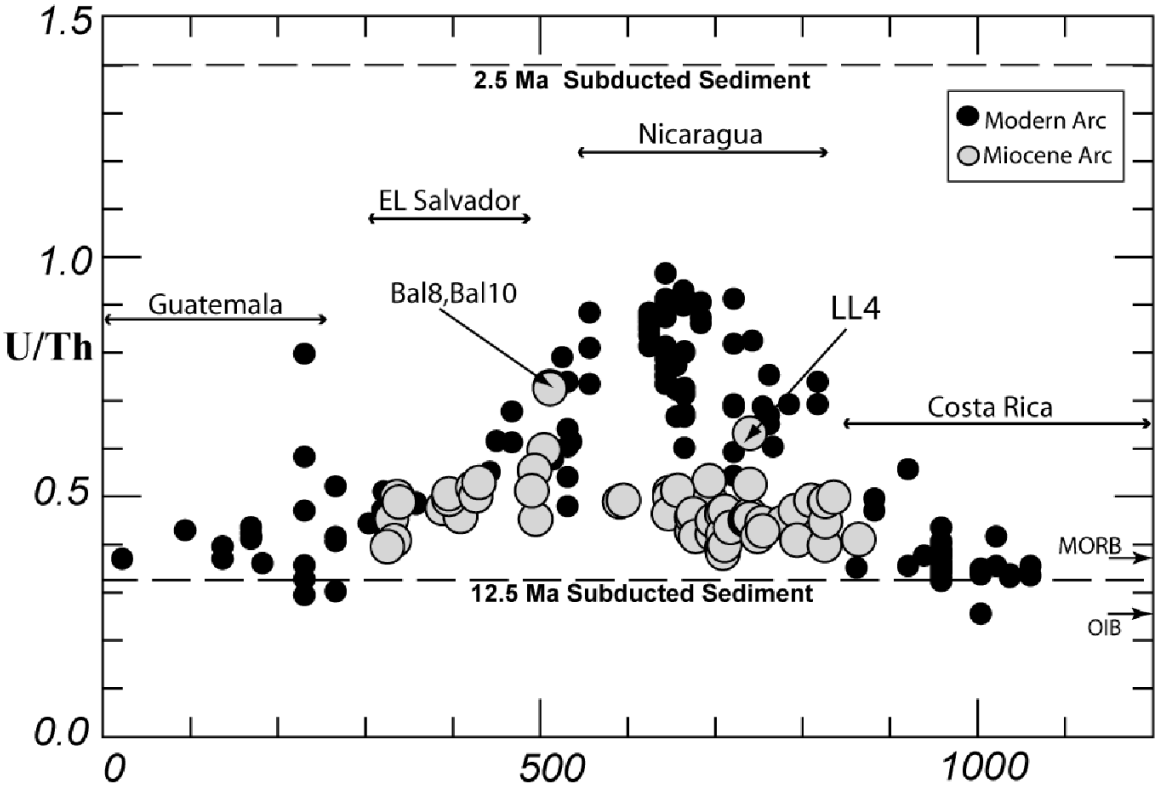

Figure 3. Along arc variation in U/Th with country section labeled. Black circles are the modern arc and gray circles are Miocene (Condie, 2005; Carr et al., 2003). 3 samples selected for dating are labeled (Carr et al. 2007; Saginor et al. see Chapter 3).

Second, an attempt was made to constrain both the timing and duration of this apparent hiatus in Nicaraguan volcanism by refining estimates for the youngest material within the Coyol Group as well as the oldest sections of the active arc. For the latter task, satellite images (https://zulu.ssc.nasa.gov/mrsid/) and topographic maps were used to identify areas within the active arc where the morphology suggested the oldest material could be found.

$^{40}Ar/^{39}Ar$ ages obtained using this method were reported in Carr et al. (2007), with a maximum age of 330 ka. Plank et al. (2002) suggested that Miocene volcanism in Nicaragua ceased ~7 Ma after the Coyol volcanic front migrated towards the southwest for at least 5 Ma. In an effort to locate Coyol volcanics younger than 7 Ma, fieldwork was focused between the active arc and the westernmost Coyol lavas (Figure 4, Carr et al., 2007).

This approach extended the geographic distribution of the Coyol Group ~10 km into the Nicaraguan Depression, although did not extend its temporal range. Two samples were found in this area with ages of 1.13 and 1.48, which places them in the Tinajas unit as defined in Saginor et al. (in prep; see Chapter 3).

We also collected samples between Cosigüina and San Cristóbal, the longest stretch of the volcanic front without an active volcano. This effort revealed two previously unknown volcanic units: The Tinajas (2.5-1.3 Ma) and the Encanto (3.6-3.2 Ma). Both of these are described in Saginor et al. (see Chapter 3). These two units also decreased the duration of the temporal gap in Nicaragua, leaving only 3.4 Ma (7 to 3.6 Ma) without known volcanism.

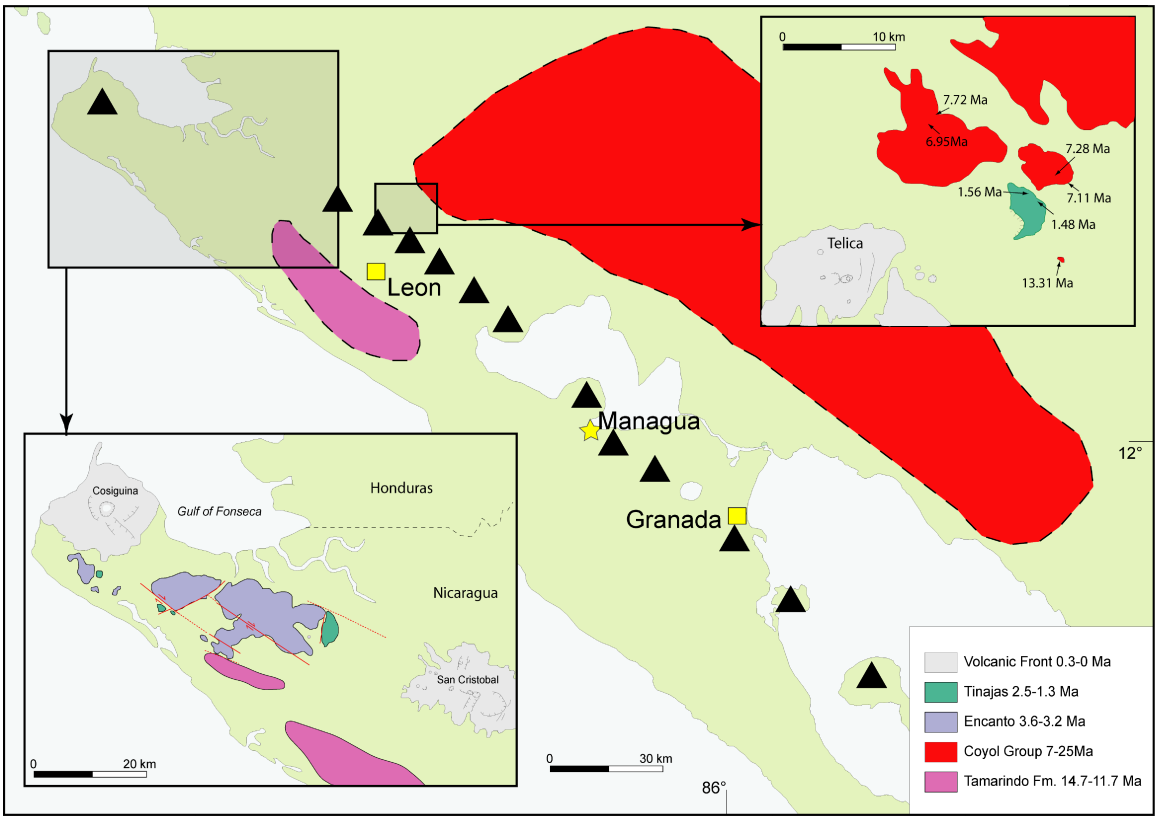

Figure 4. Map of northwest Nicaragua and two primary study areas.

Conclusions

Samples from the Nicaraguan volcanic front are generally lower in K_2O than samples from the Costa Rican front. In addition, the front may be slightly younger in Nicaragua than Costa Rica. These two factors make obtaining reliable Nicaraguan $^{40}Ar/^{49}Ar$ ages difficult because it leads to lower $^{40}Ar^*$ yields. It is also possible that efforts to locate the oldest sections of the active volcanic front were more successful in Costa Rica than Nicaragua where collected samples were actually younger than field estimates. Weathering due to the tropical Central American climate severely limits the number of samples (even on recent lava flows) acceptable for dating, because it can cause the release of $^{40}Ar^*$, although there is no evidence that weathering is more pervasive in Nicaragua than in Costa Rica.

The volcanic history in Nicaragua is incomplete and several attempts have been made to locate samples that fill in these temporal gaps. First, samples with U/Th values between the Miocene and active volcanic fronts were analyzed to see if their ages were intermediate as well. Second, satellite imagery was used to direct fieldwork toward the most weathered sections of the active Nicaraguan volcanoes and to a topographic low just behind the active front. Third, volcanic material was collected between Cosigüina and San Cristóbal, the longest stretch of the volcanic front without an active volcano. These efforts decreased the duration of the temporal gap in Nicaragua to about 3.4 Ma, which lasted from 7 to 3.6 Ma.

References

Beckinsale, R.D., and N.H. Gale (1969), A reappraisal of the decay constants and branching ratio of ^{40}K, *Earth Plan. Sci. Lett.*, 6, 289-294.

Berger, G.W., and D. York (1981), Geothermometry from $^{40}Ar/^{39}Ar$ dating experiments, *Geochim. Cosmochim. Acta*, 45, 795-811.

Carr, M.J., Feigenson, M.D., Patino, L.C., and J.A. Walker (2003), Volcanism and geochemistry in Central America: progress and problems, in *Inside the Subduction Factory,* AGU Geophysical Monograph 138, Edited by Eiler, J. and G. Abers, 153-179.

Carr, M. J., Saginor, I., Alvarado, G. E., Bolge, L. L., Lindsay, F. N., Milidakis, K., Turrin, B. D., Feigenson, M. D., and C. C. Swisher III (2007), Element fluxes from the volcanic front of Nicaragua and Costa Rica, *Geochemistry Geophysics Geosystems*, 8, 6, 1525-2027.

Ching-Hua Lo, Onstott, T.C., Chiang-Hwa Chen, and L. Typhoon (1994), An assessment of $^{40}Ar/^{39}Ar$ dating for the whole-rock volcanic samples from the Luzon Arc near Taiwan, *Chemical Geology*, 114, 1-2, 157-178.

Condie, C. (2005), Continuity (Ba) and change (U) in Central American geochemistry: New evidence from the Miocene Balsamo Formation in El Salvador, Masters Thesis, Rutgers University.

Ehrenborg, J. (1996), A new stratigraphy for the Tertiary volcanic rocks of the Nicaraguan highland, *Geol. Soc. Am. Bull.*, 108, 830-842.

Elming, S.A., Layer, P., and K. Ubieta (2001), A paleomagnetic study of Tertiary rocks in Nicaragua, Central America, *Geophys. J. Int*, 147, 294-309.

Hanson, G.N., and P.W. Gast (1967), Kinetic studies in contact metamorphic zones, *Geochim. Cosmochim. Acta*, 31, 1119-1153.

Lanphere, M. (2000), Comparison of conventional K–Ar and $^{40}Ar/^{39}Ar$ dating of young mafic volcanic rocks, *Quaternary Research*, 53, 3, 294-301.

Luff, I.W. (1982), Petrogenesis of the island arc tholeiite series of the South Sandwich Islands, PhD Thesis, University of Leeds, U.K.

Marsh, B.D. (1982), The Aleutians. *In* Andesites: Orogenic andesites and related ocks, R.S. Thorpe (ed.), Chichester: Wiley, 99-114.

Merrihue, C., and G. Turner (1966), Potassium-Argon dating by activation with fast neutrons, *J. geophys. Res.*, 71, 2852-2857.

Peccerillo, R., and S.R. Taylor (1976), Geochemistry of Eocene calc-alkaline rocks from the Kastamonu Area, northern Turkey, *Contrib. Min. Pet.*, 58, 63-81.

Plank, T., Balzer, V., and M.J. Carr (2002), Nicaraguan volcanoes record paleoceanographic changes accompanying closure of the Panama Gateway, *Geology* 30, 1087-1090.

Renne, P.R., Sharp, W.D., Deino, A.L., Orsi, G., and L. Civetta (1997), $^{40}Ar/^{39}Ar$ dating into the historical realm: Calibration against Pliny the Younger, *Science*, 277, 1279-1280.

Saginor, I, Gazel, E., Carr, M., Swisher, C., Turrin, B. (see Chapter 3), Narrowing the gap: New geochemical and geochronological results from Western Nicaragua, with an updated Miocene to recent volcanic history.

Steiger, R.H., and E. Jager (1977), Subcommision on geochronology: Convention on the use of decay constants, *Earth Plan. Sci. Lett.*, 36, 359-362.

Smith, A.L., Roobal, M.J., and B.M. Gunn, B. (1980), The Lesser Antilles – A discussion of the Island arc magmatism, *Bull. Volc.*, 43, 287-302.

Wills, J.K. (1974), The geological history of southern Dominica, and plutonic nodules from the Lesser Antilles, PhD Thesis, University of Durham, U.K.

Chapter 3

Narrowing the Gap: New geochemical and geochronological results from Western Nicaragua, with an updated Miocene to Recent Volcanic History

Ian Saginor, Esteban Gazel, Michael J. Carr, Carl C. Swisher III, Brent Turrin
Rutgers University, Department of Earth and Planetary Sciences, 610 Taylor Rd., Piscataway NJ 08854-8066

Abstract

The volcanic record of western Nicaragua documents a significant lull in Central American arc volcanic activity that has been considered to persist from the late Miocene (~ 7 Ma) to the formation of the modern volcanic front around 350 ka. The precise reasons for this lull in volcanic activity is not clear, however it is speculated to have been a consequence of slab rollback.

We report here, geochemical data and $^{40}Ar/^{39}Ar$ ages on two suites of volcanic rocks that occur between Cosigüina and San Cristóbal, Nicaugua, that appear to fill in some of this missing interval. 1) Encanto, an extinct volcanic center composed mainly of basalts dated between 3.6 to 3.2 Ma. 2) Tinajas, another extinct volcanic center, composed of primarily of basaltic andesite to andesite is dated between 2.5 and 1.3 Ma. In addition, a cluster of isolated hills just south of the Encanto unit is identified as the northwest termination of the Tamarindo Formation that ranges in age from about 14.7 to 11.7 Ma. Geochemistry of the new Tamarindo samples suggests that this formation is geochemically distinct from Coyol volcanism that occurred during the same time period.

Previously reported geochemical analyses of the active and Miocene volcanic fronts show that U/Th values increased by nearly threefold following the "carbonate crash" at 10 Ma. This transition was thought to be abrupt, however new data show that it took place

gradually over the last 7 Ma. La/Yb also increases through time and with the distance from the trench, perhaps due to backward migration of the arc towards the trench. Systematic increase in Zr/Nb towards the trench, although indicative of a stronger subduction signal near the trench, shows no correlation with age.

Both the extensive Mid-Miocene Nicaraguan volcanism and the coeval eruption of the Tamarindo and Coyol are consistent with behavior at other circum-Pacific arcs and should not be viewed as anomalous.

Introduction

The pioneering studies of Molnar and Sykes (1969) and Dengo (1962) set the stage for a series of studies trying to unravel the complexities of the Central American Volcanic Front that stretches 1100km from Guatemala to Costa Rica. These studies have generated a wealth of geochemical data currently used to interpret underlying mantle composition, the composition, angle and depth of its subducting slab, as well as the complex and variable mechanisms for the delivery of slab derived material to the zone of magma generation. To accomplish this, McBirney and Williams (1965) and Weyl (1980) relied upon interpretations of stratigraphic relationships amongst the Central America volcanics and later K-Ar and $^{40}Ar/^{39}Ar$ ages on tephra and lavas associated with the numerous Central American volcanoes as well as tephra interbedded in adjacent marine strata. The introduction of K-Ar dating in the 1960's and 70's and subsequently the more precise $^{40}Ar/^{39}Ar$ method, helped illuminate not only the evolution of the arc as a whole, but of individual volcanic centers as well. The challenge now is to integrate the geochemical and

geochronological data into a cohesive model that can be applied to other arcs throughout the world.

Tectonic Setting

The Central American volcanic front extends 1100 km from the border between Mexico and Guatemala to Costa Rica (Figure 1) and is generated by the northeasterly subduction of the Cocos Plate underneath the Caribbean Plate at a rate that ranges from 6 cm/yr off southern Guatemala to 9 cm/yr off southern Costa Rica (Demets, 2001).

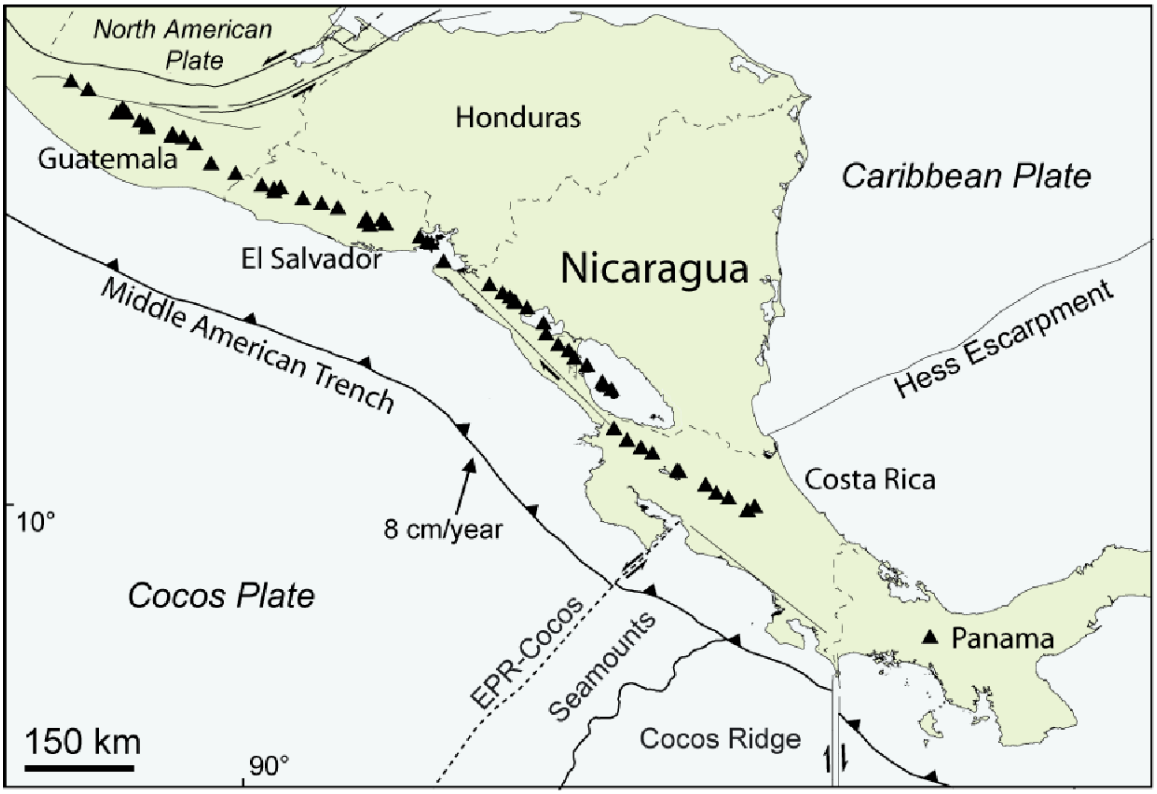

Figure 1. Map of Central American Volcanic Front. Triangles are Holocene volcanoes.

Panama, while geographically part of Central America, has a markedly different tectonic setting, and has not experienced historic volcanism. Rather, to the east of the

Cocos Plate, the Nazca Plate forms either a strike slip system with the Caribbean plate or is slowly subducting underneath Panama.

One of the most obvious arc-wide features in Central America is the physical segmentation of the arc into seven right stepping sections that vary in length from 100 to 300 km (Carr, 1984). The spacing of volcanoes within segments appears to be random with an average of 27 km, however there are a few along-arc gaps with the longest occurring between Cosigüina and San Cristóbal in Nicaragua, a distance of about 80 km.

Study Area

Lava and tephra samples reported in this study were collected primarily from two areas in western Nicaragua (Figure 2). The first area, located between San Cristóbal and Cosigüina, occurs near the northwest termination of the Nicaraguan volcanic front, where we collected 17 samples, most of which were from a low-lying region of basaltic and andesitic lavas and ignimbrites. This area has not received much prior attention perhaps because it occupies the longest stretch of the Central American Volcanic Front without an active volcano. Lack of data from this region has led to confusion of both the type and origin of these rocks.

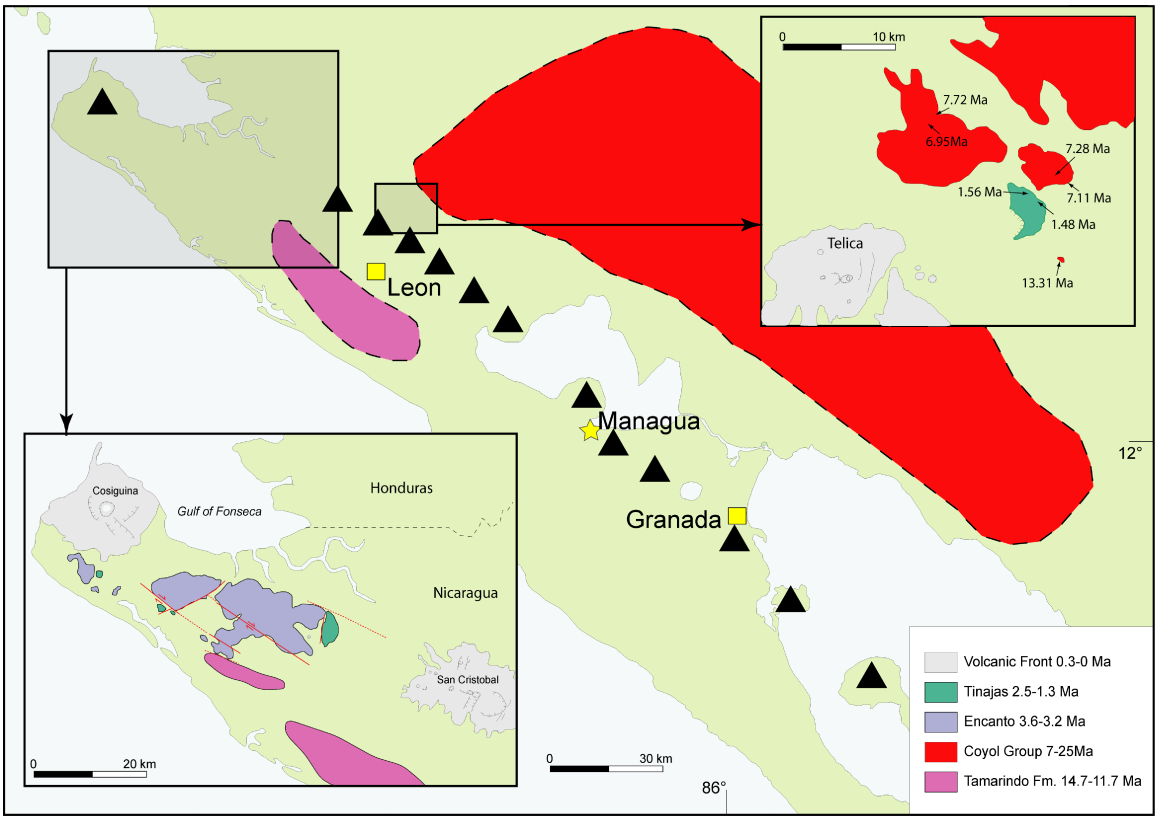

Figure 2. Map of northwest Nicaragua and two primary study areas.

McBirney and Williams (1965) described this region as a mix of Quaternary and Tertiary rocks, while the majority of studies list this region as comprising solely Tertiary volcanic material (Weyl, 1980; Nystrom et al., 1988; Darce, 1989; Elming et al., 2001). One early study mistakenly calls it Quaternary alluvium on a geologic map (Dengo, 1968). The idea that the area was Tertiary was supported by a single $^{40}Ar/^{39}Ar$ date (Elming et al., 2001) from a sample collected nearby from the Tamarindo Formation.

The second primary area of study is also shown in Figure 2 and is located between the Coyol group and active volcanic front. This area was selected in an attempt to locate material that erupted during an apparent hiatus in volcanic production between the end of Miocene volcanism at 7 Ma and the appearance of the modern arc circa 350 ka (Carr et al., 2007). This area consists mainly of weathered domes of basalts to basaltic andesites and

volcaniclastic sediments that partially fill in the Nicaraguan Depression. The volcanic features in this area are low-lying, with a maximum relief of only a few hundred meters, although recent sediments may bury additional relief.

In addition to these two areas, five additional samples were collected from El Salvador and around Masaya in Nicaragua. The El Salvadoran samples are considered to be from part of the Balsamo Formation, which is composed of Upper Miocene to Pliocene andesitic lavas, tuffs, and lahars. Reynolds (1980) also identified the Chalatenango Formation (Middle to Upper Miocene) composed of rhyolitic tuffs and lavas and the Cuscatlán Formation (Pliocene) composed of rhyolitic tuffs and volcanic sediments, both that roughly parallel the Pacific coastline in northern Central America.

Near Masaya, three samples were collected. Two (Nic-2000-2 and Nic-2000-1BM) are lavas taken from the Las Banderas group northeast of Masaya and one (LS-2000-4) is a tephra from the Las Sierras group on Masaya's southwestern flank, that is dipping toward the Pacific. Samples from the Las Sierras and Las Banderas groups near Masaya were thought to represent the earliest expressions of the active arc in Nicaragua.

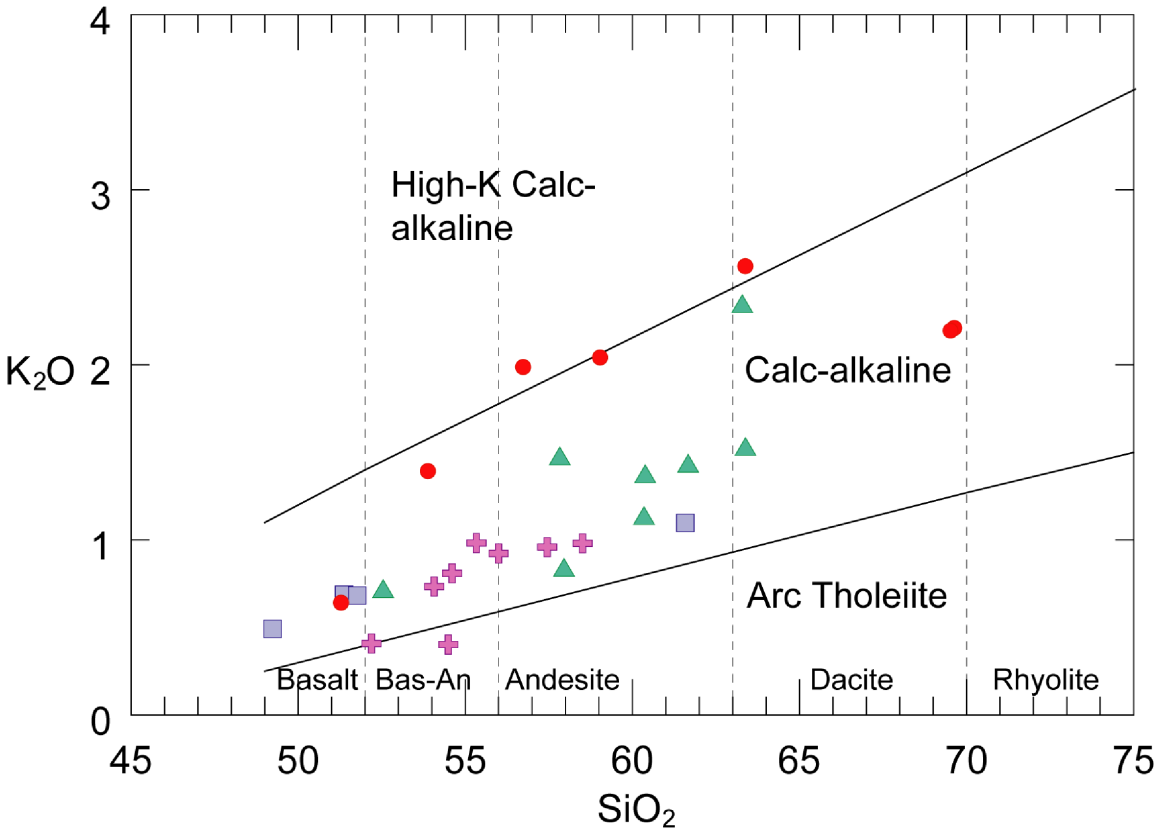

Figure 3. Rock classification diagram for all analyzed samples (Peccerillo and Taylor, 1976). Purple crosses are Tamarindo, blue squares are Encanto, green triangles are Tinajas, red circles are Coyol Group.

Tamarindo Formation

The Tamarindo Formation (Figure 2) consists of a narrow band of basaltic to andesitic lavas interlayered with thick ignimbrite deposits and volcaniclastic sediments that parallel Nicaragua's Pacific coast west of the modern volcanic front. Stretching for at least 80 km beginning 40 km northwest of Managua, the formation was first described in an unpublished report by Wilson (1942) who named it after typical exposures near the coast northwest of Managua. McBirney and Williams (1965) made a more careful description of the area and emphasized the prevalence of ignimbrite deposits over the less common lavas.

Geologic maps of Nicaragua created over the last 40 years have exposed confusion about the origin of the Tamarindo Formation. A 1968 map by Dengo (1968) included parts

of the Tamarindo in the active arc and filled in the area between the volcanic front and the Pacific coast with Quaternary alluvium and Tertiary sedimentary rocks. Nystrom et al. (1988) and Elming et al. (2001) list both the Tamarindo and Coyol as "Tertiary volcanic rocks" whereas McBirney and Williams (1965) seem to ignore the lava component of the Tamarindo entirely and label the Tamarindo as Tertiary ignimbrites, despite having noted the presence of interlayered lavas. Weinberg (1992) uses a modified map after a Ph.D. thesis by Darce (1989) and differentiates the Coyol from the Matagalpa Group, the latter being composed primarily of ignimbrites, which surround Coyol deposits on all sides. On this map, the Tamarindo is not listed by name and is included as part of the Matagalpa group. Weyl (1980) lists the age of Tamarindo variously as Eocene, Oligocene, or Miocene, despite citing a mid-Miocene K-Ar age in the text and is similarly unsure about whether to group the Tamarindo and Coyol together.

Weyl (1980) provided the first K-Ar age constraint for the Tamarindo Formation with a mid-Miocene age of 13.7 ± 0.5 Ma, which, according to Weyl, makes it equivalent in age with the Coyol Formation. This age assignment is supported by four subsequent K-Ar ages for the Tamarindo Formation ranging between 12.3 and 18.4 Ma (Ehrenborg, 1996; Elming et al., 2001; Plank et al., 2002). The upper age limit comes from a whole rock K-Ar analysis on an ignimbrite and may be anomalously old, due to possible xenolith or xenocrystic contamination.

Methods

Samples for geochemistry and $^{40}Ar/^{39}Ar$ dating were obtained from the cores of large boulders or lava blocks collected from the study areas. Most of the samples appear

fresh and unweathered despite apparent intense surficial weathering. The samples were observed under binocular and petrographic microscopes and those that showed the least amount of weathering or alteration were prepared for geochemistry and $^{40}Ar/^{39}Ar$ dating.

Matrix or mineral separates were prepared and analyzed following methods outlined in Carr et al. (2007). The samples were loaded into individual sample wells of aluminum irradiation disks, along with aliquots of the irradiation monitor mineral Alder Creek (AC-1). The loaded sample disks were wrapped in Al foil, sealed in quartz glass tubes, and then irradiated for 0.25 hours in the Cadmium-Lined, In-Core Irradiation Tube (CLICIT) facility of the Oregon State University Triga Research Reactor (OSTR).

The irradiated samples were loaded into sample wells in a stainless steel disk, loaded onto the sample extraction line and baked out at approx. 100° C overnight. Approximately 80 mgs of per sample were incrementally heated in step-wise fashion (15 increments per sample) using a CO2 laser focused through a 6 mm integrator lens. Released gases were purified using an internal cold finger to collect water vapor and C50 getter operated at approximately 2.5 amps to remove unwanted interference gases. Ar was measured on a MAP215-50 mass spectrometer using both conventional analogue and pulse counting methods. Calibration and determination of the irradiation parameter J was determined by multiple total fusion analyses of the co-irradiated monitor mineral Alder Creek Rhyolite Sanidine (ACS-1) using a published reference age of 1.194 ± 0.006 Ma (Turrin et al., 1994; Renne et al., 1998). Interference isotopes produced during irradiation of the samples were corrected using previously published values $(^{36}Ar/^{37}Ar)_{Ca} = 2.72\pm0.06$ $(x10^{-4})$, $(^{39}Ar/^{37}Ar)_{Ca} = 7.11\pm0.02$ $(x10^{-4})$, $(^{38}Ar/^{39}Ar)_{K} = 1.22\pm0.02$ $(x10^{-2})$, and $(^{40}Ar/^{39}Ar)_{K} = 7\pm3$ $(x10^{-4})$ (Renne et al., 1998; Deino et al., 2002). During the analysis of the samples

and standards, mass discrimination was regularly monitored through measurement of air aliquots delivered via an on-line automated air pipette system and varied between 1.000 and 1.007 AMU. Data reduction was made using software program MassSpec written by A. Deino.

Data are plotted on release spectra that show the apparent age, Ca/K ratio, and the percent of released ^{40}Ar of radiogenic origin for each temperature step. $^{36}Ar/^{40}Ar$ is also plotted against $^{39}Ar/^{40}Ar$ on inverse isochron diagrams. Ideally, the data for each individual step fit on a single line such that the slope provides the age and the *y*-intercept provides the initial $^{36}Ar/^{40}Ar$ value. The scatter about the isochron line is given by the mean squared weighted deviation (MSWD), which is listed on each isochron plot in the supplementary material.

Samples for major and trace element analysis were powdered using an alumina powdering mill and analyzed by LA-ICP-MS and XRF at Michigan State University according to methods outlined in Szymanski (2007) and Hannah et al. (2002). Homogeneous glass disks were produced for samples by fusing each powder (3 g) with a lithium tetraborate ($Li_2B_4O_7$) flux (9 g); approximately 0.5 g of ammonium nitrate (NH_4NO_3) was added to ensure oxidation of iron during fusion. Samples were weighed in Pt crucibles (95% Pt, 5% Au) and suspended over an oxidizing flame (~1000°C) on an orbital mixing stage for 25 minutes. Resulting melts were poured into red-hot Pt molds (40 mm diameter) and cooled on a hot plate at ~500°C. These glass disks were then analyzed for major elements and selected trace elements by X-ray fluorescence (XRF) and for trace elements by laser ablation inductively-coupled plasma mass spectrometry (LA-ICP-MS).

Fused disks were analyzed for major elements (SiO_2, TiO_2, Al_2O_3, Fe_2O_3, MnO, MgO, CaO, Na_2O, K_2O, and P_2O_5) as well as Rb, Sr, and Zr on a Bruker S4 Pioneer XRF. Data were reduced using fundamental parameters (e.g. Criss, 1980) in SPECTRAplus software (Bruker AXS, Germany) on the S4 Pioneer; trace elements were determined using standard linear regression techniques. Precision for most elements is <1% RSD, except for P_2O_5 (<2%).

Trace element concentrations were determined on the same glass disks using a CETAC LSX 200 Plus Nd:YAG (266 nm) laser on a Micromass (now Thermo Electron Corporation) Platform ICP-MS with hexapole collision cell. Samples were ablated using a single line scan, after a pre-ablation to clean and roughen the surface. A spot size of 250 μm and a 150 μm/s scan rate were used for the pre-ablation, while the ablation for data acquisition used a 200 μm spot size, a scan rate of 10 μm/s and a defocus into the sample of 50 μm. Using the Selected Ion Recording (SIR) function in the MassLynx software (Waters Corporation, U.S.A.) data for twenty-three (23) elements were acquired: V, Cr, Y, Nb, Ba, La, Ce, Pr, Nd, Sm, Eu, Gd, Tb, Dy, Ho, Er, Yb, Lu, Hf, Ta, Pb, Th and U. A set of 12-15 external rock standards, representing a wide variety of igneous rock compositions and prepared using and identical fusion method, was used for calibration. Before processing, the background signal from the Ar/He carrier gas was subtracted from each sample and standard. Strontium (or zirconium), determined by XRF on the same glass disks, was used as the internal standard for quantification. Final concentrations were determined using a standard linear regression for each element (normalized signal vs. concentration), using only standards with calculated values within 15% of preferred, published values. Precision for all elements is <5% RSD.

Results

Twenty one new geochemical analyses and twenty nine new $^{40}Ar/^{39}Ar$ analyses are presented in this paper. Samples generally plot along the calc-alkaline series and range from basalt to andesite in composition (Table 1, Figure 3).

The area between San Cristóbal and Cosigüina yielded sixteen $^{40}Ar/^{39}Ar$ dates and seventeen geochemical analyses. As mentioned earlier, the age of material from this area was not known, however it has been generally assumed to consist of a single unit. Our data reveal three geochemically and morphologically distinct units spanning at least 13 Ma ranging from 1.1 to 14.3 Ma. The first is identified as the northwestern terminus of the Tamarindo Formation. The other two do not fit into the current geochronological model of western Nicaragua making it is necessary to name and define these two previously unknown units.

	C-06-Nic-1	C-06-Nic-2	C-06-Nic-3	C-06-Nic-4	C-06-Nic-5	C-06-Nic-6	C-06-Nic-7	C-06-Nic-8	C-06-Nic-9	C-06-Nic-10	C-06-Nic-11
Easting	475660	468539	469294	469294	465859	465620	464718	462685	461284	458616	458102
Northing	1404776	1402932	1407569	1407569	1405433	1406257	1406210	1406665	1407499	1405529	1405850
Dist. along trench	603.6	598.5	596.8	596.8	595	594.3	593.6	591.6	590	588.8	588.2
Dist. from trench	178.1	173	177.4	177.4	173.9	174.4	174	173.3	173.4	170.4	170.4
Plateau age	**14.03 ± 0.05**	**13.76 ± 0.09**	**3.653 ± 0.020**	**11.71 ± 0.05**	n/a	**3.60 ± 0.03**	**14.25 ± 0.08**	n/a	**13.54 ± 0.06**	n/a	**13.90 ± 0.07**
Total fusion age	14.06 ± 0.07	13.73 ± 0.17	3.59 ± 0.03	1.75 ± 0.07	n/a	3.59 ± 0.03	14.13 ± 0.08	**11.47 ± 0.07**	12.64 ± 0.07	**12.22 ± 0.07**	12.84 ± 0.06
Isochron age	14.03 ± 0.13	13.76 ± 0.16	3.68 ± 0.04	11.40 ± 0.17	n/a	3.52 ± 0.09	14.48 ± 0.15	14.4 ± 0.7	13.78 ± 0.17	14.72 ± 0.09	14.4 ± 0.3
$^{40}Ar/^{36}Ar$ int.	294 ± 2	295.5 ± 0.9	294.2 ± 0.8	301 ± 3	n/a	300 ± 5	290.8 ± 1.6	284 ± 18	292 ± 3	227.2 ± 1.9	285.5 ± 5
MSWD	2.1	1.2	2.4	1	n/a	0.4	1.5	0.54	1.3	1.2	0.78
$\%^{39}Ar$ on plateau	63	100	93	100	n/a	100	85	n/a	62	n/a	62
SiO_2	51.65	n/a	49.42	51.6	51.99	49.35	49.95	56.24	52.94	53.42	55.14
TiO_2	1.13	n/a	0.69	0.56	1.15	0.82	1.02	1.65	1.87	1.71	1.74
Al_2O_3	15.61	n/a	20.68	18.37	15.93	17.79	16.19	13.89	13.48	14.27	13.93
Fe_2O_3	11.65	n/a	9.23	8.29	11.3	10.97	11.09	11.06	12.97	12.27	11.53
MnO	0.17	n/a	0.17	0.15	0.18	0.2	0.21	0.2	0.21	0.21	0.21
MgO	4.14	n/a	3.33	4.43	3.68	3.85	5.48	2.94	3.84	3.49	3.22
CaO	8.69	n/a	9.98	8.91	8.25	10.3	9.68	7.07	7.95	7.54	7.44
Na_2O	2.77	n/a	2.83	2.77	2.88	2.36	2.63	2.85	2.58	2.49	2.76
K_2O	0.7	n/a	0.66	0.38	0.77	0.65	0.39	0.95	0.95	0.93	0.93
P_2O_5	0.18	n/a	.13	0.06	0.21	0.13	0.17	0.35	0.35	0.33	0.34
Totals	96.69	n/a	97.12	93.52	96.34	96.42	96.81	97.2	97.14	96.69	97.24
LOI	3.17	n/a	2.73	4.36	3.51	3.43	3.06	2.57	2.62	3.08	97.24
V	385	n/a	212	220	370	345	378	329	470	400	386
Ni	29	n/a	33	25	24	21	35	23	31	26	26
Cu	129	n/a	98	152	357	205	297	318	456	326	415
Zn	88	n/a	68	61	85	77	79	106	106	110	108
Rb	12	n/a	9	7	15	9	7	23	20	12	22
Sr	339	n/a	561	318	356	409	369	341	316	344	340
Y	28.68	n/a	16.47	17.85	29.64	21.71	23.93	54.68	56.71	53.3	56.31
Zr	69	n/a	38	36	78	43	57	153	148	140	144
Nb	1.09	n/a	0.84	0.57	1.81	0.79	0.97	2.09	1.97	1.92	1.96
Ba	518	n/a	583	367	494	533	465	972	945	1004	942
La	4.41	n/a	4.59	1.96	5.8	3.94	3.95	9.1	8.95	8.46	9.06
Ce	10.59	n/a	10.23	5.38	12.53	9.25	9.93	22.22	21.16	19.9	21.34
Pr	1.82	n/a	1.57	0.88	2.16	1.52	1.71	3.92	3.88	3.62	3.77
Nd	9.79	n/a	7.74	4.87	11.61	8.03	9.12	21.17	21.18	19.57	20.34
Sm	3.2	n/a	2.21	1.73	3.57	2.5	2.9	7.04	7.05	6.46	6.68
Eu	1.03	n/a	0.84	0.69	1.16	0.86	0.99	2.06	1.97	1.95	1.99
Gd	3.54	n/a	3.27	2.08	3.96	2.71	3.13	7.45	7.58	7.19	7.36
Tb	0.61	n/a	0.4	0.39	0.68	0.48	0.54	1.26	1.29	1.21	1.24
Dy	4.34	n/a	2.52	2.62	4.57	3.27	3.65	8.74	9.08	8.31	8.82
Ho	0.86	n/a	0.49	0.54	0.91	0.65	0.73	0.1.75	1.84	1.68	1.74
Er	2.58	n/a	1.5	1.67	2.74	1.94	2.24	5.27	5.34	5.07	5.21
Yb	2.66	n/a	1.55	1.82	2.84	2.06	2.29	5.62	5.72	5.41	5.45
Lu	0.41	n/a	0.24	0.27	0.42	0.31	0.35	0.83	0.83	0.8	0.82
Hf	2.15	n/a	1.09	1.1	2.24	1.32	1.73	4.83	4.85	4.56	4.7
Ta	0.08	n/a	0.03	0.02	0.12	0.04	0.07	0.16	0.15	0.15	0.15
Pb	2.55	n/a	1.83	1.51	2.7	2.31	2.35	5.72	5.68	6.39	5.76
Th	0.31	n/a	0.61	0.18	0.4	0.39	0.26	0.73	0.64	0.7	0.72
U	0.16	n/a	0.49	0.11	0.19	0.41	0.16	0.42	0.36	0.38	0.38
Cr	20	n/a	5	8	9	4	50	2	16	2	2

	C-06-Nic-12	C-06-Nic-13	C-06-Nic-14	C-06-Nic-15	C-06-Nic-16	C-06-Nic-17	OA-3	C-51	Sa-1	MEL-1	MEL-2
Easting	479610	477630	479875	453307	439801	436857	515519	472920	544588	531139	526947
Northing	1415351	1419917	1413921	1417082	1422361	1421559	1402883	1408510	1422797	1405468	1403408
Dist. along trench	601.6	597.7	602.6	578.5	564.4	562.3	638.3	599.4	653	650.2	647.7
Dist. from trench	189.1	192.1	188.1	177.6	175.5	173.3	196.2	180	227.6	206.1	202.3
Plateau age	n/a	**1.364 ± 0.009**	**1.770 ± 0.017**	**2.49 ± 0.03**	**2.34 ± 0.03**	**3.181 ± 0.011**	**0.67 ± 0.06**	**3.590 ± 0.03**	**8.89 ± 0.07**	**7.72 ± 0.02**	**6.95 ± 0.03**
Total fusion age	n/a	1.359 ± 0.013	1.85 ± 0.04	2.46 ± 0.03	2.25 ± 0.03	3.09 ± 0.02	0.66 ± 0.09	3.550 ± 0.04	9.54 ± 0.19	7.66 ± 0.03	6.86 ± 0.10
Isochron age	n/a	1.364 ± 0.011	1.64 ± 0.06	2.66 ± 0.07	2.45 ± 0.03	3.196 ± 0.015	0.55 ± 0.16	3.640 ± 0.05	8.3 ± 0.3	7.82 ± 0.13	7.5 ± 0.3
$^{40}Ar/^{36}Ar$ int.	n/a	295 ± 6	299.7 ± 1.3	292.5 ± 1.0	251 ± 6	290.6 ± 0.7	298 ± 5	294 ± 0.8	301.0 ± 0.7	291 ± 13	285 ± 2
MSWD	n/a	0.5	2.9	0.2	0.17	1.2	1.2	1	1.1	4.7	1.2
$\%^{39}Ar$ on plateau	n/a	100	61	93	87	86	94	98	60	62	92
SiO_2	76.98	57.75	58.69	50.05	55.42	58.99	61.1	47.14	49.38	51.37	60.54
TiO_2	0.23	0.6	0.62	0.94	0.68	0.64	0.55	0.74	0.83	0.74	0.69
Al_2O_3	10.65	16.94	15.76	17.37	19.12	16.25	15.45	20.43	17.16	16.75	16.73
Fe_2O_3	2.4	6.85	6.98	10.51	6.96	7.87	6.87	10.06	9.98	8.95	4.84
MnO	0.04	0.1	0.13	0.19	0.11	0.14	0.17	0.17	0.17	0.21	0.26
MgO	0.48	2.87	2.78	4.26	1.94	2.11	2.23	3.92	6.23	4.61	1.48
CaO	1.05	6.99	6.51	9.18	7.67	6.06	5.38	11.49	1.06	9.49	5.33
Na_2O	2.56	2.82	2.92	2.9	3.06	3.33	3.73	2.23	2.58	2.56	3.39
K_2O	1.22	1.3	1.35	0.67	1.4	1.05	1.46	0.47	0.61	1.32	2.44
P_2O_5	0.33	0.1	0.13	0.24	0.17	0.13	0.14	0.1	0.22	0.17	0.25
Totals	95.94	96.32	95.87	96.31	96.53	96.57	97.08	96.75	97.22	96.17	95.95
LOI	3.92	3.52	3.97	3.53	3.3	3.25	2.74	3.11	2.64	3.63	3.82
V	50	266	207	305	170	169	138	288	277	249	102
Ni	16	20	17	25	18	24	20	21	55	33	18
Cu	51	39	77	104	116	171	67	336	92	121	47
Zn	29	62	55	88	60	66	57	67	71	76	58
Rb	15	23	22	14	28	19	24	7	7	34	70
Sr	162	361	366	478	396	340	424	518	494	477	404
Y	15.15	20.54	22.98	25.58	26.64	33.33	23.09	16.9	18.69	24.6	32.97
Zr	96	81	96	64	99	86	82	29	55	85	175
Nb	1.71	1.23	1.6	1.21	1.36	1.22	1.45	0.64	1.67	1.65	3.53
Ba	1188	996	1033	654	918	875	1093	438	429	865	1634
La	9.29	6.14	7.5	7.74	8.94	6.7	8.69	3.62	6.83	8.9	13.71
Ce	14.48	14.44	17.96	18.1	17.98	14.23	17.4	7.86	15.63	17.98	30.07
Pr	2.23	2.07	2.43	2.76	2.84	2.49	2.54	1.27	2.19	2.84	4.28
Nd	8.86	9.48	11.15	13.65	13.01	12.78	11.57	6.59	10.38	13.75	18.85
Sm	2.06	2.75	3.03	3.73	3.48	3.9	3.03	2.04	2.76	3.62	4.91
Eu	0.72	0.87	0.94	0.1.17	1.06	1.12	0.96	0.76	0.95	1.06	1.3
Gd	2.2	2.89	3.19	3.82	3.78	4.18	3.14	2.28	2.92	3.73	4.88
Tb	0.37	0.47	0.51	0.6	0.61	0.7	0.52	0.4	0.47	0.6	0.78
Dy	1.99	2.84	3.15	3.82	3.74	4.68	3.24	2.58	2.78	3.71	4.7
Ho	0.4	0.57	0.65	0.75	0.74	0.94	0.65	0.52	0.54	0.73	0.92
Er	1.28	1.74	2	2.22	2.2	2.86	2.07	1.57	1.67	2.13	2.79
Yb	1.41	1.9	2.13	2.32	2.32	2.98	2.3	1.57	1.66	2.28	2.93
Lu	0.24	0.29	0.33	0.34	0.36	0.47	0.37	0.24	0.26	0.34	0.44
Hf	2.4	2	2.33	1.67	2.61	2.44	2.35	1.01	1.3	2.39	4.3
Ta	1.21	0.05	0.06	0.04	0.11	0.12	0.13	0.02	0.06	0.11	0.38
Pb	5.21	3.47	3.75	3.78	5.77	3.41	3.99	3.97	2.75	6.43	12.38
Th	1.67	1.03	1.11	0.69	1.28	0.83	1.2	0.5	0.39	1.42	2.57
U	3.77	1.33	1.25	0.71	1.19	0.56	1.33	0.32	0.27	0.67	1.61
Cr	2	14	6	35	2	1	2	3	132	23	2

	LN-1	LN-6	LN-7	LN-11	LN-12	Ban-00-2	Ban-00-1 BM	Bal-8	Bal-10	LS-00-4
Easting	541035	543354	542503	544873	544670	61368	61263	3916464	3808123	56119
Northing	1394849	1401672	1402188	1405051	1405510	136236	13621	14610376	1461636	131557
Dist. along trench	663.9	662.5	661.5	662.1	661.7	741.7	741	504.3	494.8	720.7
Dist. from trench	201.9	208.9	209	212.6	212.9	210	209.3	184.9	180	144
Plateau age	**13.151 ± 0.017**	**1.13 ± 0.05**	**1.48 ± 0.02**	**7.188 ± 0.006**	**7.111 ± 0.008**	**1.24 ± 0.03**	**1.3 ± 0.03**	**1.067 ± 0.011**	**0.974 ± 0.017**	**1.749 ± 0.018**
Total fusion age	13.03 ± 0.04	1.06 ± 0.04	1.47 ± 0.04	7.098 ± 0.008	7.060 ± 0.010	1.25 ± 0.03	1.29 ± 0.03	1.061 ± 0.014	1.057 ± 0.013	1.75 ± 0.02
Isochron age	13.11 ± 0.10	1.56 ± 0.15	1.48 ± 0.06	7.19 ± 0.03	7.12 ± 0.03	1.21 ± 0.08	1.3 ± 0.2	1.09 ± 0.04	1.11 ± 0.06	1.68 ± 0.05
$^{40}Ar/^{36}Ar$ int.	295 ± 2	286 ± 3	295 ± 1.9	293 ± 3	294 ± 2	297 ± 4	300 ± 20	292 ± 3	273 ± 15	303 ± 6
MSWD	6.8	1	1.4	5	4	0.41	0.38	2.4	1.1	1
$\%^{39}Ar$ on plateau	80	93	100	87	78	100	100	73	78	100
SiO_2	55.99	57.61	55.52	67.06	67.12	n/a	n/a	n/a	n/a	n/a
TiO_2	0.82	0.7	0.71	0.55	0.54	n/a	n/a	n/a	n/a	n/a
Al_2O_3	17.48	17.05	17.74	14.63	14.93	n/a	n/a	n/a	n/a	n/a
Fe_2O_3	6.76	7.52	8.4	4.04	4.02	n/a	n/a	n/a	n/a	n/a
MnO	0.13	0.18	0.17	0.06	0.05	n/a	n/a	n/a	n/a	n/a
MgO	1.97	2.38	2.54	0.59	0.54	n/a	n/a	n/a	n/a	n/a
CaO	6.42	5.78	6.92	3.16	3.13	n/a	n/a	n/a	n/a	n/a
Na_2O	3.47	3.73	3.63	4.31	4.31	n/a	n/a	n/a	n/a	n/a
K_2O	1.95	1.07	0.79	2.12	2.11	n/a	n/a	n/a	n/a	n/a
P_2O_5	0.21	0.19	0.22	0.14	0.14	n/a	n/a	n/a	n/a	n/a
Totals	95.2	96.21	96.64	96.66	96.89	n/a	n/a	n/a	n/a	n/a
LOI	4.67	3.62	3.17	3.13	2.91	n/a	n/a	n/a	n/a	n/a
V	144	115	182	109	112	n/a	n/a	n/a	n/a	n/a
Ni	19	20	19	32	18	n/a	n/a	n/a	n/a	n/a
Cu	44	47	167	232	73	n/a	n/a	n/a	n/a	n/a
Zn	63	83	74	50	51	n/a	n/a	n/a	n/a	n/a
Rb	39	13	9	38	39	n/a	n/a	n/a	n/a	n/a
Sr	354	467	539	278	288	n/a	n/a	n/a	n/a	n/a
Y	26.26	29.44	42.69	34.47	79.67	n/a	n/a	n/a	n/a	n/a
Zr	140	55	47	166	165	n/a	n/a	n/a	n/a	n/a
Nb	2.98	1.17	1.25	4.09	4.12	n/a	n/a	n/a	n/a	n/a
Ba	523	984	807	1348	1347	n/a	n/a	n/a	n/a	n/a
La	10.39	7.89	11.96	13.92	32.16	n/a	n/a	n/a	n/a	n/a
Ce	22.57	14.62	19.58	29.34	49.45	n/a	n/a	n/a	n/a	n/a
Pr	3.17	2.44	4.31	3.9	8.97	n/a	n/a	n/a	n/a	n/a
Nd	14.41	12.25	21.98	16.6	39	n/a	n/a	n/a	n/a	n/a
Sm	3.73	3.5	6.07	4.18	9.27	n/a	n/a	n/a	n/a	n/a
Eu	1.06	1.23	2.2	1.17	2.75	n/a	n/a	n/a	n/a	n/a
Gd	3.87	3.67	6.16	4.41	9.8	n/a	n/a	n/a	n/a	n/a
Tb	0.64	0.6	0.96	0.72	1.39	n/a	n/a	n/a	n/a	n/a
Dy	3.87	3.86	6.44	4.25	9.09	n/a	n/a	n/a	n/a	n/a
Ho	0.75	0.76	1.23	0.87	1.82	n/a	n/a	n/a	n/a	n/a
Er	2.23	2.31	3.59	2.68	5.41	n/a	n/a	n/a	n/a	n/a
Yb	2.31	2.44	3.88	2.95	5.86	n/a	n/a	n/a	n/a	n/a
Lu	0.36	0.38	0.55	0.45	0.88	n/a	n/a	n/a	n/a	n/a
Hf	3.4	1.64	1.33	3.26	3.3	n/a	n/a	n/a	n/a	n/a
Ta	0.23	0.08	0.1	0.54	0.59	n/a	n/a	n/a	n/a	n/a
Pb	5.66	4.07	2.48	9.38	9.77	n/a	n/a	n/a	n/a	n/a
Th	1.98	0.54	0.51	1.91	1.91	n/a	n/a	n/a	n/a	n/a
U	0.85	0.58	0.85	1.64	1.84	n/a	n/a	n/a	n/a	n/a
Cr	2	1	3	3	3	n/a	n/a	n/a	n/a	n/a

Table 1. ICP-MS, XRF, and $^{40}Ar/^{39}Ar$ data. Bold indicates preferred age.

Unit 1: Tamarindo Formation

The Tamarindo Formation has been well-studied, but was never thought to extend this far to the northwest (Plank et al., 2002). Eight lavas and one tephra were collected and analyzed from the Tamarindo Formation producing eight $^{40}Ar/^{39}Ar$ dates and eight geochemical analyses. Rare Earth Element (REE) patterns for these samples are flat (La/Yb values between 1 and 2) and are consistent with previously published values for the Tamarindo Formation (Plank et al., 2002). Although all Tamarindo samples show similar REE patterns, four of these samples have distinctly elevated REE (up to 40 times chondritic, Figure 4) and TiO_2 values (>1 wt.%).

$^{40}Ar/^{39}Ar$ ages on these samples range from 13.8 to 14.7 Ma with one sample significantly younger with an age of 11.7 Ma.

Unit 2: Encanto

The Encanto unit is named after a small hill (12.7146ºN/87.2771ºW), located near the first collected sample (C-51, Figure 5), makes up the bulk of volcanic material between San Cristóbal and Cosigüina. Characterized by low-lying heavily weathered hills, it is also found on the southern flank of Cosigüina approximately three kilometers from the coast. SiO_2 values generally range from 47 to 49 wt.%, with one sample having the significantly higher value of 59 wt.%. Chondrite normalized REE patterns are slightly steeper than Tamarindo with the LREEs being elevated relative to HREEs, with La/Yb values between 2 and 3 (Figure 4).

$^{40}Ar/^{39}Ar$ dating of four samples from the Encanto ranged in age from 3.6 to 3.2 Ma.

Unit 3: Tinajas

Named after one of its characteristic small smooth round hills of basalt, (12.7960ºN/87.1981ºW) the Tinajas unit distinguishes itself morphologically from the deeply eroded Encanto. REE patterns are slightly steeper than Encanto and significantly steeper than Tamarindo with La/Yb values between 3 and 4. SiO_2 values are generally higher than Encanto and range from 55.4-58.7 wt.%

$^{40}Ar/^{39}Ar$ ages for the Tinajas range from 1.3 to 2.5 Ma, with three samples from the area between San Cristóbal and Cosigüina and the fourth from the southern flank of Cosigüina. A step-heating spectrum for sample C-06-Nic-13 is shown in Figure 6.

Of the samples collected between the Coyol and active volcanic fronts two were found have similar $^{40}Ar/^{39}Ar$ ages, 1.1 and 1.5 Ma, as well as similar La/Yb and U/Th values as the Tinajas and are considered to be part of the Tinajas unit.

It is not clear whether the El Salvadoran Balsamo samples or the Nicaraguan Las Sierras and Las Banderas samples should be included in the Tinajas unit, because those samples have not been geochemically analyzed. Our $^{40}Ar/^{39}Ar$ ages for these samples range from 974 ka to 1.75 Ma compared to the Tinajas range of 1.3 to 2.5 Ma, however, given the large distance separating the Tinajas from the Balsamo (~50 km), Las Sierras (~125 km), and Las Banderas samples (~150 km), it is impossible to say with certainty that they are all part of the same volcanic episode.

Regardless of which samples are included as part of the Tinajas, it is important to note that between 1 and 2 Ma, there was active volcanism in El Salvador, Nicaragua, and Costa Rica where the Monteverde Formation was found to be 1.1-2.2 Ma (Carr et al., 2007).

Coyol Group

Six samples collected from the low lying area just behind the active arc were found to have geochemistry and ages (6.95 to 13.31 Ma) in the range of previously reported data (Plank et al., 2002) from the Coyol Group. The Coyol Group is characterized by relatively steep REE patterns compared to the Tamarindo samples. Sample LN-1 (13.3 Ma) is contemporaneous to the Tamarindo Formation, but shares a geochemical affinity to Coyol (relatively steep REE patterns).

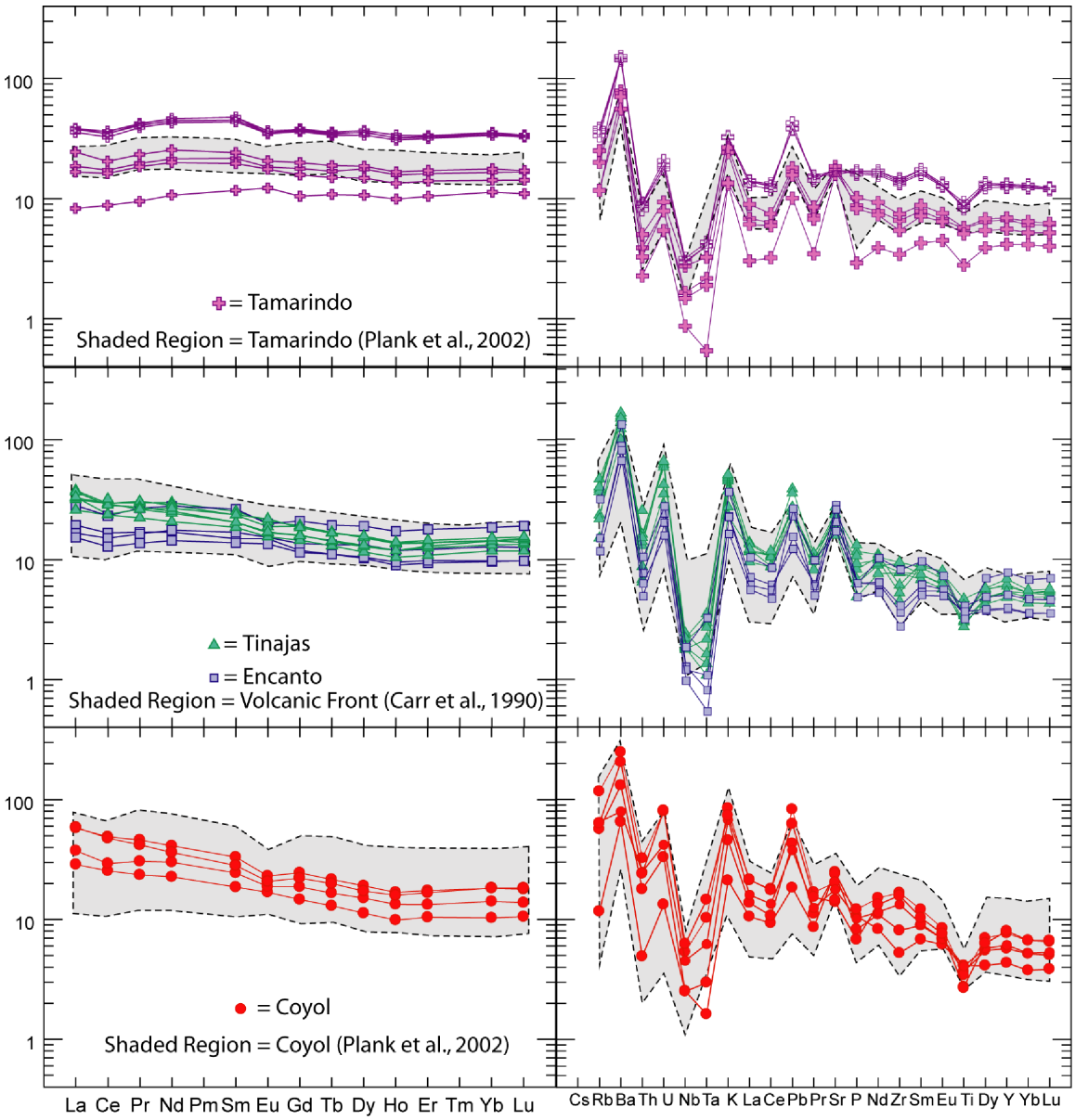

Figure 4. Chondrite and mantle normalized trace elememt patterns. Purple crosses are Tamarindo, blue squares are Encanto, green triangles are Tinajas, red circles are Coyol Group.

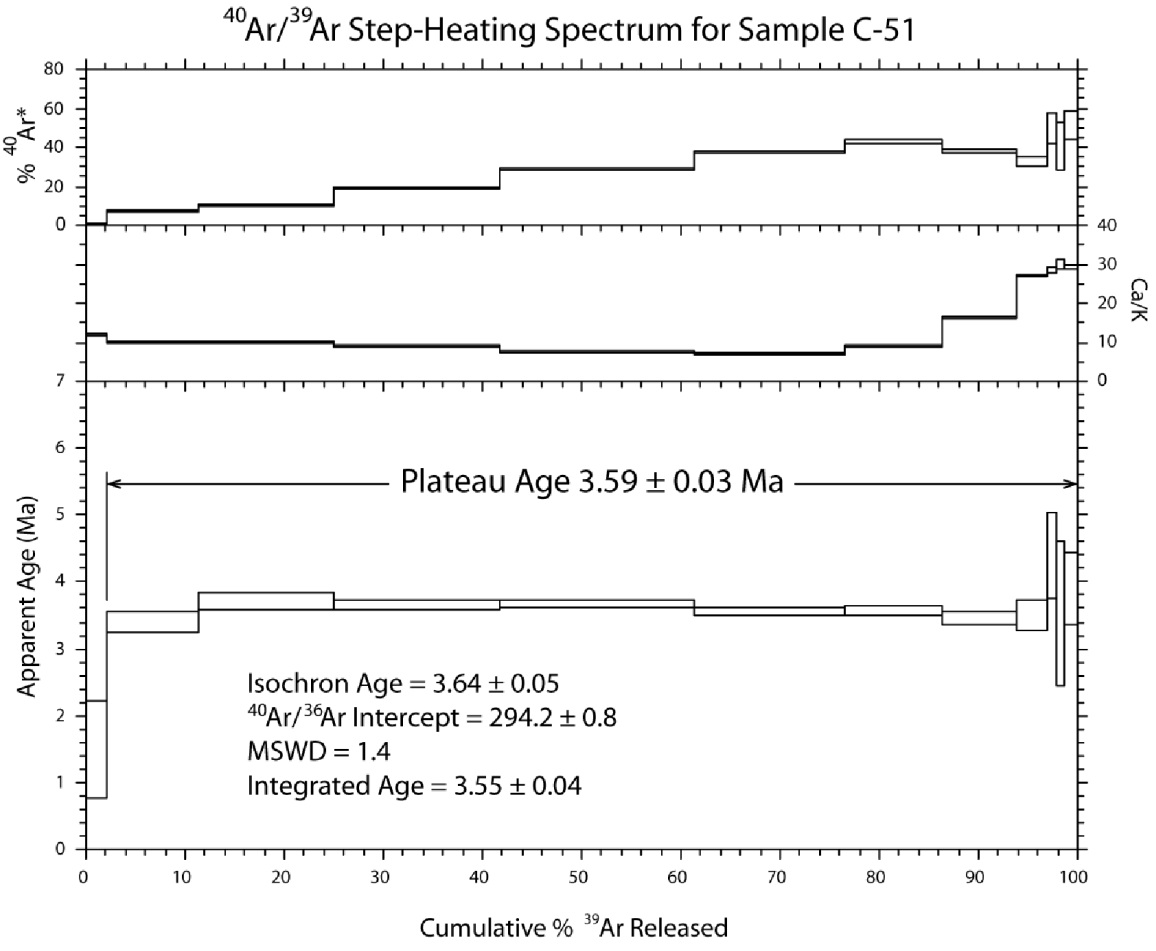

Figure 5. Step Heating Spectrum for Sample C-51.

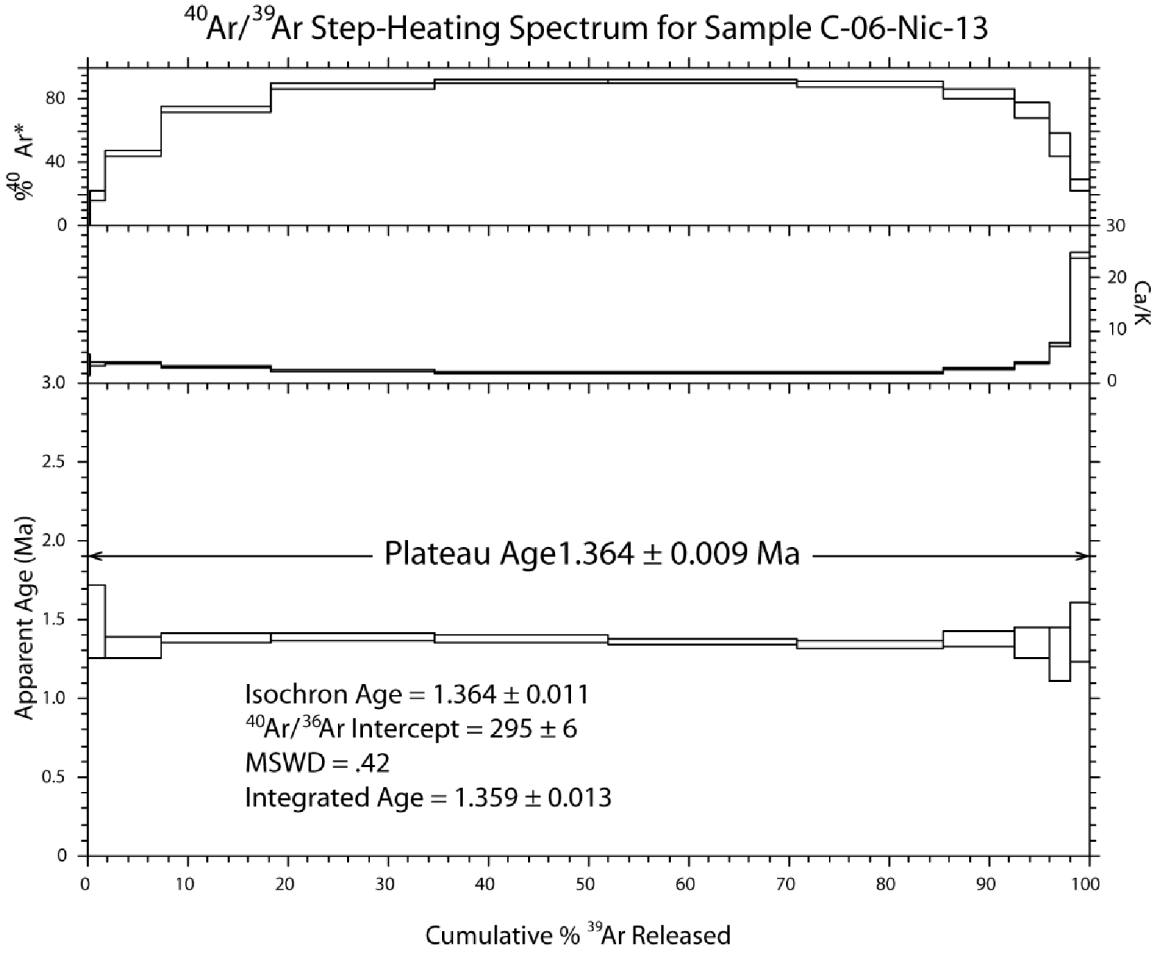

Figure 6. Step Heating Spectrum for Sample C-06-Nic-13

Discussion

Volcanic History

Ehrenborg (1996) describes Middle Tertiary to Recent volcanism of Nicaragua. During the Oligocene, rhyolite shield volcanism resulted in the formation of the Highland Ignimbrite. This was followed by basaltic to andesitic Miocene magmas of the Coyol Group. The Coyol Group records relatively continuous volcanic production and migration of eruptive centers to the southwest for at least 60 km before ceasing volcanism abruptly

~7 Ma (present paper; Carr et al., 2007; Plank et al., 2002; Elming et al., 2001; Ehrenborg, 1996).

Widespread volcanism does not appear to have resumed until ~350 ka, with the formation of the present volcanic arc front (Carr et al., 2007). At least 20 km separate the westernmost lavas of the Coyol Group from the modern arc, with the area between them dominated by low-lying topography broken only by minor volcanism intermingled with weathered volcanoclastic sediments. We hypothesize that either slab rollback or steepening caused the southwestward migration of the volcanic front throughout the Miocene and that this process continued until the front established its current position. It is unclear why this process would be accompanied by a gap in volcanism between 7 Ma and 350 ka, however a volcanic hiatus during this time may explain the presence of a physical volcanic gap between the Coyol and active volcanic front.

Despite the lack of widespread Nicaraguan volcanism between 7 Ma and 350 ka, we present new evidence that the arc was not entirely silent during this "hiatus" and that there were two pulses of volcanism between 3.6 and 1.3 Ma; the younger corresponding in time to Costa Rican volcanism known as the Monteverde Formation (Carr et al., 2007; Alvarado et al., 1993).

The temporal gap appears in satellite imagery as an area of low topography between the active front and Miocene volcanism and seems to extend into Honduras, El Salvador, and to a lesser extent, Costa Rica raising the possibility that it is caused by a pervasive arc-wide tectonic mechanism.

Geochemical evolution

The data presented in this paper allow a more detailed look at the evolution of volcanism in Nicaragua, because samples were recovered from time periods where volcanic activity was thought to be absent (Plank et al., 2002).

The increase in U/Th values in Nicaraguan volcanic material since the Miocene has been attributed to changes in the subducting sediments following the "carbonate crash" (Plank et al., 2002) at 10-12 Ma. At that time, the Central American isthmus began to close, which shut off an important flow of water from the Caribbean to the Pacific (Coates et al., 1992; Lyle et al., 1995; Farrell et al., 1995). This caused the carbonate compensation depth to rise and sediments to become enriched in organic carbon at the expense of carbonate (Hoffmann et al., 1981). The result is that Cocos plate sediments consist mainly of a lower carbonate layer and an upper hemipelagic layer, with the latter unit showing enrichment in U (Patino et al., 2000). This increase in uranium content of subducted sediments is reflected in Nicaraguan lavas in the form of a substantial increase in U/Th values between the Miocene and active volcanic front (Patino et al., 2000; Plank et al., 2002). The timing and rate of this increase could not be determined because there was gap in the volcanic record between 7 Ma and 0.3 Ma (Carr et al., 2007). The data presented here reduce the length of this gap roughly by half, leaving only the period between 7 and 3.6 Ma without known volcanism and Figure 7 shows that the transition from low to high U/Th was more gradual than previously thought.

If the subduction rate has varied between 8 and 10 cm/yr since the Miocene, and the slab dip varied between 45º and 84º and the depth of melt was between 140 and 200 km (ranges from Carr et al., 1990; Protti et al., 1995), it would take 1.4-2.5 Ma for subducted

sediments to reach the depth of melt. Given that flux-melted mantle can reach the surface in less than 8000 years, essentially instantaneous for our purposes (Clark et al. 1998), our data suggest a lag of between 2 and 3 Ma from the time of the carbonate crash to the first increases in the U/Th values of the erupted products. Because the high uranium sediments must build up for a period of time before they are thick enough to influence arc geochemistry, the lower estimate of 1.4 Ma may be more likely.

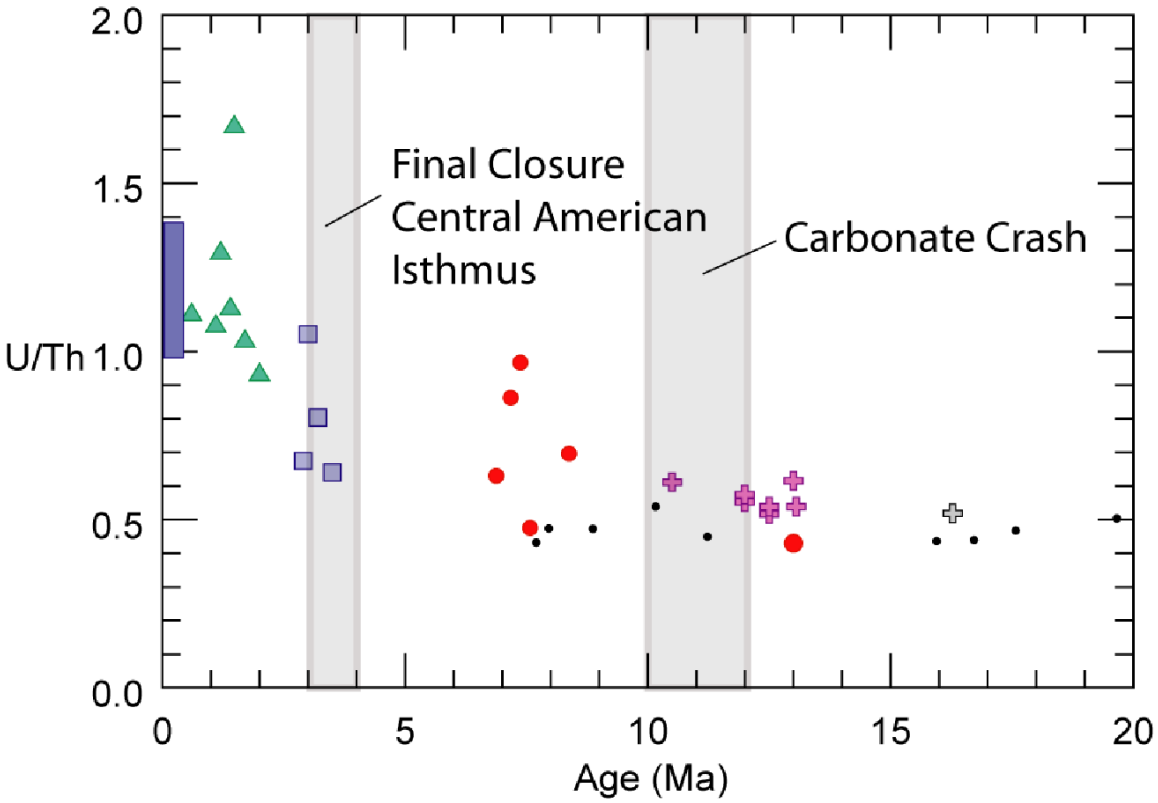

Figure 7. U/Th values for all dated samples vs age. Purple crosses are Tamarindo, blue squares are Encanto, green triangles are Tinajas, red circles are Coyol Group, black dots are Coyol from Plank et al. (2002), Grey crosses are Tamarindo from Plank et al., 2002, and gray shaded regions are from Plank et al. (2002). Blue shaded region is active volcanic front (Carr et al., 1990).

Although the range of La/Yb values are extremely small, two interesting trends are observed: A positive correlation between La/Yb and distance from the trench (Figure 8) and an increase in La/Yb through time (Figure 9). La/Yb values in volcanic material have

been used as a proxy for degree of mantle melt assuming that the source composition does not change, with high values correlating to low degrees of melt and low values correlating to high degrees of melt (Carr et al., 1990). The correlation between La/Yb and distance from trench suggests that the degree of melt is highest near the trench and decreases away from it assuming that the mantle source composition or trench location relative to the volcanic front has not changed significantly since the Miocene. This is not surprising, because if the subducting slab is being progressively dehydrated, then less water is available for lowering the solidus of the mantle peridotite as subduction proceeds (Peacock, 1991). This correlation may not extend to Coyol samples, which have slightly lower La/Yb values than their geographic location suggests. This could be explained if the trench was closer to the Coyol Group during the Miocene than it is now or if the source composition has changed since the Miocene. While the Tinajas samples do not seem to exhibit this trend when viewed alone, as a group, their La/Yb values and distance from trench is consistent with being slightly lower degree melts than either the Encanto or Tinajas.

The correlation between La/Yb and age is not immediately clear because values for all analyzed samples do not fit on a single trend. However, the samples are from two distinct areas (between San Cristóbal and Cosigüina and samples from behind the active arc, Figure 9) and if those two areas are looked at separately, two parallel trends emerge. In each case La/Yb increases through time, which suggests that the degree of melt has been decreasing at least for the last 20 Ma. We interpret this trend as well as the steepening of REE patterns through time as a result of slab roll back, which moved the trench towards the southwest over time and deprived the front of the fluids necessary for producing high degree melts. This mechanism is most clearly manifested in the Tinajas and Encanto units.

These two units along with samples from the Tamarindo Formation form an episodic record of volcanism stretching 13 Ma within a narrow geographic area. Although the degree of melt appears to be decreasing through time as the slab rolls back toward the southwest, volcanism in the area does not migrate with it. This suggests that, despite the migrating slab, the crustal plumbing system that fed the Tamarindo may have remained a convenient pathway to the surface up to the time that the Tinajas unit formed.

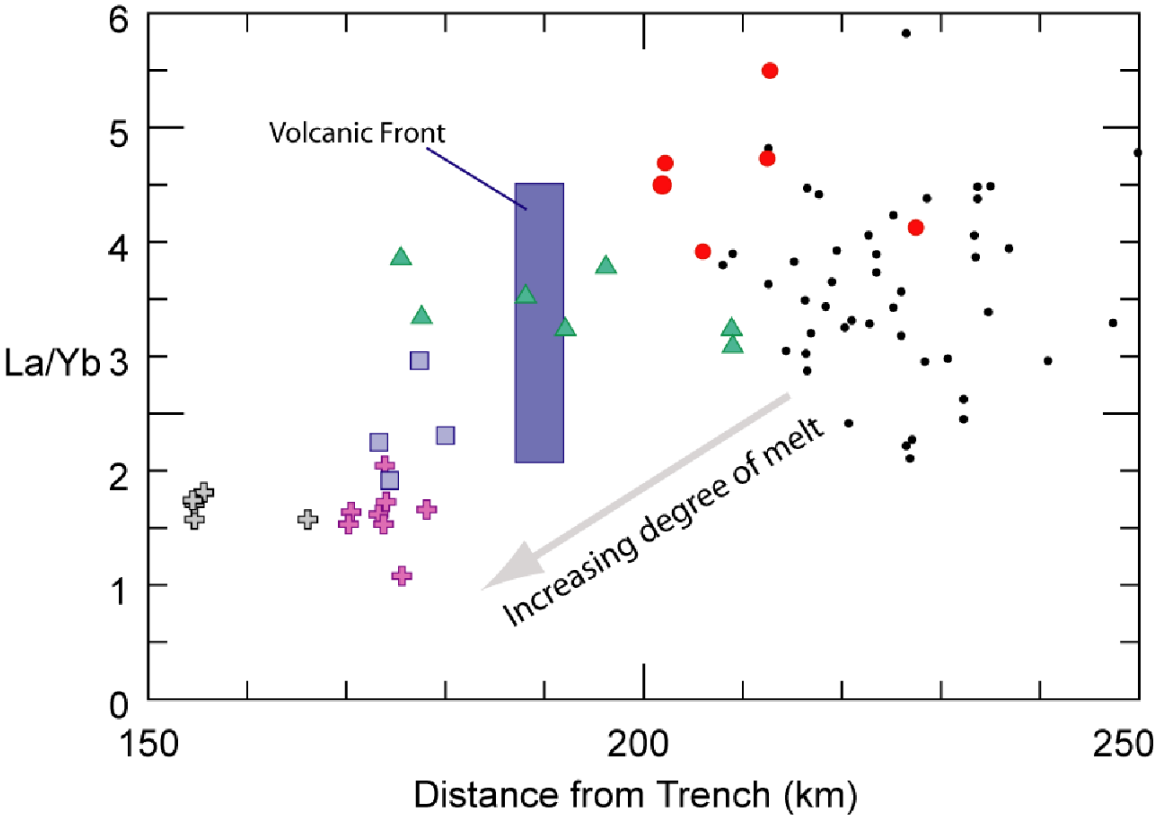

Figure 8. La/Yb values vs. distance from trench. Purple crosses are Tamarindo, blue squares are Encanto, green triangles are Tinajas, red circles are Coyol Group, black dots are Coyol from Plank et al. (2002), Grey crosses are Tamarindo from Plank et al., (2002). Blue shaded region is active volcanic front (Carr et al., 1990).

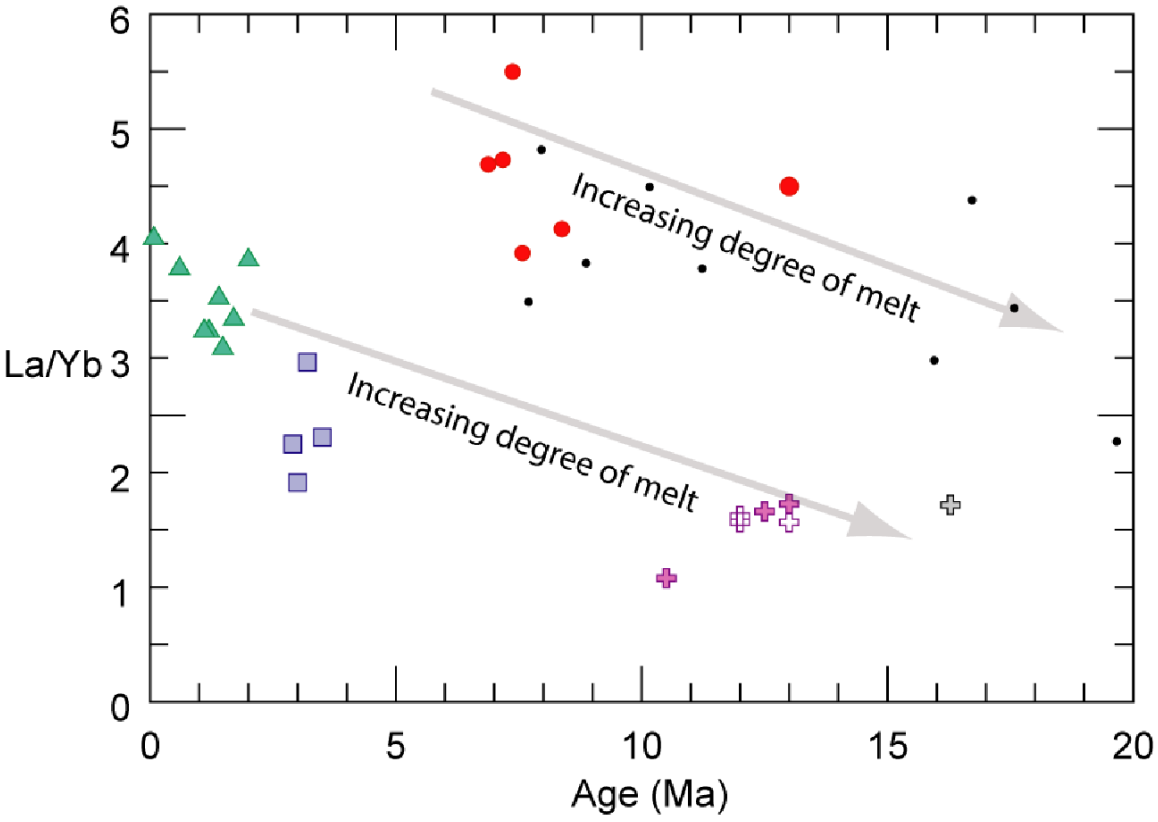

Figure 9. La/Yb values vs. age. Purple crosses are Tamarindo, blue squares are Encanto, green triangles are Tinajas, red circles are Coyol Group, black dots are Coyol from Plank et al., 2002, Grey crosses are Tamarindo from Plank et al. (2002). Blue shaded region is active volcanic front (Carr et al., 1990).

Subduction zone volcanics are typically depleted in High Field Strength Elements (HFSE) relative to Large Ion Lithophile (LILE) (see Kelemen et al., 1990 for review). There is some disagreement as to the cause of this depletion; however, it is generally assumed to result from the presence of residual titanite minerals or amphibole in the subducting slab or the mantle wedge, which favorably partition HFSEs relative to other incompatible trace elements (Kelemen et al., 1990; Walker et al., 2001). Zr/Nb values allow us to examine the ratio of a more compatible HFSE (Zr) with a less compatible one (Nb) and quantify the degree of HFSE depletion. Figure 10 shows a negative correlation between Zr/Nb and distance from the trench, suggesting that the HFSE depletion is related with residual minerals in the subducting slab and not in the mantle wedge. There is also no

evidence that this correlation reveals a change in the mantle source, because there is no correlation between Zr/Nb and age.

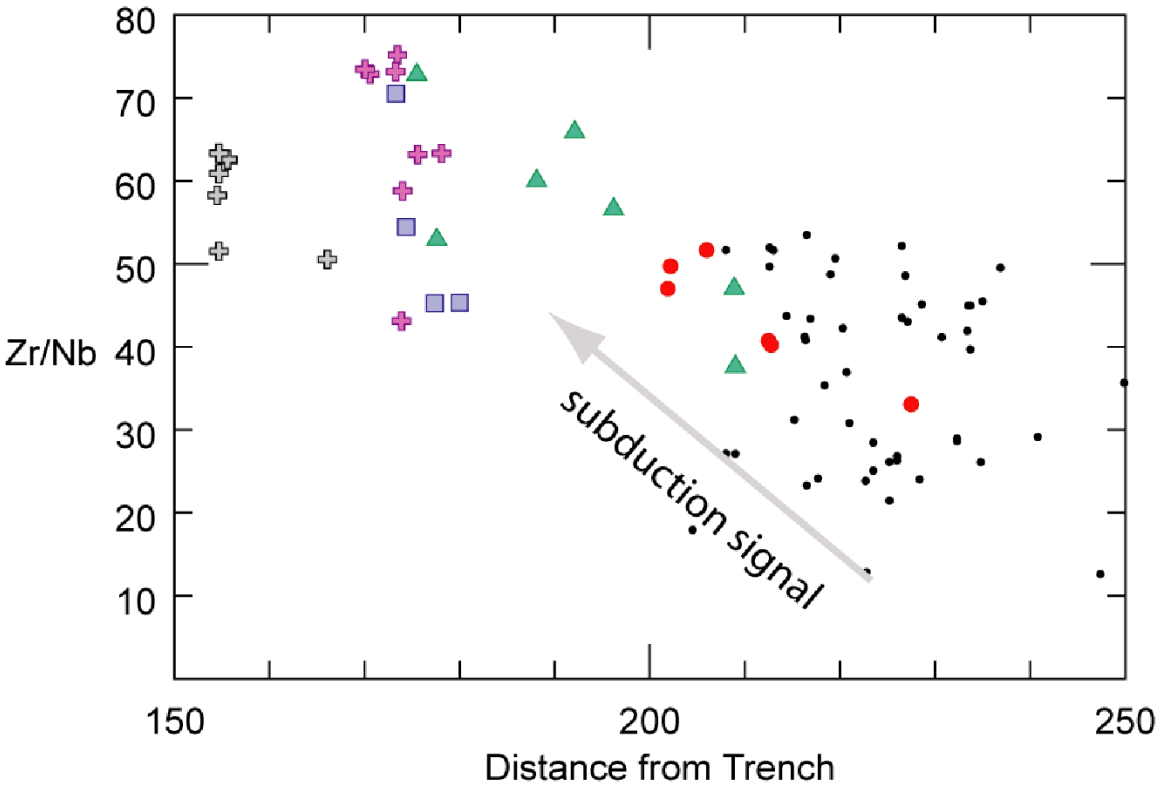

Figure 10 Zr/Nb values vs. distance from trench. Purple crosses are Tamarindo, blue squares are Encanto, green triangles are Tinajas, red circles are Coyol Group, black dots are Coyol from Plank et al. (2002), Grey crosses are Tamarindo from Plank et al. (2002).

Origin of the Tamarindo Formation

Explanations about the origin of the Tamarindo Formation generally fall into three categories.

1) It began as part of the Coyol and was later tectonically separated by normal faulting. In this view, the Tamarindo Formation and Coyol Group are "fully equivalent" as Weyl (1980) concluded and the Nicaraguan Depression is a fault-bounded pull-apart basin as argued by Weinberg (1992). Key to this view is determining the depth of the sediment fill within the depression and the height of the faults on either side. Weyl cites unnamed

"personal communication" to place the depth at 2000m and the maximum exposed fault displacement at 900m, for a total displacement of almost 3km (Weyl, 1980). However, a closer examination by van Wyk de Vries (1993) found that sediment fill in the Nicaraguan depression is much thinner than previously thought and cites a well log from a geothermal plant near Momotombo where the sediment is only 150m deep. In addition, faults such as the Mateare were found to be local features, which precludes the possibility that the Nicaraguan Depression is a typical fault-graben system. Calculations by McKenzie (1978) suggest that the limited regional subsidence is not enough to accommodate the 80 km of extension that separates the Tamarindo from the Coyol. To tectonically accomplish this would either require the formation of ocean crust to fill the gap or subsidence that far exceeds even the largest estimates of offset associated with the Nicaraguan Depression. Also, data presented here suggest that the Tamarindo Formation is geochemically distinct from Coyol. REE patterns for Tamarindo are remarkably flat, while Coyol samples of Tamarindo age (14-16 Ma) are elevated in LREEs relative to HREEs (See Figure 4).

2) The Tamarindo Formation was emplaced elsewhere and transported along strike from either the northwest of southeast. With an age of at least 14 Ma, the Tamarindo certainly had enough time to be transported it to its present location from a great distance away. For example, a rate of only 3cm/yr corresponds to 450km over a 15 Ma period. Although it is mathematically possible to have transported the Tamarindo from another location, the geochemistry presented in this paper suggest that is not the case. There are several along-arc geochemical indicators that reach a maximum or minimum in Nicaragua (Carr et al., 1990) that are useful in determining if the Tamarindo was formed somewhere other than its current location. A plot of Ba/La vs. distance along arc reveals a chevron pattern centered

on a Nicaraguan maximum and tapering off to either side. La/Yb shows the opposite pattern with minimum values located in Nicaragua (Carr et al., 1990). These two chevron patterns apply to samples from both the Coyol and active volcanic fronts. Tamarindo Ba/La values are generally higher and La/Yb values lower than samples to the northwest and southeast suggesting that they are consistent with being emplaced near the center of these geochemical highs and lows. Finally, no evidence has been presented of a right or left lateral fault system that is extensive enough to have transported the Tamarindo to its current location.

3) The Tamarindo Formation was emplaced in situ. Geochemically, this is the most likely explanation. As mentioned above, Ba/La values are higher and La/Yb are lower in Nicaragua than anywhere else along the volcanic front. If the Tamarindo Formation was emplaced in its current location, its Ba/La and La/Yb values should be within the range typical of other Nicaraguan samples. The data confirm that Tamarindo's high Ba/La and low La/Yb are consistent with its current along-arc location (Figure 11). The Tamarindo's La/Yb values not only constrain its origin to the Nicaragua, but also provide evidence that it was emplaced closer to the trench than Coyol. La/Yb values in Nicaragua increase with distance from the trench (Figure 8) and Tamarindo's distinctly low values suggest that its distance to the trench relative to other Nicaraguan units has not changed.

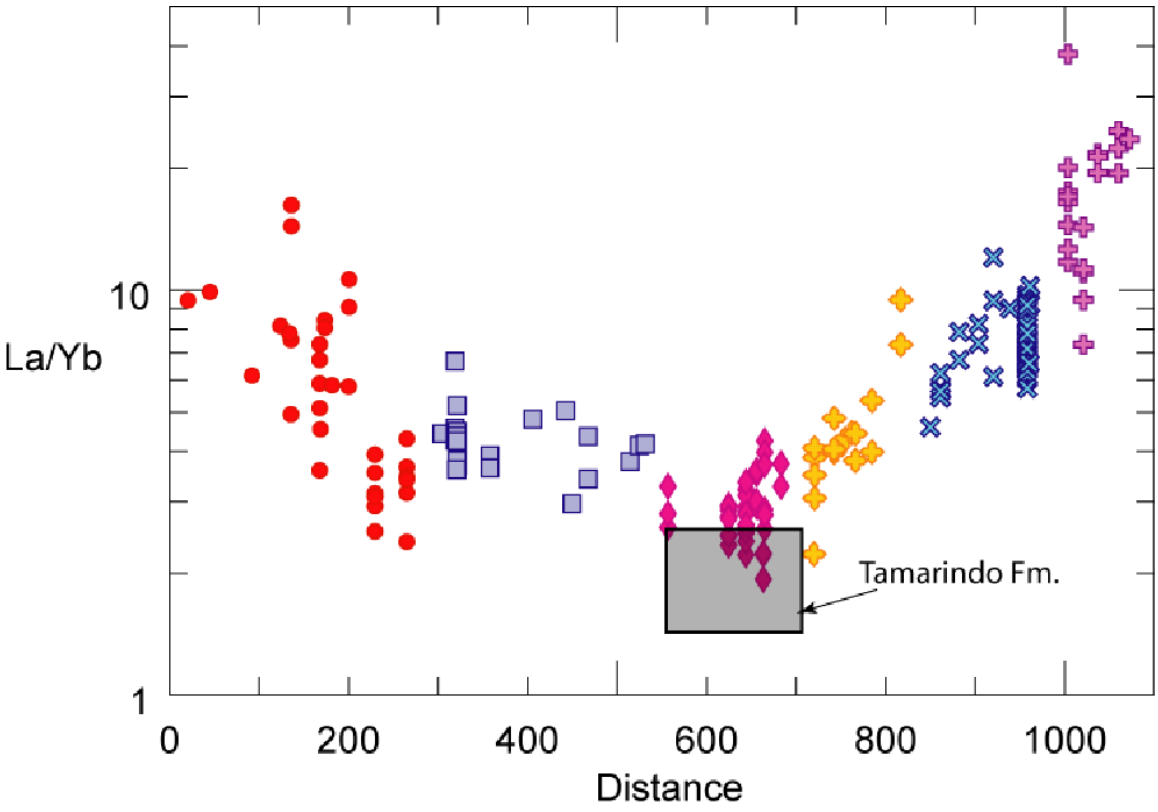

Figure 11. La/Yb values vs. Distance along volcanic front. All symbols are active volcanic front from Carr et al. (1990). Shaded box is Tamarindo.

Mid Miocene Volcanism

The geochemical and geochronological data suggests that the Tamarindo Formation was emplaced in situ and was not transported tectonically to its current location. At the same time, Coyol Group volcanism was active at least 80 km inland (Plank et al., 2002) and one sample (LN-1) collected between the Coyol and active fronts yielded an age of 13.31 Ma. This coeval volcanism suggests that Nicaraguan Mid-Miocene volcanism was not restricted to a narrow volcanic front as is today and that the maximum width of Mid-Miocene volcanism was at least 80 km, compared to no more than 20 km for the active front. If the Tamarindo Formation formed in situ, we are required to explain the presence of extensive Mid-Miocene volcanism as well as the presence of a wider arc.

Many authors have described a sharp increase in circum-Pacific volcanism in the early to mid Miocene and have included studies from the Cascade Range of Oregon (McBirney et al., 1974), the Peruvian Andes (Noble et al., 1974), the Japan arc (Jolivet and Tamaki, 1992), and the Kamchatka-Kurile and Aleutian arcs (Prueher and Rea, 2000). Others have compiled data from numerous arcs that show that the increase in mid Miocene volcanism is truly a circum-Pacific phenomenon (Kennett and Thunell, 1977; Kennett et al., 1977; Cambray and Cadet, 1994). There is some evidence that this early to mid Miocene increase extends to the eastern side of the Central American isthmus. Siggurdson et al. (2000) describes early Miocene peaks at 3 sites in the Caribbean, while Cambray and Cadet (1994) include data from the Lesser Antilles volcanic arc that show a peak between 13 and 17 Ma.

Cambray and Cadet (1994) offer a particularly thorough analysis of six circum-Pacific arcs (Tohuku, Seinan, Bonin, Mexico, Central America, Lesser Antilles) and provide compelling evidence that the mid Miocene volcanic peak is synchronous throughout the Pacific. They also cite Vogt (1979) as evidence that the Hawaiian islands, although far removed from any subduction zone, experienced a significant Mid Miocene peak as well. The extensive Mid-Miocene volcanism in Nicaragua described in this paper fits easily into the Pacific volcanic chronology. In addition, although the proposed 80 km width of Mid-Miocene Nicaraguan volcanism is greater than most arcs, Tatsumi (2005) shows that several active arcs exceed this width.

There are a number of mechanisms that could explain the systematic shifting of the Central American volcanic arc over time and others that could explain why the arc experienced such a dramatic downturn in production. One way to shut off an arc is to

subduct a seamount ridge (Abratis and Worner 2001). In this model the ridge is composed of hotter, thicker, and therefore more buoyant oceanic crust that partially resists forces causing subduction as it collides into the opposing plate. As it does subduct, it does not plunge into the mantle, but slides along the bottom of the upper plate. This not only keeps the subducted lithosphere above the depths required to dehydrate the slab, but pinches out the mantle wedge as well. These two processes may have been responsible for the cessation of volcanism above the subducted Cocos ridge in southern Costa Rica ~8 Ma (Abratis and Worner 2001). Although, ridge collision is a viable mechanism for shutting down arc volcanism, there is no geochemical or tectonic evidence ridge collision/subduction ever occurred in Nicaragua.

The same applies to slab windows, another mechanism for dramatically altering the nature of arc volcanism. Slab windows occur when a mid-ocean ridge is subducted, as happened in southern Costa Rica between 6 and 10 Ma (Johnston and Thorkelson 1997). As the spreading center begins to subduct, the Cocos and Nazca plates continue to spread apart, but now that the spreading occurs at depth, the upwelling mantle does not form new oceanic crust. Instead, it caused partial melting of the buoyant crust making up the Cocos ridge, which forms the trailing edge of the slabs that surround the window (Johnston and Thorkelson 1997, Abratis and Worner 2001). This mechanism potentially explains the adakitic composition of dacitic and rhyolitic volcanism above the window and the enriched OIB mantle source for basalts in this area. While it is not clear that a slab window could shut down arc volcanism on a large scale, the case in southern Costa Rica demonstrates the power of slab windows in altering the nature of subduction related volcanics. However, a

first-order observation of the tectonic history of the Cocos plate makes it unlikely that a slab window was ever subducted in Nicaragua.

Trenchward migration of the Coyol arc in Nicaragua may be related to the more common and well-understood process of slab rollback. If this were true, faulting of the subducting Cocos slab would cause its faulting axis to progressively shift away from the direction of subduction, causing a corresponding shift of the volcanic arc above it. This may explain the observed shift in volcanism over time, but does not necessarily explain the downturn in volcanism that constitutes the gap discussed here. It is possible that this slab rollback happened fast enough, such that the volcanism left in the receding slab's wake could not build up to substantial volumes before the front moved on. In this scenario, the mechanism behind Nicaraguan volcanism never actually shut off and the gap simply represents an increase in the speed of slab rollback. It is also possible that this slab rollback caused a decrease in the speed of the subducting slab, which would deprive the mantle wedge of sufficient fluids needed to drive large scale volcanism.

Slab detachment is known to occur in some convergent margins (Wortel and Spakman 2000). Rogers et al. (2002) use tomographic images to show that northern Central America overlies a detached slab that can account for some topographic highs east of the modern volcanic arc. They estimate that the detachment occurred sometime between 10 and 3.8 Ma, although the younger estimate assumes that slab detachment does not slow subduction, which is almost certainly not the case. Slab detachment could potentially cause a hiatus in volcanic production as the trailing end of the slab stalls near the surface as the forces pulling it into the mantle decrease dramatically. Arc volcanism would not resume until the trailing edge of the slab reaches sufficient depth to cause dehydration of

the sediments and fluid flux into the overlying mantle. It would be difficult to imagine that this process could occur without some decompression melting as the hot mantle rises to through the newly formed slab gap, but the presence of apparent back arc volcanism so close to the active arc in Guatemala and Honduras (Walker et al. 2000) may be evidence of this phenomenon.

Conclusions

- Our new data reduces the duration of the Nicaraguan volcanic hiatus since the Miocene from ~7 Ma to 3.4 Ma.
- The increase in U/Th values between the Miocene and active arc was gradual and due to the carbonate crash brought on by the closure of the Central American isthmus.
- The Tamarindo Formation was emplaced in situ and was not tectonically separated from the Coyol Group.
- Both the extensive Mid-Miocene Nicaraguan volcanism and the coeval eruption of the Tamarindo and Coyol are consistent with behavior at other circum-Pacific arcs and should not be viewed as anomalous.
- Increasing La/Yb values through time in Nicaragua is likely due to slab rollback, which decreases the degree of melt for a given location through time.
- Volcanism between San Cristóbal and Cosigüina has maintained a limited geographic footprint over 13 Ma, while the trench migrated to the southwest. This suggests that conduits feeding lava to this area remained the preferred volcanic path throughout this time period.

References

Abratis, M., and G. Worner (2001), Ridge collisions, slab-window formation, and the flux of Pacific aesthenosphere into the Caribbean realm, *Geology*, 29, 2, 127-130.

Alvarado, G.E., Kussmaul, S., Chiesa, S., Gillot, P.-Y., Appel, H., Wörner, G., and C. Rundle (1993), Resumen cronostratigráfico de las rocas ígneas de Costa Rica basado en dataciones radiométricas, *J. South American Earth Sciences*, 6, 151-168.

Borgeois, J., Azema, J., Baymgartner, P.O., Tournen, J., Desmet, A., and J. Aubouin (1984), The geologic history of the Caribbean-Cocos plate boundary with special reference to the Nicoya Ophiolite Complex (Costa Rica) and D.S.D.P. results (Legs 67 and 84 off Guatemala): A synthesis. *Tectonophysics*, 108, 1-32.

Carr, M.J. (1984), Symmetrical and segmented variation of physical and geochemical characteristics of the Central American volcanic front, *J. Volcanology and Geothermal Research*, 20, 231-252.

Carr, M.J., Feigenson, M.D., and E.A. Bennett (1990), Incompatible element and isotopic evidence for tectonic control of source mixing and melt extraction along the Central American arc, *Contrib. Mineral. Petrol*, 105, 369-380.

Carr, M.J., R. E. Stoiber (1990), Volcanism, *from: The Geology of North America Vol. H: The Caribbean Region*, The Geological Society of America, 375-391.

Carr, M.J., Feigenson, M.D., Patino, L.C., and J.A. Walker (2003), Volcanism and geochemistry in Central America: progress and problems, in *Inside the Subduction Factory,* AGU Geophysical Monograph 138, Edited by Eiler, J. and G. Abers, 153-179.

Carr, M. J., Saginor, I., Alvarado, G. E., Bolge, L. L., Lindsay, F. N., Milidakis, K., Turrin, B. D., Feigenson, M. D., and C. C. Swisher III (2007), Element fluxes from the volcanic front of Nicaragua and Costa Rica, *Geochemistry Geophysics Geosystems*, 8, 6, 1525-2027.

Clark, S.K., Reagan, M.K., and T. Plank (1998), Trace element and U-series systematics for 1963-1965 tephras from Irazú Volcano, Costa Rica: implications for magma generation processes and transit times, *Geochim. Cosmochim. Acta*, 62, 15, 2689-2699.

Coates, A.G., Jackson, J.B.C., Collins, L.S., Cronin, T.M., Dowsett, H.J., Bybell, L.M., Jung, P., and J.A. Obando (1992), Closure of the Isthmus of Panama; the near-shore marine record of Costa Rica and western Panama, *Bull. Geo. Soc. Am*, 104, 7, 814-828.

Condie, C. (2004), Continuity (Ba) and change (U) in Central American geochemistry: New evidence from the Miocene Balsamo Formation in El Salvador, Masters Thesis, Rutgers University.

Darce, M. (1989), Mineralogical alteration patterns, chemical mobility and origin of the La Libertad Gold Deposits, Nicaragua, Ph.D. Thesis, University of Stockholm, Sweden.

Deino, A., Tauxe, L., Monaghan, M., and A. Hill (2002), $^{40}Ar/^{39}Ar$ geochronology and paleomagnetic stratigraphy of the Lukeino and lower Chemeron Formations at Tabarin and Kapcheberek, Tugen Hills, Kenya, *J. Human Evolution*, 42, 117-140.

Demets, C. (2001), A New estimate for present-day Cocos-Caribbean plate motion: Implications for slip along the Central American Volcanic Arc, *Geophys. Res. Lett.*, 28, 21, 4043-4046.

Dengo, G. (1962), Tectonic-igneous sequence in Costa Rica, *in*: Engel, A. E. J., James, H. J., Leonard, B. F. (Eds.), A volume to honor A. F. Budington, *Geol. Soc. Am. Special Volume*, 133-161.

Dengo, G. (1968), Estructura geologica, historia tectonica, y morfologia de America Central, Centro Regional de ayuda tecnica, Mexico, 1-50.

Ehrenborg, J. (1996), A new stratigraphy for the Tertiary volcanic rocks of the Nicaraguan highland, *Geol. Soc. Am. Bull.*, 108, 830-842.

Elming, S.A., Layer, P., and K. Ubieta (2001), A paleomagnetic study of Tertiary rocks in Nicaragua, Central America, *Geophys. J. Int*, 147, 294-309.

Farrell, J., Raffi, I., Janacek, T.R., Murray, D.W., Levitan, M., Dadey, K.A., Emeis, K.-C., Lyle, M., Flores, J.-A., and S. Hovan (1995), Late Neogene sedimentation, patterns, in the eastern equatorial Pacific Ocean, *in* Pisias, N.G., Mayer, L.A., Janecek, T.R., and T.H. van Andel (Eds.), *Proceedings of the Ocean Drilling Program, Scientific Results*, 138, 717-753.

Hannah, R., Vogel, T., Patino, L., Alvarado, G., Pérez, W., and D. Smith (2002), Origin of silicic volcanic rocks in Central Costa Rica: A study of a chemically variable ash-flow sheet in the Tiribí Tuff, *Bull. Volc*, 64, 117–133.

Hoffmann, E.E., Busalacchi, A.J., and J.J. O'Brien (1981), Wind generation of the Costa Rica Dome, *Science*, 214, 552-554.

Johnson, S., and D. Thorkelson (1997), Cocos-Nazca slab window beneath Central America, *Earth Plan. Sci Lett.*, 146, 3-4, 465-474.

Jolivet, L., and K. Tamaki (1992), Neogene kinematics in the Japan Sea region and volcanic activity on the Northwest Japan Arc, In: Tamaki, K., Suyehiro, K., Allan, J., McWilliams, M., (Eds.), *Proceedings of the Ocean Drilling Program, Scientific Results*, 127/128, 1311-1331.

Kelemen, P.B., Johnson, K.T.M., Kinzler, R.J., and A.J. Irving (1990), High-field-strength element depletions in arc basalts due to mantle–magma interaction, *Nature*, 345, 521-524.

Kennett, J.P., and R.C. Thunell (1977), On explosive Cenozoic volcanism and climate implications, *Science*, 196, 1231-1234.

Lyle, M., Dadey, K.A., and J.W. Farrell (1995), The Late Miocene (11-8 Ma) Eastern Pacific carbonate crash: Evidence for reorganization of deep-water circulation by the closure of the Panama Gateway, *in* Pisias, N.G., Mayer, L.A., Janecek, T.R., and T.H. van Andel (Eds.), *Proceedings of the Ocean Drilling Program, Scientific Results*, 138, 821-838.

McBirney, A, Williams, H. (1965), Volcanic History of Nicaragua, *University of California Publications in Geological Sciences*, 55, 1-73.

McBirney, A.R., Sutter, J.F., Naslund, H.R., Sutton, K.G., and C.M. White (1974), Episodic volcanism in the Central Cascade Range, *Geology*, 2, 585-590.

McKenzie, D., (1978), Some Remarks on the Development of Sedimentary Basins, Earth and Planetary Science Letters, 40, 25-32.

Molnar, P., and L.R. Sykes (1969), Tectonics of the Caribbean and Middle America Regions from focal mechanisms and seismicity, *Geo. Soc. Am. Bull.*, 80, 1639-1684.

Noble, D.C., McKee, E.H., Farrar, E., and U. Peterson (1974), Episodic Cenozoic volcanism and tectonism in the Andes of Peru, *Earth Plan. Sci. Lett.*, 21, 13-23.

Nystrom, J., Levy, B., Troeng, B., Ehrenborg, J., and G. Carranza (1988), Geochemistry of volcanic rocks in a traverse through Nicaragua, *Reviste Geological America Central*, 8, 77-109.

Patino, L.C., Carr, M.J., and M.D. Feigenson (2000), Local and regional variations in Central American arc lavas controlled by variations in subducted sediment input, *Contrib. Mineral. Petrol*., 138, 265-283.

Peccerillo, R., and S.R. Taylor (1976), Geochemistry of Eocene calc-alkaline rocks from the Kastamonu Area, Northern Turkey, *Contrib. Min. Pet.*, 58, 63-81.

Peacock, S.M. (1991), Numerical simulation of subduction zone pressure-temperature-time paths: Constraints on fluid production and arc magmatism, Philos. *Trans. R. Soc. Lond.*, 335, 341-353.

Plank, T., Balzer, V., and M.J. Carr (2002), Nicaraguan volcanoes record paleoceanographic changes accompanying closure of the Panama Gateway, *Geology* 30, 1087-1090.

Prueher, L.M., and D.K. Rea (2001), Tephrochronology of the Kamchatka-Kurile and Aleutian arcs: evidence for volcanic episodicity, *J. Volc. Geotherm. Res.*, 106, 67-84.

Renne, P.R., Swisher, C.C., Deino, A.L., Karner, D.B., Owens, T.L. and D.J. DePaolo (1998), Intercalibration of standards, absolute ages and uncertainties in $^{40}Ar/^{39}Ar$ dating, *Chemical Geology*, 145, 117-152.

Rogers, R., Karason, H, and R. van der Hilst (2002), Epeirogenic uplift above a detached slab in Northern Central America, *Geology*, 30, 1031-1034.

Reynolds, J.H. (1980), Late tertiary volcanic stratigraphy of northern central America, *Bull. Volc.*, 43, 3, 601-607.

Sun, S.-s., and W.F. Mcdonough (1989), Chemical and isotopic systematics of oceanic basalts: implications for mantle composition and processes, *Geo. Soc., London, Spec. Pub.*, 42, 313-345.

Szymanski, D.W. (2007), Magmatic evolution of ignimbrites in the Bagaces Formation, Guanacaste Province, Costa Rica, Ph.D. Thesis, Michigan State University, 1-340.

Tatsumi, Y. (2005), The subduction factory: How it operates in the evolving Earth, *GSA Today*, 15, 7, 4-10.

Turrin, B.D., J.M. Donnelly-Nolan, and B.C. Hearn Jr. (1994), $^{40}Ar/^{39}Ar$ ages from the rhyolite of Alder Creek, California; age of the Cobb Mountain normal-polarity subchron revisited, *Geology*, 22-3, 251-254.

van Wyk de Vries, B. (1993), Tectonics and magma evolution of Nicaraguan volcanic systems, Ph.D. Thesis, Open University, Milton Keynes, UK, 1-328.

Vogt, P.R. (1979), Global magmatic episodes: New evidence and implications for the steady state mid-oceanic ridges, *Geology*, 7, 93-98.

Walker, J., Patino, L, Cameron, B., and M. Carr (2000), Petrogenic insights provided by compositional transects across the Central American Arc: Southeastern Guatemala and Honduras, *J. Geophys Res.*, 105, 18,949-18,963.

Walker, J.A., Patino, L.C., Carr, M.J., and M.D. Feigenson (2001), Slab control over HFSE depletions in central Nicaragua, *Earth Plan. Sci. Lett.*, 192, 533-543.

Weinberg, R.F. (1992), Neotectonic development of Western Nicaragua, *Tectonics*, 11, 5, 1010-1017.

Weyl, R. (1980), Geology of Central America, Beiträge zur regionalen Geologie der Erde, 15, 1-371.

Wortel, M., and W. Spakman (2000), Subduction and Slab Detachment in the Mediterranean-Carpathian Region, *Science*, 290, 1910-1917.

Chapter 4

Geochemical variations along the Central American volcanic front controlled by subducting input and melting mechanism: A new look at Ba/La and U/Th ratios

Ian Saginor, Esteban Gazel, Claire Condie, Michael J. Carr
Rutgers University, Department of Earth and Planetary Sciences, 610 Taylor Rd., Piscataway NJ 08854-8066

Abstract

New geochemical analysis of Tertiary volcanic rocks in El Salvador add to existing data from Nicaragua and Costa Rica to greatly increase the geographic range of high quality geochemical data for Tertiary Central American volcanics. Combined with $^{40}Ar/^{39}Ar$ available ages, these data provide further insight into our understanding of the temporal geochemical evolution of the Central American volcanic arc. Our findings support those of Plank et al. (2002) for Nicaragua in which the Miocene and modern volcanics have similar Ba/La profiles along the volcanic front, both in magnitude and spatial distribution; whereas, Miocene and modern volcanics have dissimilar U/Th profiles along the front, the modern volcanics having higher U/Th ratios, particularly in Nicaragua. The change in U/Th contents in the volcanics coincide temporally with similar change noted in Cocos Plate sediments. The oldest subducting Cocos Plate sediments were Middle to Lower Miocene carbonates with little U, whereas, the younger Quaternary to Upper Miocene sediments are hemipelagic muds, rich in organic material and U. The high U/Th values of the modern arc are the result of the cycling of this U-rich sediment via subduction and subsequent volcanism. The cause and timing of the change in U/Th in the sediments is not fully known.

Ba/La has been traditionally used as a geochemical proxy for contributions from the subducting slab. It defines a chevron pattern with a peak centered in Western Nicaragua with lower values towards both ends of the volcanic front (Guatemala and Central Costa Rica). However, our analyses indicate that the Ba concentrations, both in subducting sediment and in the arc itself, do not vary along strike. Therefore, the chevron pattern is controlled primarily by changes in La, an indicator of the degree of partial melting. Trace element models of four segments of the volcanic front in Nicaragua and Costa Rica indicate that the mantle most likely has been modified by a higher percentage of sediment underneath Nicaragua than in Costa Rica, but not a result of more sediment entering the subduction zone. Instead, the sediment component most likely makes up a smaller percentage of the MM source in Costa Rica, because of the additional seamount component

Introduction

The Central American volcanic front extends 1100 km from the border between Mexico and Guatemala to Costa Rica (Figure 1) and is generated by the northeasterly subduction of the Cocos Plate underneath the Caribbean Plate at a rate that ranges from 6 cm/yr off southern Guatemala to 9 cm/yr off southern Costa Rica (Demets, 2001). One of the obvious features in Central America is the physical segmentation of the volcanic front into seven right stepping lines that vary in length from 100 to 300 km (Carr, 1984). The spacing of volcanic centers within segments averages 27 km, however there are a few along-arc gaps with the longest occurring between Cosigüina and San Cristóbal in Nicaragua, a distance of about 80 km.

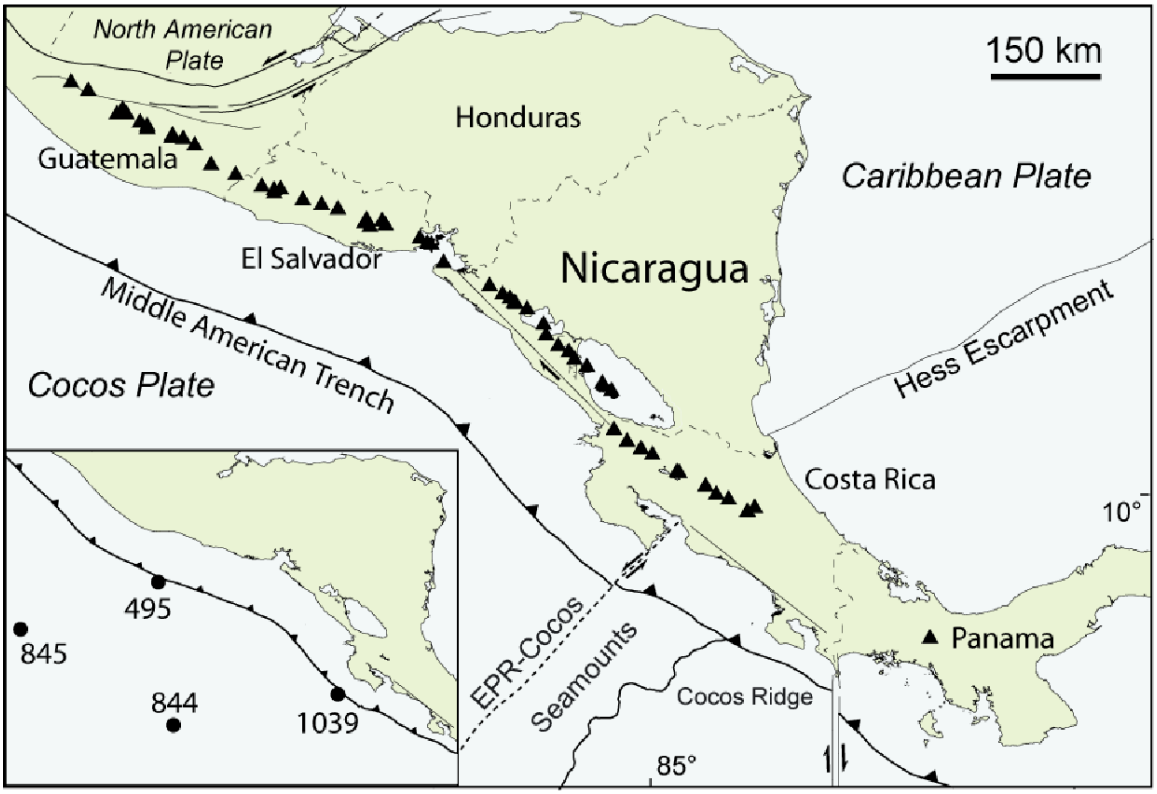

Figure 1. Map of Central American Volcanic Front. Triangles are Holocene volcanoes. Inset shows locations of core sites.

Reynolds (1980) summarized the late Tertiary volcanic stratigraphy of Northern Central America, using many of the units defined by Wiesemann (1975). An elongate Tertiary volcanic belt strikes N 70° W, roughly parallel to the Pacific Coast for 800 km through Guatemala, El Salvador, and into Honduras. In central and eastern Honduras and northern Nicaragua, the Tertiary belt widens significantly. Reynolds divided the Tertiary volcanic sequence into three lithostratigraphic formations that roughly parallel the Pacific Coastline: the Chalatenango Formation (Middle to Upper Miocene) composed of rhyolitic tuffs and lavas, the Balsamo Formation (Upper Miocene to Pliocene) composed of andesitic lavas, tuffs, and lahars, and the Cuscatlán Formation (Pliocene) composed of rhyolitic tuffs and basaltic lavas. The Chalatenango Formation occurs inland from the

presently active volcanic belt. The Balsamo Formation is coincident with or on the Pacific coastal side of the currently active volcanic belt. In eastern and central El Salvador, the Cuscatlán Formation overlies the Balsamo Formation on the coastal side of the volcanic belt. In western El Salvador, the Cuscatlán Formation occurs on the northern side of the Tertiary volcanic belt, where it overlies the Chalatenango Formation.

In Nicaragua, the Tertiary was dominated by basaltic and andesitic lavas of the Coyol and Tamarindo Formations, with the latter being the only Miocene Nicaraguan volcanism to the southwest of the active front. The Coyol is often found associated with Miocene ignimbrites of the Matagalpa Formation (McBirney and Williams, 1965). Costa Rica was similarly active during this time period with the exception of 10-7 Ma, when a gap in volcanism was associated with pluton emplacement (Gans et al., 2002).

It is now clear that the volcanic front has shifted through time (Plank et al., 2002; Carr et al. 2007; Saginor et al., in prep). Available geochronological data indicate that the currently active volcanic front started approximately 600 kyr in the same location as the earlier front that was active from 2 Ma to 1 Ma (Carr et al., 2007). For the most part, the Tertiary volcanic fronts were inland from the Quaternary (2-1Ma) and Modern (<600 ka) volcanic front with the exception of Costa Rica where the modern front is underlain by volcanism of Early Miocene to Pliocene age (Figure 6). Volcanic activity has generally migrated westward since the middle Miocene towards the Pacific Coast. The character of the volcanics changed from dominantly silicic tuffs to andesitic flows to basaltic flows during the late Pliocene to Quaternary (Reynolds, 1980). A secondary type of volcanism, composed of bimodal basalt-rhyolite suites and termed the Cuscatlán, occurred since the late Pliocene in the region behind the volcanic front. The extensive flows and tuffs of the

middle Miocene, the Chalatenango Formation, occur inland of the present volcanic front and along the central and northern parts of the Tertiary volcanic belt. These extensive, predominantly silicic deposits represent a substantially more productive, broader, and longer lasting volcanic episode.

Over the last 20 Ma, the volcanic front of Central America has migrated, usually in the trenchward direction, allowing the geochemical history to be sampled Carr et al., 2007; Plank et al., 2002; Ehrenborg, 1996). The subducting Cocos plate has a simple sedimentary stratigraphy consisting primarily of an upper hemipelagic layer overlying a carbonate sedimentary layer (Patino et al., 2000). It is generally thought that, outside of central Costa Rica, these sediments are not accreted and that the complete subduction of the Cocos plate allows comparison of the subducted input and volcanic output (Patino et al., 2000 and Plank et al., 2002; Solomon et al., 2006). However, significant ^{10}Be enrichment in Nicaraguan front volcanoes may suggest incomplete subduction of the hemipelagic sediments towards the edges of the margin in Guatemala and Costa Rica (Leeman et al., 1994).

Plank et al. (2002) sought to trace the geochemical history of Nicaraguan volcanism from the Miocene to present. Remarkably, they showed that the Ba/La profile for the Tertiary and modern volcanics is essentially the same, while the U/Th profile along the Tertiary volcanic front in Nicaragua is very different from the profile derived from the presently active volcanoes. We report here new geochemical data on Tertiary rocks from El Salvador, which allow us to extend the along arc profiles in Ba/La and U/Th for the Tertiary arc. The main objective of this work is to reexamine the temporal variation in the U/Th profile and the lack of variation in the Ba/La profile using this wider reference frame.

Stratigraphy of the Cocos Plate

ODP Sites 844 and 845 (Plank et al., 2002), DSDP Site 495 (Patino et al., 2000), ODP site 1039 (Solomon et al., 2006) provide a sedimentological and chemical stratigraphy for the Cocos Plate (Figure 2, core locations in Figure 1). The sedimentary column consists largely of two units: pelagic carbonate overlain by diatomaceous hemipelagic clayey ooze. The two closest sites to the trench are Site 1039 off the Nicoya Peninsula of Costa Rica and Site 495 off of Guatemala. Despite being 600 km apart, these two sites have very similar lithologies and barium distributions throughout both the carbonate and hemipelagic layers. Uranium values of 495, 844, and 845 all increase sharply in the upper hemipelagic layer at the same time, when corrected for distance from trench (Figure 2). It is unfortunate that no cores are available at the trench offshore of Nicaragua that would allow us to confidently assert that the composition of the subducting sediment does not vary along strike. However both site 844 (600 km offshore Nicaragua) and 845 (435 km offshore Guatemala) have similar Ba profiles as 1039 and 495 (Patino et al., 2000; Solomon et al., 2006). Both 844 and 845 lack the organic carbon and related uranium enrichment of 495 and 1039, which is most likely due to their distance from the terrestrial sources of organic carbon. The similar barium values in these four cores, suggests that barium levels are relatively constant throughout sedimentary layers on the Cocos Plate and are not controlled solely by distance from the shallower waters of the margin.

In the carbonate section, incompatible elements are in low concentration or vary little with depth (e.g. Sr, Ba). In the hemipelagic section, there are some strong gradients:

Ba, and Pb increase with depth and U decreases. Th, K, Rb, Cs, and Sr show little variation with depth. The mean values of Ba, La, Y, and Pb are only slightly higher in the hemipelagic section than in the carbonate section. However, the mean values of U, Cs, Th, K and Rb are much higher in the hemipelagic section.

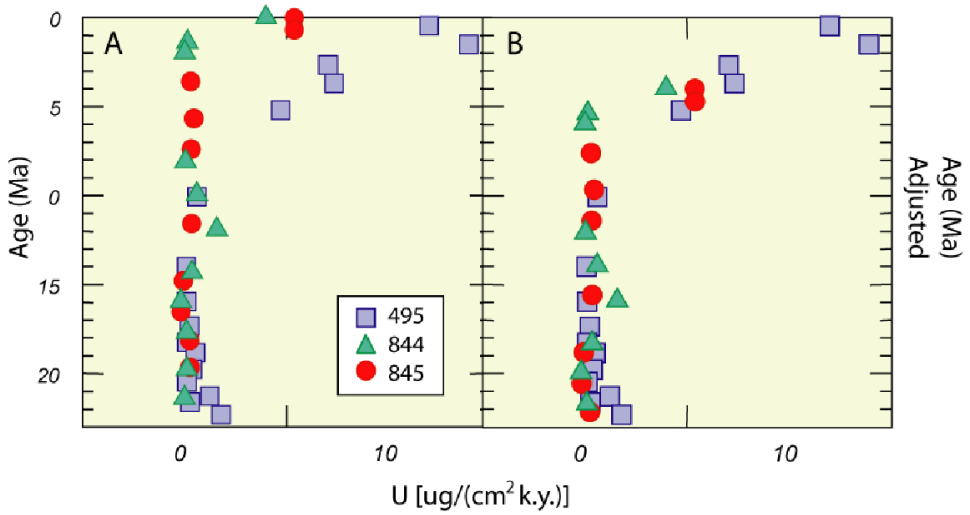

Figure 2. A) U concentration in core samples vs. age (after Plank et al., 2002). B) U concentration in core samples vs. adjusted age (from Condie, 2004).

The Slab Contribution

Large geochemical variations occur in Central American front lavas (Figure 3, Carr et al., 1990; Morris et al., 1989; Leeman et al., 1994). Both Na_2O content (Plank and Langmuir, 1993) and La/Yb (Carr et al., 1990) indicate that the degree of melting is highest beneath Nicaragua and that extent of melting decreases to the northwest and southeast. Similarly, the element ratios that trace slab input, Ba/La, U/Th, and Ba/Th, are highest in Nicaragua and decrease to the northwest and southeast.

It has been determined that slab contribution for Central American volcanics originates from both the sedimentary layers and the altered oceanic crust subducting along the Middle American trench (Patino et al., 2000). Patino et al. (2000) have shown that the

sediment signal is a mixture between the upper organic rich hemipelagic section of the Cocos Plate (with low Ba/Th and high U/La) and the lower pelagic carbonate section (with high Ba/Th and low U/La) of the Cocos Plate. Well-sampled volcanoes such as Arenal and Telica support the conclusion that the slab component was produced by mixing between these two end members (Olney, 2006; Bolge et al., 2006).

Oxygen isotopes ($\delta^{18}O_{olivine}$) from basalts and basaltic-andesites from the Central American Volcanic Front, vary from a minimum of 4.6‰, centered in western Nicaragua to a maximum of 5.7‰ in Guatemala (Eiler et al., 2005). This variation correlates with major and trace elements, and Sr and Nd isotope values of the host lavas. Eiler et al. (2005) interpreted this trend as variations in $\delta^{18}O$ slab component contribution to the mantle. Models suggest that these variations are produced by two end members, a water rich flux with low $\delta^{18}O$ produced by de-watering of serpentine from the altered oceanic crust of the Cocos Plate and a relatively water poor sediment melt with high $\delta^{18}O$. The first end member dominates the slab component in the center of the arc, the second is more evident in the northwestern part of the arc. In Central Costa Rica both fluxes are small or even insignificant (Eiler et al., 2005).

Recently reported geochronological and geological data define an approximate age for the volcanic front of Costa Rica and Nicaragua of 600 ka and 330 ka respectively (Carr et al., 2007). Based on this age constraint the estimated extrusive volcanic flux ranges from 1.3×10^{10} kg/m/Ma in western Nicaragua to 2.4×10^{10} kg/m/Ma in Central Costa Rica, both within the calculated error. This suggests that the subduction component flux is not significantly different across Nicaragua and Costa Rica and that the regional variations of Ba/La are not related with the total amount of released slab component but the mechanism

of fluid delivery into the mantle wedge. A focused fluid mechanism that produces high degree melts (low La/Yb) is preferred for Nicaragua meanwhile a diffuse mechanism that will produced low degree (high La/Yb) melts is more possibly Costa Rica (Carr et al., 2007).

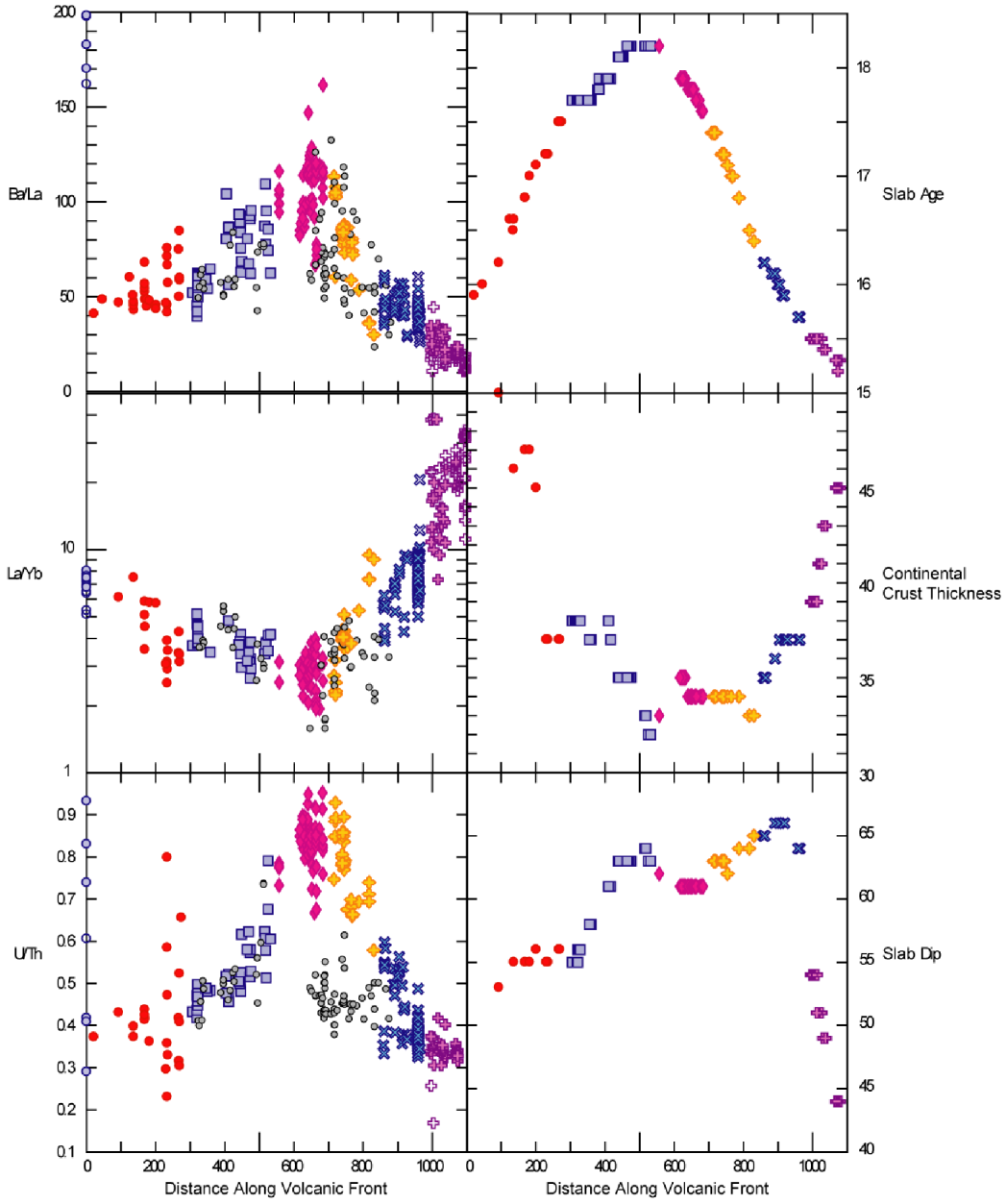

Figure 3: Colored symbols for geochemistry are from the active front and gray circles are Miocene. Colored symbols for geophysical measures refer to present day. Samples from the active arc from Carr et al. (2003). Slab age and crustal thickness is from Carr et al. (1990). Slab dip is from Syracuse and Abers (2005).

Barium Cycle

Biogenic barium ($BaSO_4$) has emerged as a useful proxy of primary productivity in both modern and past paleo-environments (Sanchez-Vidal et al., 2004). Seawater is usually undersaturated in barite (Monnin et al., 1999), but biological processes can create the proper conditions for barite formation (Dehairs et al., 1980). There is debate regarding the specific mechanisms that cause barite to precipitate, however there is evidence to suggest that these are not purely chemical. Ganeshram et al. (2003) found that barite crystals formed during the decay of planktonic diatoms and noted that only a small amount (2-4%) of the barium released by decomposition was converted to barite, suggesting that the availability of barium saturated microenviroments is a limiting factor in barite formation. The oxidation of organic sulfur during the decay of organic matter (Bishop, 1988) as well as the release of barium and sulfur from acantharian shells made of celestite (Bernstein et al., 2002) have also been proposed to generate the proper conditions for barite formation in seawater.

Despite the variety of ways that barite has been shown to precipitate from the decay of organic material, they may not account for the abundance of barite in the oceans or ocean sediments. Gonzalez-Munoz et al. (2003) showed that *Myxococcus xanthus*, a heterotrophic bacteria found in soil and marine environments, can facilitate precipitation of sulfates in seawater. Although the relative contribution of each of these mechanisms to the barite budget of the oceans remains a matter of substantial debate, there appears to be a consensus that barite is biologically mediated; a conclusion that is important to the present paper.

There are, of course, significant non-biogenic sources of barium in seawater, such as hydrothermal vents, which contribute increasing amounts of barium as one moves closer to a mid-ocean ridge. Barite can also form as barium-rich pore fluids in sediment come into contact with sulfate-rich seawater (Paytan et al., 2002). However, Dymond (1981) found that for most samples, particularly those far from these ridges, biogenic barium accounted for more than 90% of barium in the sediment. Because seawater is typically undersaturated with respect to barite, a large amount of the biogenic barite that makes it to the deep ocean enters into solution before entering the sediment. However, Dymond et al. (1992) found that, on average, approximately 30% of the biogenic barium that reaches the ocean floor is preserved in sediment.

The Papagayo Wind

Since, barium concentrations in ocean sediments are mediated by primary production mechanisms, we need to evaluate mechanisms that might affect primary productivity; particularly those that could cause along strike variations in barium concentrations. One of these mechanisms relates to regional wind patterns.

The Papagayo Wind is a narrow jet of air that flows through a low-lying pass between the Costa Rican volcanic front and Nicaraguan Miocene volcanics (Brenes et al., 2003). There are two other similar regional wind currents that take advantage of high-pressure systems in the Caribbean and Gulf of Mexico and of rare gaps in the largely unbroken topography: The Tehuano Winds in Southern Mexico and the Panama Winds, which gust through the area of the Panama Canal. The net effect of these winds is seasonal upwelling that brings nutrients from the deep sea to the surface. NASA SeaWiFS images

(McClain et al., 2002) clearly show positive chlorophyll anomalies of at least 8 mg/m^3 associated with each of these winds systems relative to the surrounding ocean water. Although the size, shape, and extent of the Papagayo chlorophyll anomaly changes throughout the year these images show that the ocean surface offshore Nicaragua is consistently more enriched than the water offshore Guatemala and Costa Rica.

If this increase in primary productivity is dramatic enough to increase the concentration of organically derived barium in the ocean sediments offshore Nicaragua, then this anomaly could potentially affect along strike variations barium in the volcanic front. However, Carr et al. (2007) determined Ba fluxes from the volcanoes of Nicaragua and Costa Rica and found that there is no significant variation between the two volcanic sections.

Methods

To address the lack of analyses of Miocene volcanics from the northern segment of the volcanic front, we collected twenty samples from the Balsamo Formation across El Salvador. Sample locations were documented using GPS. The stratigraphic positions of three samples (Bal-4, Bal-15, and Bal-17) were not mapped as Balsamo (Weiseman et al., 1975), however, chemical analysis of these samples revealed the low U/Th that is characteristic of the rest of the Balsamo samples, indicating that they are indeed from the Balsamo Formation.

Major element data for the Balsamo samples were obtained using an SMAX Rigaku X-ray Fluorescence (XRF) Spectrograph at Michigan State University following procedures outlined in Hannah et al. (2002). XRF major element analyses were reduced by

the fundamental parameter data reduction method (Criss, 1980) using XRFWIN software (Omni Instruments) (Hannah et al., 2002).

Trace element data were determined from rock sample solutions analyzed on a Finnigan MAT Element, a high resolution Inductively Coupled Plasma Mass Spectrometer (HR-ICP-MS) (Table 3) at Rutgers University. Sample digestion, dilution, run preparation, instrument tuning parameters and method were conducted following RU laboratory procedures outlined in Bolge et al. (2006). The analytical run consisted of 20 rocks sample solutions, two digestion blanks, two USGS rock standards, five duplicate samples, and three standard additions (consisting of nine samples). Standard additions were distributed evenly through the run. Indium was added to all the samples during solution preparation. Drift was reduced by normalizing the Indium intensities of all the measurements in the run to the first measurement in the run. The Indium drift was about 20% during the run.

Accuracy was estimated by analysis of the USGS rock standard BHVO-1 and comparison to certified concentrations. The percent difference between the calculated and given reference values were below 6% with the exception of Cs (-26%), Eu (-11%), Ta (-9%), W (-15%), Ti (-26%), Pb (-19%), Th (-16%), Y (-10%). The large percent deviations result from the very low concentration of the elements in the rock sample. Pb and Th have poor agreement with the values from Govindaraju (1989), but agree within 6% of the ICP-MS data reported by Jenner et al. (1990). Precision was determined by duplicate analyses. The majority of the standard deviations are below 7%. All blank concentrations are less than 2% with the exception of Li (2.82%), Ba (3.01%), Pb (3.20%), Cr (6.30%), Ni (2.68%), and Zn (6.01%).

Results

The new geochemical data from the Balsamo Formation in El Salvador obtained in this study support those of Plank et al. (2002) for the Tertiary lavas of Nicaragua. First, the Ba/La profile for the Tertiary samples El Salvador is continuous with the Nicaraguan profile and also roughly coincident with the profile for the modern volcanic front (Figure 3). The U/Th profile for the Tertiary El Salvador samples is continuous with the flat profile obtained for Nicaraguan Miocene samples. Modern Nicaraguan values are significantly higher than in the Miocene while values towards the edges of the arc have not changed substantially since that time (Figures 3).

As a result, we concur with Plank et al. (2002) that the Miocene U/Th results from normal U/Th values in the subducting Cocos Plate. The unusually high ratios found in samples from the active volcanic front result from subduction of anomalously high U contents in the upper organic-rich hemi pelagic muds.

Trace Element Modeling

Previous Central American trace element models were handicapped by poor estimates of the composition of the mantle wedge. For the present model, we inverted the depleted mantle (DM) composition from an East Pacific Rise basalt subducting off Nicaragua (sample SO144-1, Werner et al., 2004). Furthermore, Hoernle et al. (2008) has shown the subducting Galapagos derived volcanics is a necessary component for modeling isotopic and trace element data in southern Central America and we include this component as well.

Trace element concentrations for the modern volcanic front were modeled for four segments along the volcanic front (Figure 4): Northwest Nicaragua (Cosigüina to Momotombo), Southeast Nicaragua from (Apoyeque to Maderas), Northwest Costa Rica from (Orosi to Tenorio), and Central Costa Rica from (Platanar to Irazu-Turrialba). The northern segments of the front were not modeled, because the volcanic material from that region shows evidence of crustal contamination most likely due to relatively thicker continental crust (Feigenson and Carr, 1986).

Carr et al. (2007) modeled trace element concentrations by varying the degree of melt between volcanic front segments in Nicaragua and Costa Rica, but the cause of geochemical differences along the front may be more complicated. Our model incorporates metasomatism of DM by a variable contribution from the slab as well as the seamounts subducting in southern Costa Rica. To do this, DM was metasomatized (Gazel et al., in prep) by the varying input from a 20% partial melt of sediments (50% carbonate sediment and 50% hemipelagic sediment; Patino et al., 2000) and a 20% partial melt of the

Galapagos seamount component (Gazel et al., in prep). Of course, with the seamounts subducting in southern Costa Rica, their contribution could not be equal along the volcanic front and metasomatism of the mantle wedge depends on the subduction input in each segment. The Northwest Nicaraguan source was modeled with the highest sediment component of the four segments (1%) and no seamount component, while Central Costa Rica was modeled with the lowest sediment component (0.1%) and the highest seamount component (1%). Eiler et al. (2005) argued that an additional solute-rich aqueous fluid component is required to explain the variation in oxygen isotopes along the volcanic front. That may be true, however it is not necessary to explain observed Ba/La or U/Th values and there is no direct evidence that more water is entering the Nicaraguan trench relative to the rest of the margin. Therefore, this component will not be included in the present model.

The metasomatized mantle (MM) was then melted over a range of partial melts chosen to bracket the range of actual compositions found within each of these four segments (Figure 4; Carr et al., 2003). The modal MM composition was varied slightly between the four segments and the proportion of garnet in the mantle was adjusted to fit the Heavy Rare Earth Elements (HREEs). The MM composition for Northwest and Southeast Nicaragua was 60% ol, 25% opx, 14.5% cpx, and 0.5% ga. Northwest Costa Rica was 60% ol, 25% opx, 14.7% cpx, and 0.3% ga. Central Costa Rica was 60% ol, 25% opx, 13.5% cpx, and 1.5% ga. A summary of model parameters is given in Table 1.

These data show that the modeled MM compositions along the arc vary due to the varied proportions of the slab and seamount contribution as well as the variation in garnet abundance.

	Northwest Nicaragua	Southeast Nicaragua	Northwest Costa Rica	Central Costa Rica
Degree of Partial Melting	8-20%	4-10%	4-10%	4-6%
Sediment Component	1%	0.5%	0.5%	0.1%
Seamount Component	0%	0.3%	0.4%	1%
DM Composition				
Ol	60%	60%	60%	60%
Opx	25%	25%	25%	25%
Cpx	14.5%	14.5%	14.7%	13.5%
Ga	0.5%	0.5%	0.3%	1.5%

Table 1. Model Parameters.

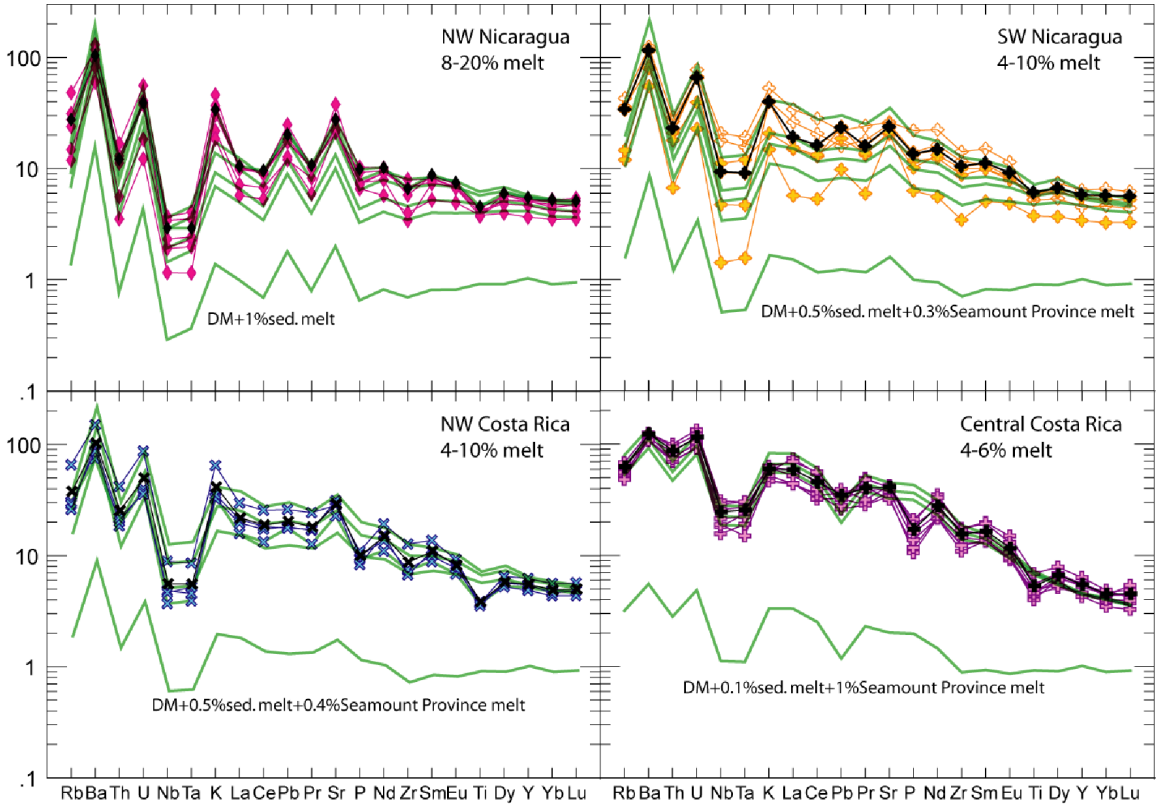

Figure 4: Modeled trace element concentrations for NW Nicaragua, SE Nicaragua, NW Costa Rica, and Central Costa Rica. Green lines are modeled concentrations. Northwest Nicaragua modeled using 8, 10, 15, and 20% melt of a MM source (1% sediment + 99% DM. Southeast Nicaragua modeled using 4, 6, 8, and 10% melt of a MM source (0.5% sediment + 0.3% seamount + 99.2% DM. Northwest Costa Rica modeled using 4, 6, 8, and 10% MM source (0.5% sediment + 0.4% seamount + 99.1% DM). Central Costa Rica modeled using 4, 5, and 6% melt of a MM source (0.1% sediment + 1% seamount + 98.9% DM.

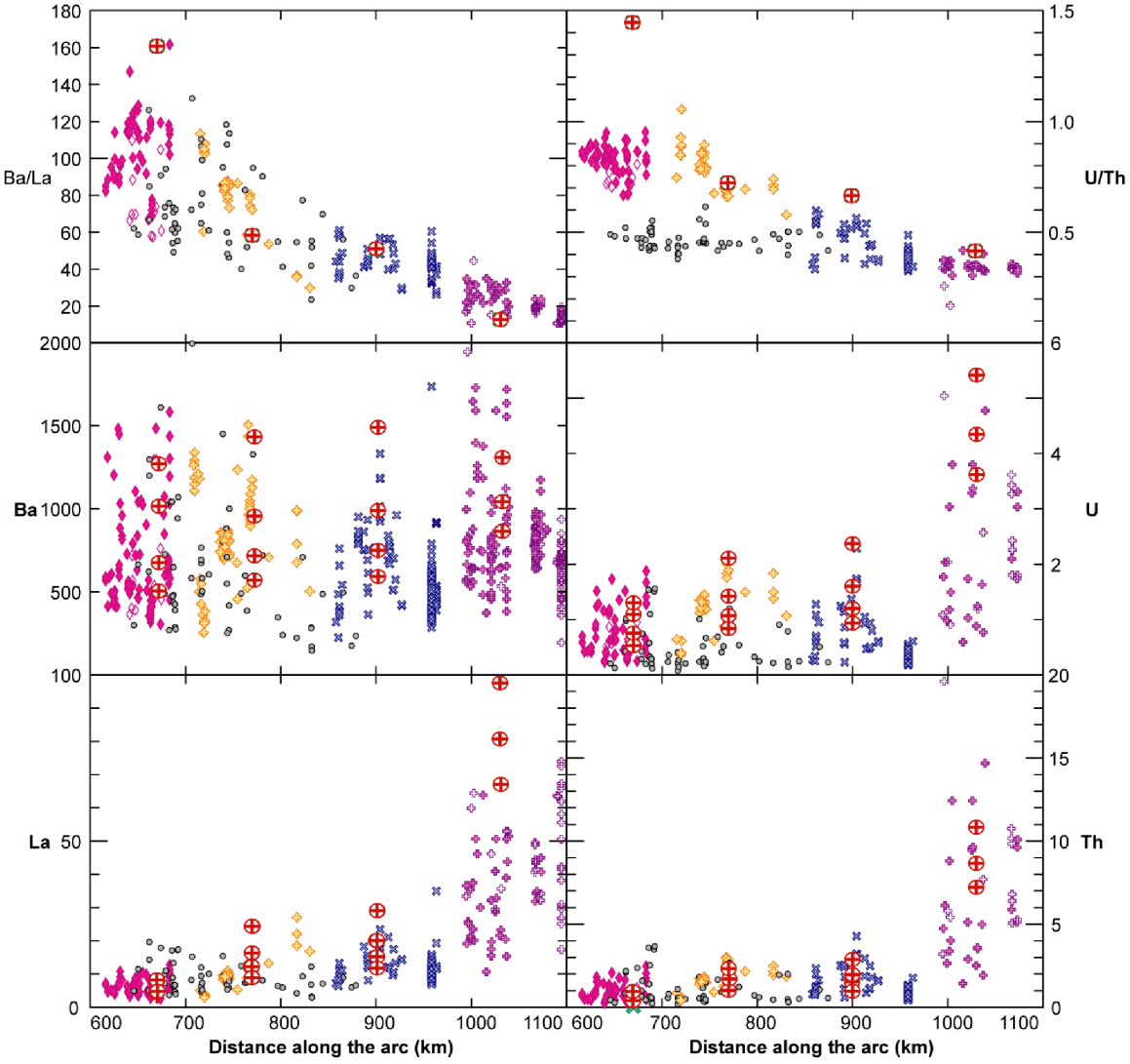

Figure 5. Colored data symbols are volcanic front data from Carr et al. (2003) plotted against distance along arc. Gray circles are Miocene samples from Plank et al. (2002). Red symbols are modeled values at different degrees of partial melting.

Mean trace element concentrations for each segment are in agreement with modeled values and are generally bracketed by the modeled ranges of degree of partial melting. The exceptions are P and Ti, which are generally elevated in modeled compositions. This is most likely because our model does not take into account melt fractionation in the crust, which depletes P through apatite fractionation and Ti through

titanomagnetite fractionation (Claque et al., 1981). Modeled Ba/La and U/Th (Figure 5) values also reflect the decrease toward Costa Rica seen in the data, although model values for both are slightly elevated in the Northwest Nicaraguan segment, which suggests that we have overestimated the sediment component. Modeled values for Ba, La, U, and Th closely match actual data.

According to the models, the mantle underneath Nicaragua has been modified by a higher percentage of sediment than in Costa Rica, however, this does not necessarily mean that more sediment is entering the subduction zone offshore Nicaragua. Rather, the sediment component makes up a smaller percentage of the MM source in Costa Rica, because of the additional seamount component. This supports the conclusion of Carr et al. (2007) that the flux of incompatible elements to the volcanic front does not change significantly along strike. The model also shows that the seamount component decreases from Costa Rica to Nicaragua, which is expected because the Galapagos hotspot tracks collide with the margin in Southern Costa Rica.

Discussion

Ba/La in Central American volcanic rocks has been used as a geochemical indicator of slab input, primarily because Ba is fluid mobile under subduction conditions relative to La and because Ba is highly enriched in ocean sediments relative to mantle values. Carr et al. (1990) suggested that high Ba/La should be expected in Nicaragua because the slab's steep dip caused a more focused flux of material from the subducting slab. However, if Ba is plotted by itself vs. distance along the arc, it is clear that the absolute value of Ba does not change significantly along strike, as this model predicts and that the variation is

controlled by variations in La (Figure 5). Furthermore, data from ODP Sites 844, 845, and 1039 combined with data from DSDP Site 495 reveal that the Ba profile in offshore sediments are remarkably similar throughout the Cocos plate, which is somewhat unexpected given the increase in primary productivity offshore of Nicaragua due to the Papagayo winds. Given these factors, we do not believe that Ba alone is a reliable indicator of sediment input in Central America, although Ba/La does correlate well with $^{10}Be/^{9}Be$, a tracer of the upper portion of the sediment section (Leeman et al., 1994). This does not mean that Ba cannot provide insight into the mechanisms that deliver slab-derived material from the slab to the volcanic front. Rather, it simply means that any model attempting to trace the evolution of Ba from sediments to the arc itself, must explain how Ba remains virtually unchanged along strike both in the subducting sediments and the resulting arc material.

La, rather than Ba controls Ba/La variations. La/Yb values have been used as a proxy for degree of melt and along arc La/Yb values in Central America suggest that the degree of melt is highest in Nicaragua (Carr et al., 1990).

Carr et al. (1990) suggested that the higher degree melts in Nicaragua could be explained by the steeper slab dip, which focuses the flux of slab-derived fluids into a smaller volume of mantle causing higher degrees of melting than occurs where dip is shallower. Models in this paper also suggest that Nicaragua does represent the highest degree of melt along the Central American Volcanic Front. According to Ranero et al. (2003), this variation in along-strike slab dip was governed by the orientation of faults formed at the East Pacific Rise and the Galapagos Spreading Centers. These faults are optimally reactivated by subduction where they strike parallel to the trench. The steepest

dip proposed in Nicaragua is associated with well-developed trench-parallel faults. The authors also suggest that the shallower slab dip in Costa Rica is caused by a tectonic fabric that is perpendicular in the South and oblique in the North. Although slab age (oldest in Nicaragua, Figure 3; Carr et al., 1990) vary along strike, it was not thought to significantly influence either slab bend-faulting or slab dip. However, given the correlation between slab dip with slab age, it suggests that factors other than fault orientation also control slab dip.

We propose the following model to explain the along arc variation in degree of melt: Offshore of Nicaragua, relatively older and cooler lithosphere enters the subduction zone. These factors promote the development of a steeper slab dip in Nicaragua. In addition, the preferential orientation of cracks formed at the ridge also allow steepening of the slab (Ranero et al., 2003). To either side of Nicaragua, younger and warmer lithosphere promotes the development of a shallower slab dip. This is particularly the case in southern Central America where the subduction of the buoyant Galapagos Hot Spot tracks resists steep subduction (Ranero et al., 2003). The oblique to perpendicular orientation of cracks formed at the ridge also inhibit steepening of the slab (Ranero et al., 2003).

Regardless of the mechanism for generating bend faults at the subduction zone, seismic imagery supports the argument that these faults lead to serpentinization that can penetrate into the upper mantle (Ranero et al., 2003). Since this faulting is most pronounced in Nicaragua, it is possible that the Nicaraguan slab carries more water into the subduction zone than in Costa Rica. In addition, p-wave velocities suggest that the Nicaraguan slab contains at least 5 wt.% water, which is several times greater than found in

other slabs using this method (Abers et al., 2003). However, there is no direct evidence of variable water contents at Central American volcanic front volcanoes and it is not necessary to invoke water to explain variations in the degree of melt.

Variation in slab dip means that the depth of the slab as well as the height of the melt column under the volcanic front is 75 km greater in Nicaragua than Costa Rica (Syracuse and Abers, 2006). In Nicaragua, the steep slab focuses the flux of slab-derived fluids into a narrower column, which leads to high degrees of melt (Carr et al., 1990). In Costa Rica, the shallower slab releases the flux of fluids into a broader melt column, which leads to lower degrees of melt. Along-strike La/Yb values (Figure 3) support these variations in degree of melt throughout the Central American Volcanic Front (Carr et al., 1990).

Regional variations in along arc U/Th and Ba/La (with peaks in Nicaraguan volcanic front lavas) have been considered to reflect varying intensity of the flux of slab-derived components (Carr et al., 1990; Patino et al., 2000). However, the overall flux of Ba does not vary significantly along strike (Carr et al., 2007) and the concentration of Ba within Central American volcanics is similarly constant. We propose the following to explain how Ba concentrations can both enter and exit the subduction system without changing its along strike profile: Carr et al. (1990) first suggested that the steeper slab dip in Nicaragua caused a focusing of the flux of slab-derived fluids into the mantle wedge. This focused flux causes a higher degree of partial melting under Nicaragua. This focused flux does not lead to high Ba levels in the resulting volcanic material, because the focused flux is at the same time diluted by the higher degree of melt that it produces. The opposite would be true where the slab dip is shallower, where a more diffuse slab flux modifies a

lager volume of mantle producing low degree of melts. Since the extrusive flux does not appear to vary significantly between Nicaragua and Costa Rica (Carr et al., 2007), it is likely that the focused slab flux under Nicaragua produces a higher degree of melt from a smaller volume of mantle relative to Costa Rica. A higher Ba flux could occur in Nicaragua because the mass of intrusive magmatic bodies is much greater than in Costa Rica. However, this is unlikely given the more mafic character of Nicaraguan volcanics compared to those of Northwest Costa Rica.

Why then has Ba/La has remained essentially the same for 23 Ma (Plank et al., 2002), while U/Th has increased, particularly in Nicaragua. The constancy of Ba/La has survived major reorganizations of the volcanic front. Figure 6 shows the approximate past positions of the volcanic front for El Salvador, Costa Rica and Nicaragua, which appear to have shifted location over time. In general, the volcanic belt has migrated toward the trench, implying either a steeper slab dip over time or slab rollback, however there are substantial differences along the margin. In Nicaragua, the modern front has been moving trenchward for at least 10 Ma (Plank et al., 2002) and there is a gap in age determinations between 7 Ma and 3.6 Ma (Saginor et al., see Chapter 3). In western Costa Rica, the strike of the volcanic front has rotated 30 degrees counterclockwise since about 13 Ma (Gans et al., 2002). Rogers et al. (2002) argued that a slab detachment occurred between 10 and 6 Ma, causing major uplift in Honduras and Northern Nicaragua. Through all this turbulence the regional variation in Ba/La has continued with minimal change. Because the regional variation in Ba/La is primarily controlled by La (an indicator of degree of melt), the constant Central American Ba/La ratios may indicate that fundamental tectonic factors such as slab dip have not changed over this time period.

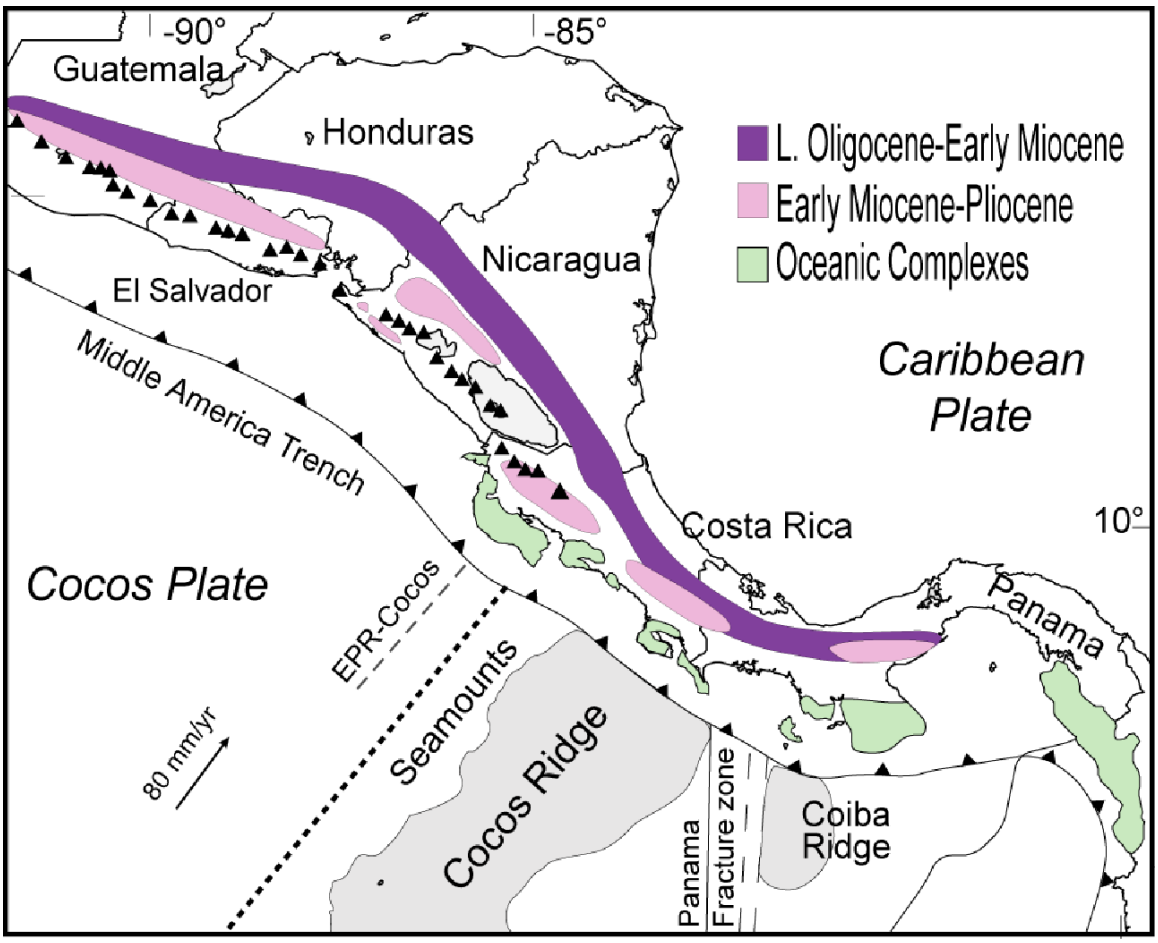

Figure 6: Location of Miocene to present volcanic front. (Bundschuh and Alvarado, 2007)

The high Ba content of Cocos Plate sediments is the cause of the high Ba/La in Central America relative to other arcs (Plank and Langmuir, 1993). Ba is elevated in this region relative to many other arcs because of high oceanic primary productivity caused by the low latitude band of upwelling (Solomon et al., 2006). At 24 Ma, plate reconstructions, relative to a fixed hotspot frame, place Central America essentially at the same latitude as the present, or at most a degree to the south (Rogers, 2003). Therefore, any parameter that varies with latitude, such as oceanic productivity, should not be greatly affected. The source of the highest Ba/La ratios in the Tertiary and modern volcanics seems constant,

however, the remarkable aspect of the subduction signal in Central America, both now and during the Tertiary, is the substantial regional variation, with its maximum in Nicaragua, at roughly the center of the margin. This regional variation occurs over just 5 degrees of latitude and the belt of high primary productivity (and high Ba) extends over the entire region. However, whether this high productivity existed in the Miocene is unknown.

The increase in U/Th values in Nicaraguan volcanic material since the Miocene has been attributed to changes in the subducting sediments following the "carbonate crash" (Plank et al., 2002) at 10-12 Ma. At that time, the Central American isthmus began to close, which shut off an important flow of water from the Caribbean to the Pacific (Coates et al., 1992; Lyle et al., 1995; Farrell et al., 1995). This caused the carbonate compensation depth to rise and sediments to become enriched in organic carbon at the expense of carbonate (Hoffmann et al., 1981). The result is that Cocos plate sediments consist mainly of a lower carbonate layer and an upper hemipelagic layer, with the latter unit showing enrichment in U (Patino et al., 2000). This increase in uranium content of subducted sediments is reflected in Nicaraguan lavas in the form of a substantial increase in U/Th values between the Miocene and active volcanic front (Patino et al., 2000; Plank et al., 2002). The timing and rate of this increase could not be determined because there was a gap in the volcanic record between 7 Ma and 0.3 Ma (Carr et al., 2007) until data from Saginor et al. (see Chapter 3) reduced the length of this gap roughly by half, leaving only the period between 7 and 3.6 Ma without known volcanism. Saginor et al. (see Chapter 3) also showed that the transition from low to high U/Th was more gradual than previously thought. Uranium levels along the active volcanic front are generally higher than in the Miocene with the exception of a few high U Miocene Nicaraguan samples. Along strike, U

does not vary significantly throughout Central America in either the Miocene or active fronts. Instead, along arc variations in modern lavas U/Th are primarily controlled by Th, which is lowest in Nicaragua. The low Th in Nicaragua may simply reflect the higher degrees of melt relative to the rest of the arc.

Along arc $^{10}Be/^{9}Be$ values (Tera et al. 1986; Morris et al., 1990; Reagan et al., 1994; Kelly, 2003) offers the best evidence the entire sediment package is not subducted outside of Nicaragua. ^{10}Be is a cosmogenic radionuclide with a half-life of 1.5×10^{6} years (Yiou and Raisbeck, 1972). Because of its relatively short half-life, ^{10}Be is only found in high concentration in the upper tens of meters of marine sediment (Tera et al., 1986). Central American $^{10}Be/^{9}Be$ values show a systematic variation with a chevron pattern centered on a Nicaraguan maximum (Morris et al, 1990; Kelly, 2003), which indicates that the entire sediment package is subducted near the middle of the arc and not toward the edges. This process only requires that small amounts of sediment fail to subduct, which means that the flux of sediment indicators, such as Ba, that are found in similar concentrations throughout the entire sediment section will not be greatly affected. Sediment indicators, such as U, which are elevated in the upper hemipelagic layer, may be slightly affected although the models suggest that the bulk subducted sediment composition does not vary significantly. Kelly (2003) argues that this upper ^{10}Be enriched sediment layer is subducted in Nicaragua because offshore basement faulting is great enough to accommodate the entire sediment section, while the throw of basement faults towards the edges of the margin leave the uppermost ^{10}Be-bearing layer prone to accretion.

Conclusions

- Along arc U/Th values in Nicaragua experienced a significant increase since the Miocene, due to increases in U-bearing sediment following the carbonate crash.
- Variations in Ba/La are primarily controlled by changes in La, which indicates changes in the degree of partial melting.
- Along arc Ba/La values have not changed significantly since the Miocene suggesting that the degree of melt has been highest in Nicaragua and lowest near the edges of the arc since that time.
- Trace element modeling suggest that the mantle under Nicaragua is metasomatized by a higher percentage of the sediment component than in Costa Rica, because the sediment signal in Costa Rica is may be diluted by the subducting seamount component.

References

Abers, G., Plank, T., and B. Hacker (2003), The wet Nicaraguan slab, *Geophys. Res. Lett.*, 30, 2, DOI 10.1029/2002GL015649.

Bernstein, R., Byrne, R., Betzer, P., and A. Greco (1992), Morphologies and transformations of celestite in seawater: The role of Acantharians in strontium and barium geochemistry. *Geochim. Cosmochim. Acta*, 56, 3273-3279.

Bundschuh, J., Alvarado, G. (2007), Central America: Geology, Resources, Hazards, Taylor and Francis, London.

Bishop, J. (1988), The barite-opal-organic carbon association in oceanic particulate matter. *Nature*, 331, 341–343.

Bolge, L., Carr, M., Feigenson, M., and G. Alvarado (2006), Geochemical stratigraphy and magmatic evolution at Arenal volcano, Cost Rica, *J. Volc. Geotherm. Res*,157, 34-48.

Brenes, C., Coen, J., Chelton, D., Enfields, D., Leo, S., and D. Ballestero (2003), Wind driven upwelling in the Gulf of Nicoya, Costa Rica, *International Journal of Remote Sensing*, 24, 5, 1127-1133.

Cannariato, K., and A. Ravelo (1997), Pliocene–Pleistocene evolution of the eastern Pacific surface water circulation and thermocline depth: *Paleoceanography*, 12, 805-820.

Carr, M.J. (1984), Symmetrical and segmented variation of physical and geochemical characteristics of the Central American volcanic front, *J. Volcanology and Geothermal Research*, 20, 231-252.

Carr, M.J., Feigenson, M.D., and E.A. Bennett (1990), Incompatible element and isotopic evidence for tectonic control of source mixing and melt extraction along the Central American arc, *Contrib. Mineral. Petrol*, 105, 369-380.

Carr, M.J., R. E. Stoiber (1990), Volcanism, *from: The Geology of North America Vol. H: The Caribbean Region*, The Geological Society of America, 375-391.

Carr, M.J., Feigenson, M.D., Patino, L.C., and J.A. Walker (2003), Volcanism and geochemistry in Central America: progress and problems, in *Inside the Subduction Factory,* AGU Geophysical Monograph 138, Edited by Eiler, J. and G. Abers, 153-179.

Carr, M. J., Saginor, I., Alvarado, G. E., Bolge, L. L., Lindsay, F. N., Milidakis, K., Turrin, B. D., Feigenson, M. D., and C. C. Swisher III (2007), Element fluxes from the volcanic front of Nicaragua and Costa Rica, *Geochemistry Geophysics Geosystems*, 8, 6, 1525-2027.

Coates, A. Jackson, J., Collins, L., Cronin, T., Dowsett, H., Bybell, L., Jung, P.,and J. Obando, J. (1992), Closure of the Isthmus of Panama; The near-shore marine record of Costa Rica and western Panama, *Bull. Geo. Soc. Am.*, 104, 7, 814-828.

Condie, C. (2004), Continuity (Ba) and change (U) in Central American geochemistry: New evidence from the Miocene Balsamo Formation in El Salvador, Masters Thesis, Rutgers University.

Claque, D., Frey, F., Thompson, G., and S. Rindge (1981), Minor and trace element geochemistry of volcanic rocks dredged from the Galapagos spreading center: Role of crystal fractionation and mantle heterogeneity, *J. Geophys. Res.*, 86, 9469-9483.

Criss J. (1980), Fundamental parameters calculations on a laboratory microcomputer. *Advan. X-ray Anal.*, 23, 93–97.

Dehairs, F., Chesselet, R., and J. Jedwab (1980), Discrete suspended particles of barite and the barium cycle in the open ocean, *Earth Plan. Sci. Lett.*, 49, 2, 528-550.

Dymond, J. (1981), Geochemistry of Nazca plate surface sediments: An evaluation of hydrothermal , biogenic, detrital, and hydrogenous sources, Nazca Plate, Crustal Formation and Andean Convergence, *edited by* L. Kulm, *Geo. Soc. Am. Memoirs*, 154, 133-174.

Dymond, J., Suess, E., and M. Lyle (1992), Barium in Deep Sea Sediment: A Geochemical Proxy for Paleoproductivity, *Paleoceanography*, 7, 163-181.

Ehrenborg, J. (1996), A new stratigraphy for the Tertiary volcanic rocks of the Nicaraguan highland, *Geol. Soc. Am. Bull.*, 108, 830-842.

Eiler, J., Carr, M., Reagan, M., and E. Stolper (2005), Oxygen isotope constraints on the sources of Central American arc lavas, *Geochem. Geophys. Geosyst.*, 6, 7, 1-28.

Farrell, J., Raffi, I., Janacek, T.R., Murray, D.W., Levitan, M., Dadey, K.A., Emeis, K.-C., Lyle, M., Flores, J.-A., and S. Hovan (1995), Late Neogene sedimentation, patterns, in the eastern equatorial Pacific Ocean, *in* Pisias, N.G., Mayer, L.A., Janecek, T.R., and T.H. van Andel (Eds.), *Proceedings of the Ocean Drilling Program, Scientific Results*, 138, 717-753.

Feigenson, M., and M. Carr (1986), Positively correlated Nd and Sr isotope ratios of lavas from the Central American Volcanic Front, *Geology*, 14, 79-82.

Ganeshram, R., Francois, R., Commeau, J., and S. Brown-Leger (2003), An experimental investigation of barite formation in sea-water. *Geochim. Cosmochim. Acta*, 67, 2599-2605.

Gans, P., MacMillan, I., Alvarado, G., Perez, W., and C. Sigaran (2002), Neogene evolution of the Costa Rican arc, Geol. Soc Amer., 2002 Annual Meeting, Abstracts with Programs.

Gonzalez-Munoz, M., Fernandez-Luque, B., Martinez-Ruiz, F., Chekroun, K., Arias, J., and M. Rodriguez-Gallego (2003), Precipitation of barite by Myxococcus xanthus: Possible implications for the biogeochemical cycle of barium, *Applied and Environmental Microbiology*, 69, 5722–5725.

Govindaraju , K. (1989), Compilation of working values and sample description for 272 Geostandards, *Geostand. Newslett*., 13, 1-114.

Hannah, R., Vogel, T., Patino, L., Alvarado, G., Pérez, W., and D. Smith (2002), Origin of silicic volcanic rocks in Central Costa Rica: A study of a chemically variable ash-flow sheet in the Tiribí Tuff, *Bull. Volc*, 64, 117–133.

Haug, G., Tiedemann, R., Zahn, R., and A. Ravelo (2001), Role of Panama uplift on oceanic freshwater balance, *Geology*, 29, 207–210.

Hoernle, K., Abt, D., Fischer, K., Nichols, H., Hauf, F., Abers, G., van den Bogaard, P., Heydolph, K., Alvarado, G., Protti, M., and W. Strauch (2008), Arc-parallel flow in the mantle wedge beneath Costa Rica and Nicaragua, *Nature*, 451, 1094-1097.

Hoffmann, E.E., Busalacchi, A.J., and J.J. O'Brien (1981), Wind generation of the Costa Rica Dome, *Science*, 214, 552-554.

Hovan, S. (1995), Late Cenozoic atmospheric circulation intensity and climatic history recorded by eolian deposition in the eastern Equatorial Pacific Ocean, Leg 138, *in* Pisias, N.G., Mayer, L.A., Janecek, T.R., and T.H. van Andel (Eds.), *Proceedings of the Ocean Drilling Program, Scientific Results*, 138, 821-838.

Jenner, G., Longerich, H., Jackson, S., and B. Fryer (1990), ICP-MS a powerful tool for high precision trace element analysis in Earth Sciences: Evidence from analysis of selected USGS reference samples, *Chemical Geology*, 83, 133-148.

Lyle, M., Dadey, K., and J. Farrell (1995), The Late Miocene (11-8 Ma) Eastern Pacific carbonate crash: Evidence for reorganization of deep-water circulation by the closure of the Panama Gateway, *in* Pisias, N.G., Mayer, L.A., Janecek, T.R., and T.H. van Andel (Eds.), *Proceedings of the Ocean Drilling Program, Scientific Results*, 138, 821-838.

Kelly, R. (2003), Subduction dynamic at the Middle America Trench: New constraints from swath bathymetry, multichannel seismic data, and ^{10}Be, Phd Thesis, MIT/WHOI, 1-334.

McBirney, A, Williams, H. (1965), Volcanic History of Nicaragua, *University of California Publications in Geological Sciences*, 55, 1-73.

McClain, C., Christian, J., Signorini, S., Lewis, M., Asanuma, I., Turk, D., and C. Dupouy-Douchement (2002), Satellite ocean color observations of the tropical Pacific Ocean, *Deep-Sea Res.*, 2533-2560.

Monnin, C., Jeandel., C., Cattaldo, T.,and F. Dehairs (1999), The marine barite saturation state of the world oceans, *Marine Chemistry*, 65, 253-261.

Morris, J., Leeman, W., and F. Tera (1990), The subducted component in island arc lavas: constraints from Be isotopes and B-Be systematics, *Nature*, 344, 31-36.

Olney, J. (2006), The age and geochemical history of the Telica Volcanis Complex, Ph.D. Thesis, Northern Illinois University.

Paytan, A., Mearon, S., Cobb, K., and M. Kastner (2002), Origin of marine barite deposits: Sr and S isotope characterization, *Geology*, 30, 8, 747–750.

Patino, L.C., Carr, M.J., and M.D. Feigenson (2000), Local and regional variations in Central American arc lavas controlled by variations in subducted sediment input, *Contrib. Mineral. Petrol*., 138, 265-283.

Plank, T., Balzer, V., and M.J. Carr (2002), Nicaraguan volcanoes record paleoceanographic changes accompanying closure of the Panama Gateway, *Geology* 30, 1087-1090.

Plank, T. and C.H. Langmuir (1993), Tracing trace elements from sediment input to volcanic output at subduction zones, *Nature, 362*,739-743.

Ranero, C., Morgan, J., McIntosh, K., and C. Reichert (2003), Bending-related faulting and mantle serpentinization at the Middle America Trench, *Nature*, 425, 367-373.

Reagan, M., Morris, J., Herrstrom, E., and M. Murrell (1994), Uranium series and beryllium isotope evidence for an extended history of subduction modification of the mantle below Nicaragua, *Geochim. Cosmochim. Acta*, 58, 4199-4212.

Rogers, R., Karason, H., and R. van der Hilst (2002), Epeirogenic uplift above a detached slab in northern Central America, *Geology*, 30, 11, 1031-1034.

Rogers, R. (2003), Jurassic-recent tectonic and stratigraphic history of the Chortis Block of Honduras and Nicaragua, Ph.D. Thesis, University of Texas at Austin.

Sanchez-Vidal, A., Collier, R., Calafat, A., Fabres, J., and M. Canals (2004), Particulate barium fluxes on the continental margin: A study from the Alboran Sea (western Mediterranean), *Marine Chemistry*, 93, 2-4, 105-117.

Solomon, E., Kastner, M., and G. Robertson (2006), Barium cycling at the convergent Costa Rican Margin, *In* Morris, J.D., Villinger, H.D., Klaus, A., (Eds.), *Proc. ODP, Sci Results*, 205, 1-22.

Syracuse, E., Abers, G. (2005), Global compilation of variations in slab depth beneath arc volcanoes and implications, *Geochem. Geophys. Geosyst*., 7, 5, DOI: 10.1029/2005GC001045.

Schroeder, J., Murray, R., Leinen, M., Pflaum, R., and T. Janacek (1997), Barium in equatorial Pacific carbonate sediment: Terrigenous, oxide, and biogenic associations, *Paleoceanography*, 12, 125–146.

Tera, F., Brown, L., Morris, J., Selwyn Sacks, I., Klein, J., and R. Middleton (1986), Sediment incorporation in island-arc magmas: Inferences from ^{10}Be, *Geochim. Cosmochim. Acta*, 50, 535-550.

Werner, R., Hoernle, K., Barckhausen, U., and F. Hauff (2003), Geodynamic evolution of the Galapagos hotspot system (central East Pacific) over the past 20 m.y.: Constraints from morphology, geochemistry, and magnetic anomalies, *Geochem. Geophys. Geosyst*. 4, 12, DOI: 10.1029/2003GC000576.

Wiesemann, G., (1975) Remarks on the geologic structure of the Republic of El Salvador: Mitteilungen des Geologische-Palaontologischen Institut der Universite Hamburf, 44, 557-574.

Yious, F., and G.M. Raisbeck (1972), Half-life of ^{10}Be, *Phys. Rev. Lett.*, 29, 372-375.

Curriculum Vita

Ian Saginor

Education

Rutgers University, New Brunswick, NJ, Department of Geological Sciences, Ph.D., 10/08

Vassar College, Poughkeepsie, NY, B.A., Geology, May 2001

Macquarie University, North Ryde, Australia, Study Abroad, July 1999 - December 1999, Courses in Australian Politics, History, and Culture

Teaching Experience

Lecturer, Earthquakes and Volcanoes, Rutgers University, Fall 2007

Fellow, National Science Foundation GK12 Program, academic years 2005-2007

Instructor, Rutgers Science Explorer, 2005-2007

Other Educational Experience

Educational Testing Service (ETS), Item Writer and Freelance Consultant, 2006-Present

Chrysalis Publishing Group, Assistant Editor/Writer, 2002-2003

Publications

Carr, Michael J., Saginor, Ian, Alvarado, Guillermo E., Bolge, Louise L., Lindsay, Fara N., Milidakis, Kathy, Turrin, Brent, Feigenson, Mark D., Swisher, Carl C. III, Element Fluxes from the Volcanic Front, Geochemistry, Geophysics, Geosystems, Vol 8, no. 6. 2007.

Saginor, Ian, Condie, Claire, Gazel, Esteban, Carr, Michael J., Reevaluation of Ba/La as an indicator of slab input in the Central American Subduction Zone, in prep.

Saginor, Ian, Carr, Michael J., Gazel, Esteban, 40Ar/39Ar Dating in Central American Volcanics: A Review of Progress and Problems, Revista Geológica de América Central, in prep.